Alma Mater Studiorum – Università di Bologna

DOTTORATO DI RICERCA

IN EMATOLOGIA CLINICA E SPERIMENTALE

Ciclo XX

Settore scientifico disciplinare di afferenza: **med15**

MECHANISMS OF RESISTANCE TO TYROSINE KINASE INHIBITORS IN PHILADELPHIA-POSITIVE ACUTE LYMPHBLASTIC LEUKAEMIA (ALL): FROM GENETIC ALTERATIONS TO IMPAIRED RNA EDITING

Presentata da: **Dott.ssa ILARIA IACOBUCCI**

Coordinatore Dottorato — **Chiar.mo Prof. Stefano Pileri**

Relatore — **Chiar.mo Prof. Giovanni Martinelli**

Esame finale anno 2008

MECHANISMS OF RESISTANCE TO TYROSINE KINASE INHIBITORS IN PHILADELPHIA-POSITIVE ACUTE LYMPHOBLASTIC LEUKAEMIA (ALL): FROM GENETIC ALTERATIONS TO IMPAIRED RNA EDITING

1. BACKGROUND

1.1 Acute Lymphoblastic Leukemia

Acute lymphoblastic leukemia (ALL) is a malignant disorder that originates in a single B- or T-lymphocyte progenitor. Proliferation and accumulation of leukaemic cells result in the suppression of normal haematopoiesis and involves various extramedullary sites, especially the liver, spleen, lymphnodes, thymus, meninges and gonads. The disease is most common in children, but can occur in any age group. A vastly improved understanding of ALL pathophysiology has emerged from two decades of progress in defining the lineage-related development, antigen expression and genetic abnormalities of leukaemic cells, and in elucidating the multistep mechanisms by which changes in the function of specific genes disrupt key signalling pathways, which ultimately lead to leukaemic transformation.

1.1.1 Epidemiology

ALL is the most frequently diagnosed childhood acute leukemia, constituting 25% of childhood malignancies. It represents only 20% of adult acute leukemias. The incidence is 4–5 per 100,000 population between the ages of 2–4, which decreases during later childhood, adolescence, and young adulthood before a second, smaller peak occurs in patients older than 50 years (incidence 1 per 100,000 population). Among children, white children are affected more frequently than African-American children. There is little difference in incidence rates by gender among children, but in older age groups, ALL is more predominant in males.

1.1.2 Clinical presentation

Symptoms of ALL at onset are primarily produced by the detrimental effects of the expanding cell population on bone marrow, and secondarily by infiltration of other organs and by metabolic disturbances [1,2]. Bone marrow is usually infiltrated with >90% blast cells. Infiltration with less than 50% blasts represents only 4% of cases. The classical triad of

symptoms related to bone marrow failure is the following: fatigue and increasing intolerance to physical exercise (caused by anaemia), easy bruising and bleeding from mucosal surfaces and skin (caused by thrombocytopenia especially when platelets are $<20 \times 10^9\ l^{-1}$), and fever with infections (40% of all cases, caused by absolute granulocytopenia). Headache and cranial or other nerve palsy are related to meningeal or extradural nerve involvement, which occurs in 5–10% of cases at presentation, being most prevalent in B-ALL and T-ALL. Enlargement of superficial lymph nodes, liver and spleen each occur in approximately one-half of cases; mediastinal lymph nodes are enlarged in the majority of T-ALL and can cause cardiorespiratory problems. The involvement of other organs at a clinically detectable level is consistently below 5%: kidney, skin, eye, retina, lungs, pleura, heart, pericardium, testis, ovary, abdominal or retroperitoneal lymph nodes can be affected. Hyperleukocytic leukaemias with >100.000 blast cells rarely lead to the leukostasis syndrome and catastrophic early bleeding [3].

1.1.3 Diagnostic study

Diagnostics is based on bone marrow aspirate, morphological analysis, immunophenotyping and cytogenetic study.

1.1.3.1 Morphological classification

Morphology is the main criterion for primary diagnosis of ALL and differentiation from AML [4]. The diagnosis of acute lymphoblastic leukaemia (ALL) can be established when the bone marrow examination reveals a lymphoid blast cell content in excess of 20% of total cellularity. Three major morphological subtypes, according to the French–American–British (FAB) committee criteria can be distinguished[5]:

- L1/small lymphoid cells, homogeneous chromatin, no nucleoli, scanty cytoplasm, regular nuclei/25–30%;

- L2/large heterogeneous cells, lacy chromatin, irregular nuclear shape, nucleoli present, cytoplasm/65–70%:
- L3/large homogeneous cells with finely stippled nuclear chromatin, prominent nucleolus, strongly basophilic and vacuolated cytoplasm/5–10%.

The subclassification of groups L1 and L2 is of minor relevance since it has no prognostic implications. The new WHO classification scheme for both T- and B-lineage ALL no longer considers this distinction but does rather distinguish between precursor B or T lymphoblastic leukaemia[6], with different immunophenotypes and cytogenetic characteristics. The subgroup L3 gives a hint of the presence of B-lineage ALL (B-ALL), but again this distinction is not absolute, since occasional B-ALLs display L1/L2 morphology and, conversely, L3-like morphology can be seen in acute non-lymphocytic leukaemia.

1.1.3.2 Immunophenotyping

Immunophenotyping is an essential component of the diagnostic work-up of ALL and it can be used to subclassify cases according to the recognized stages of normal B- and T-cell maturation. Clinically, the only distinctions with therapeutic importance are those between T-cell and B-cell precursors (including the early pre-B, pre-B and transitional pre-B immunophenotypes) and between these cell types and mature B cells. Comprehensive immunophenotyping is also useful in immunological monitoring for minimal residual leukaemia and in immunotherapy.

The antigen-expression profiles of leukaemic lymphoblasts parallels the normal stages of B- and T-cell differentiation and maturation. Roughly 75% of cases of adult ALL are of B-cell lineage. B-lineage markers are CD19, CD20, CD22, CD24, and CD79a. The earliest B-lineage markers are CD19, CD22 (membrane and cytoplasm) and CD79a. A positive

reaction for any two of these three markers, without further differentiation markers, identifies pro-B ALL. The presence of CD10 antigen (CALLA) defines the “common” ALL. subgroup. Cases with additional identification of cytoplasmatic IgM (heavy chain of mu type only) constitute the pre-B group, whereas the presence of surface immunglobulin light chains defines mature B-ALL. T-cell ALL constitutes approximately 25% of all adult cases of ALL. T-cell markers are CD1a, CD2, CD3 (membrane and cytoplasm), CD4, CD5, CD7 and CD8. CD2, CD5 and CD7 antigens are the most immature T-cell markers, but none of them is absolutely lineage-specific, so that the unequivocal diagnosis of T-lineage ALL (T-ALL) rests on the demonstration of surface/cytoplasmic CD3 (Fig.1)[7,8]. ALL blasts coexpress myeloid markers in 15–50% of adults and in 5–35% of children[9]. The most frequently coexpressed myeloid markers are CD13 and CD33[10].

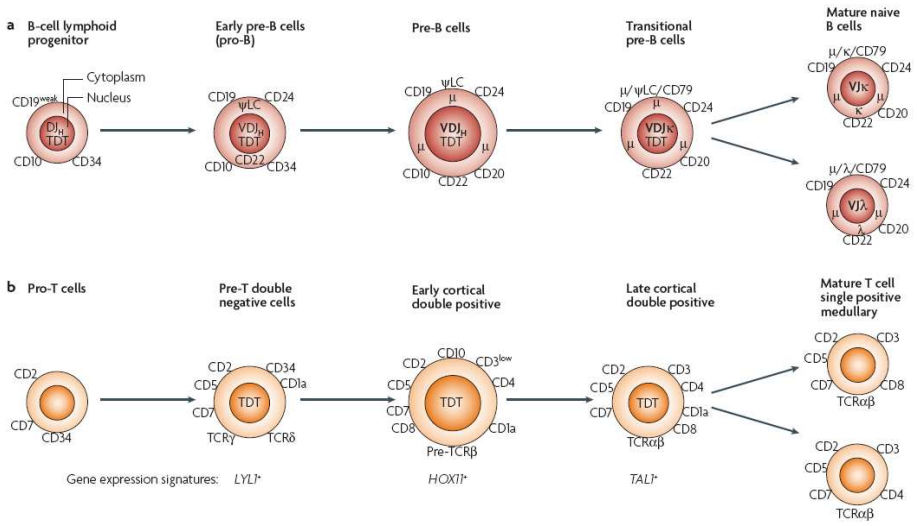

Figure 1. Schematic of B- and T-cell development. The hallmark of bone-marrow B-cell development is the ordered rearrangement of gene segments that encode the variable portion of the antibody molecule. Distinct gene-expression signatures are associated with leukaemic cell samples with recognized stages of thymocyte differentiation: LYL1+ corresponds to pre-T, HOX11+ corresponds to early cortical, and TAL1+ corresponds to late cortical.

1.1.3.3 Cytogenetic and molecular genetic abnormalities

The cloning and characterization of recurrent chromosomal translocations has allowed the identification of genes critical for the leukemogenic process[11] (Fig.2). Furthermore the presence of particular translocations often has prognostic importance and can be used to stratify patients into those who require more-intensive therapy. The use of gene expression analysis to characterize the differences in gene expression between leukemias with different chromosomal aberrations has solidified the notion that specific chromosomal abnormalities specify unique leukemias[12,13].

<u>B-lineage ALL</u>

In children, 85% of ALL cases are of B-lineage origin, and about 80% of these can be further classified by cytogenetics and characteristic genetic translocations (Fig.2):

- *t(1;19)(q23;p13.3)*: it fuses the transactivation domain of the transcription factor E2A on chromosome 19, to the homeobox (HOX) gene PBX1 on chromosome 1. E2A contains a basic helix-loop-helix domain responsible for sequence specific DNA binding and dimerization, and plays a critical role in lymphocyte development. Given that E2Adeficient mice show significant defects in lymphoid development and the t(1;19) impairs one copy of the E2A locus, loss of E2A function may contribute to leukemogenesis in this subtype of ALL. Furthermore, given the clear role of HOX genes in leukemogenesis, and the ability of PBX1 to alter HOX gene dependent regulatory programs, dysregulation of PBX1 function likely contributes to leukemogenesis[14].
- *t(4;11)(q21;q23)*: the rearrangement that involves MLL on chromosome 11 is the most common genetic abnormality in ALL cells in children younger than 1 year of age (85% of cases), and it is found in 3–8% of adults[15]. The AF4 gene on chromosome 4 is most often the fusion partner, but about 40 different partners have been shown to fuse with MLL. Any rearrangement of MLL is commonly considered a high-risk feature in ALL.

- *t(8;14)(q24;q32)* and its less common variants, t(8;22)(q24;q11) and t(2;8)(p12;q24), are characteristic of mature–B-cell ALL. All three translocations result in deregulation, increased transcription, and overexpression of c-MYC. In 80% of patients, 8q24 is juxtaposed to the IgH gene locus on 14q32, whereas the Ig lamba gene locus on 22q11 is involved in 15% of patients and the Ig kappa gene locus on 2p12 is involved in 5% of patients. Mature–B-cell ALL and Burkitt lymphoma typically are associated with 8q24 rearrangements.
- *t(9;22)(q34;q11)*: translocation of parts of chromosomes 9 and 22 to create the BCR–ABL fusion, also called the Philadelphia chromosome. This genetic abnormality occurs in about 3% of ALL cases in children and in approximately 33% of cases in adults. It is associated with an unfavourable prognosis.
- *t(12;21) (p13;q22)*: this translocation can be identified in up to 30% of children with ALL,making it the most frequent recurring cytogenetic molecular abnormality in pediatric ALL. It is rare in adults (i.e., it occurs in 1–3% of adults)[16]. The translocation involves TEL (ETV6), a transcription-regulating gene of the Ets family of transcription factors on 12p11, and AML1 on 21q22.94 The outcome of patients with a TEL-AML1 fusion is favorable in children with pre-B ALL, independent of age or leukocyte count at presentation. Its prognostic significance is undetermined in adults. Microarray-based gene expression studies have shown that TEL-AML1–rearranged ALLs represent a unique biologic subset of B-precursor ALL[13].
- Hyperdiploidy: this is defined as ALL cells with more than 50 chromosomes. Hyperdiploidy is a relatively favourable prognostic feature and is found in about 25% of all cases of paediatric ALL. Mutations in the receptor tyrosine kinase FLT3 were identified in approximately 20% of hyperdiploid ALL[17].

T-lineage ALL

Basic helix-loop-helix domain (bHLH), HOX, and other developmental genes.

Transcription factor genes are the preferred targets of chromosomal translocations in the acute T-cell leukemias. Notable examples include the bHLH genes MYC[18], TAL1(SCL)[19], and LYL1[20], which are essential for the development of other lineages such as erythroid cells (TAL1), but with the exception of MYC, they are not normally expressed in T-lymphoid cells. When rearranged near enhancers within the TCRβ-chain locus on chromosome 7, band q34, or the α/δ-chain locus on chromosome 14, band q11, these regulatory genes become active, and their protein products bind inappropriately to the promoter or enhancer elements of downstream target genes.

In addition to genes encoding bHLH proteins, additional classes of regulatory genes are rearranged near TCR loci, including those encoding the proteins LMO1 (formerly known as RBTN1 or TTG1) and LMO2 (formerly known as RBTN2 or TTG2) within the cysteine-rich LIM family[21]. Both LMO1 and LMO2 possess zinc-finger–like structures in their LIM domains but lack the DNA-binding domains common to other transcription factors in this family, suggesting that the LIM domain functions in protein-protein rather than protein-DNA interactions. The t(11;14)(p15;q11) and t(11;14)(p13;q11) are thought to affect similar T-cell developmental pathways by inducing ectopic expression of either LMO1 or LMO2.

HOX11, HOX11L2, and also major HOX genes complete the list of developmental genes that are inappropriately placed under the control of TCR loci. Located on chromosome 10, band q24[22], HOX11 encodes a homeodomain transcription factor that can bind DNA and transactivate specific target genes. Activation of HOX11 expression by chromosomal translocations, either the t(10;14)(q24;q11) or the t(7;10)(q35;q24), in developing T cells must interfere with normal regulatory cascades to promote malignant transformation. Interestingly, HOX11 expression by T-ALL blasts is associated with a favorable prognosis in children treated with modern intensive therapy, possibly because these leukemias have a

gene expression signature reflecting an arrest at the early cortical thymocyte stage with downregulation of anti-apoptotic proteins such as BCL2 and BCLXL[23]. In addition, the HOX11L2 gene, located at chromosome 5 band q35, has been found to be activated by translocation near the BCL11B locus as a result of the t(5;14)(q35;q32), or by fusion to the TCRδ locus as a result of the t(5;14)(q35;q11). More recently, a new recurrent translocation has been recognized that targets and dysregulates expression from the whole HOXA cluster[24]. Thus, this translocation mimics the global HOXA gene dysregulation characteristic of T-ALLs with MLL gene fusions.

Fusion genes in T-ALL.

Although most chromosomal translocations in T-ALL patients lead to inappropriate activation of structurally intact cellular proto-oncogenes such as MYC, TAL1, HOX11 or LMO2, some can produce fusion genes. MLL-ENL fusion results from the translocation t(11;19)(q23;p13), and is associated with acute myeloid leukemia, B-cell precursor ALL, and T-ALL. Strikingly, in one series, all 11 T-ALL patients with the MLL-ENL fusion became long-term survivors, suggesting that this rearrangement is associated with a good prognosis[25]. CALM-AF10 fusions were identified in 12 (9%) of 131 consecutive patients with T-ALL. Of note, all of the patients with CALM-AF10 fusions had either immature T-cell lymphoblasts that expressed no TCR genes or γ/δ-positive lymphoblasts. None of the patients with CALM-AF10 fusions expressed TCR α/β, suggesting that such fusions are restricted to the TCR δ lineage[26].

NOTCH1 gene mutations in T-ALL.

Very rare cases of T-ALL harbor chromosomal translocations that produce a truncated and activated form of NOTCH1, a gene that normally encodes a transmembrane receptor, that is involved in the regulation of normal T-cell development and may other tissues during

embryologic development. NOTCH-1 had previously been shown to be truncated and activated by a rare t(7;9) in T-cell ALL. Specific mutations in sequences encoding both the heterodimerization and PEST domains of NOTCH1 were identified in over 50% of primary patient T-cell ALL samples[27-30].

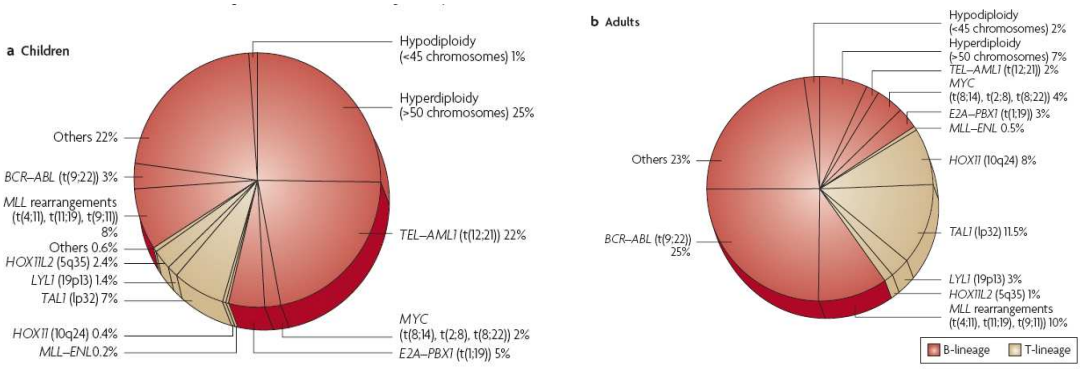

Figure 2. **Cytogenetic and molecular genetic abnormalities of childhood and adult acute lymphoblastic leukaemia (ALL)**. Data for childhood (a) and adult (b) acute lymphoblastic leukaemia. The genetic lesions that are exclusively observed in T-cell acute lymphoblastic leukaemia are illustrated in beige colour, and all other genetic subtypes are either exclusively or primarily observed in B-lineage ALL.

1.2 Molecular basis of the Philadelphia chromosome translocation

The Philadelphia (Ph) chromosome is observed in 95% of adult chronic myeloid leukaemia (CML), 15–20% of adult ALL, 3–5% of childhood ALL and very rarely in acute myeloid leukaemia[31,32]. It was the first specific genetic lesion identified in a human cancer and was subsequently shown to be t(9;22). The translocation creates a fusion of human homologue of the Abelson Murine leukaemia virus ABL on 9q34 with breakpoint cluster region BCR on 22q11. Immunophenotyping is pre-B (CD19+, CD10+), often asociated to the expression of myeloid markers (CD13+, CD33+).

1.2.1. Structure and functions of the Bcr and Abl proteins

The BCR and ABL genes are expressed ubiquitously.

Bcr is a 160-kd cytoplasmic protein with several functional domains. The N-terminal 426 amino acids of Bcr, encoded by the first exon, are retained in all Bcr-Abl fusion protein isoforms. This region contains a serine-threonine kinase domain, whose only known substrates are Bcr and Bap-1 (a member of the 14-3-3 family of proteins), and two serine/threonine–rich regions that bind Src homology (SH)2 domains. The proximal SH2-binding domain is essential for transformation of rat fibroblasts by Bcr-Abl[33]. The two key motifs of the first BCR exon are tyrosine 177 and the coiled-coil domain contained in amino acids 1 to 63. Phosphorylated tyrosine 177 forms a binding site for Grb-2 (an adapter molecule that links Bcr to the Ras pathway) and is required for the induction of myeloid leukemia [34]. The coiled-coil is crucial for dimerization of Bcr-Abl[35], which in turn is required for activation of Abl kinase activity and oncogenicity of Bcr-Abl. Bcr regions of exon 1 are not essential to oncogenicity but influence the specific phenotype of the leukaemia (Fig.3).

The **ABL** gene, the human homolog of v-abl (the oncogene of the Abelson murine leukemia virus), codes for a 145-kd nonreceptor tyrosine kinase. Two isoforms exist that differ in the

first exon (1a and 1b). Only Abl type 1b protein contains a myristoylation site and, therefore, can be anchored to the plasma membrane. Three domains located toward the N-terminus of Abl are named after their homology to the respective domains in Src, the prototype non-receptor tyrosine kinase. The SH1 domain carries the tyrosine kinase function, the SH2 domain binds phosphotyrosine-containing consensus sites, and the SH3 domain binds to proline-rich consensus sequences in proteins like Crk [36] and Crkl [37].Abl differs from Src in having a long (~90-kd) C-terminal region that contains actin-and DNA-binding domains[35], three nuclear localization signals, and one nuclear export signal. Another unique feature of Abl is the N-terminal ‘‘Cap’’ region that is critical to the regulation of kinase activity. Abl is expressed predominantly in the nucleus[38] but shuttles between nucleus and cytoplasm. The functions of the Abl protein are complex and include cell cycle inhibition, cellular responses to genotoxic stress[39], and signal transduction from growth factor receptors and from integrins[40] (Fig.3).

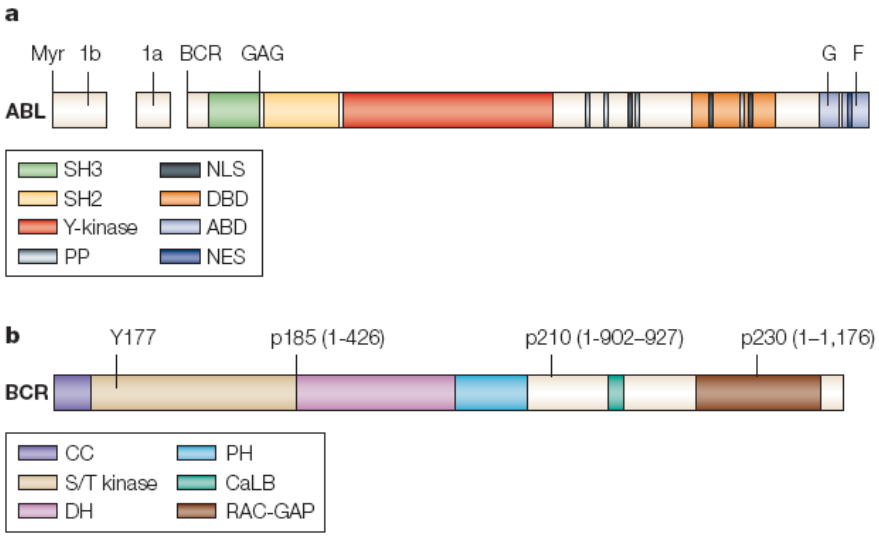

Figure 3. Schematic representation of the ABL (a) and BCR (b) proteins. There are several important domains that make up ABL and BCR proteins.

1.2.2. BCR-ABL fusion gene

Breakpoints in ABL

Breakpoints within the ABL gene can occur anywhere within a 50 segment that extends for over 300 kilobases (kb)[41]. Typically, breakpoints form within intronic sequences, most frequently between the two alternative first exons of ABL. Thus, BCR-ABL fusion genes may contain both exons 1b and 1a, exon 1a alone, or neither of the alternative first exons. BCR-ABL mRNA lacks exon 1, regardless of the structure of the fusion gene, with the transcript consisting of BCR exons fused directly to ABL exon a2.

Breakpoints in BCR

The breakpoints within the BCR gene on chromosome 22 are found within three defined regions. In 95% of patients with Chronic Myeloid Leukemia (CML) and approximately one third of patients with ALL, the BCR gene is truncated within a 5.8-kb region known as the major breakpoint cluster region. This region contains five exons, originally named b1 to b5, but now referred to as e12 to e16, according to their true positions in the gene. Most breakpoints form within introns immediately downstream of exon 13 (b2) or exon 14 (b3). Because processing of BCR-ABL mRNA results in the joining of BCR exons to ABL exon a2, hybrid transcripts are produced that have an e13a2 (b2a2) or an e14a2 (b3a2) junction. In both cases, the mRNA consists of an 8.5-kb sequence that encodes a 210-kd fusion protein, p210Bcr-Abl (Fig. 4). In two-thirds of patients with Ph-positive ALL and in rare cases of CML and acute myelogenous leukemia, the breakpoint in BCR occurs in a region upstream of the major breakpoint cluster region known as the minor breakpoint cluster region. This region consists of the 54.4-kb intron between the two alternative second exons of the BCR gene, e20 and e2. BCR-ABL fusion genes that have breakpoints within the minor breakpoint cluster region contain both BCR alternative first exons (e1 and e10)

together with the alternative second exon (e20). The hybrid mRNA consists of sequences that are approximately 7 kb in length in which exon e1 from BCR is joined to exon a2 of ABL. The translated product is a 190-kd fusion protein, p190Bcr-Abl (also referred to as p185Bcr-Abl). Interestingly, transcripts with an e1a2 junction are detectable at very low levels in patients with a major breakpoint cluster region rearrangement. The third defined breakpoint cluster region within the BCR gene was named ‘‘micro’’ breakpoint cluster region [42]. In this case, the breaks occur within a 30 segment of the BCR gene between exons e19 and e20 (known as c3 and c4 in the original nomenclature) (Fig. 4). Transcription of the hybrid gene yields an e19a2 BCRABL fusion transcript that encodes a 230-k protein, p230Bcr-Abl.

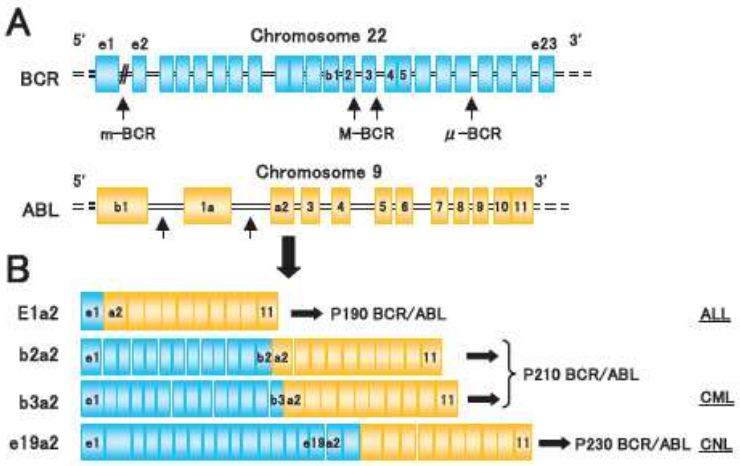

Figure 4. Three BCR-ABL variants and association of leukemia types. (A) Locations of the breakpoints in the ABL and BCR genes and (B) structure of the chimeric BCR-ABL mRNA transcripts derived from the various breaks. (C) Functional domains of P210 BCR-ABL.

1.2.3. Mechanisms of BCR-ABL-mediated leukaemogenesis

Tyrosine kinase enzymatic activity is central to cellular signaling and growth, and constitutively elevated kinase activity has been associated with transformation in several systems. The Abl protein is a non-receptor tyrosine kinase whose enzymatic activity is under close physiologic control[43]. In contrast, Bcr-Abl proteins are constitutively active tyrosine kinases. The degree of transforming activity of Bcr-Abl correlates with the degree of tyrosine kinase activity. p190Bcr-Abl, which has higher tyrosine kinase activity, is therefore associated with the development of the more aggressive acute leukemia phenotype, while p210Bcr-Abl plays a role in the more indolent chronic leukemia phenotype.

1.2.3.1 Altered cellular adhesion

In normal hematopoiesis, progenitor cells adhere to the stromal cells of the bone marrow and their associated extracellular matrix. The latter contains proteins such as fibronectin that function as adhesive ligands for receptors expressed on the surface of hematopoietic progenitor cells. Current thinking holds that the process of adhesion is essential for the regulation of hematopoiesis, providing a means of anchoring progenitors within the vicinity of cytokine-secreting cells [44], exposing them to specific signals that determine their fate. Ph-positive progenitors exhibit reduced adhesion to stromal cells and the extracellular matrix[45], which ‘‘liberates’’ them from the regulatory signals that are supplied to normal, adherent hematopoietic progenitors. It also may explain why their homing to the bone marrow is disturbed, leading to the appearance of immature cells in the peripheral blood. There is evidence that the function of β integrins on the surface of CML progenitor cells is perturbed, the net effect being reduced adhesion and increased proliferation[44]. In addition, migration, in response to certain chemokines such as MIP-1a, is abnormally high[46].

1.2.3.2 Activation of mitogenic signaling pathways

Bcr-Abl is known to activate several signaling pathways with mitogenic potential [47]. It is important to remember that in many cases, the available data comes from experiments in BCR-ABL–positive cell lines, and activation of some of these pathways in primary CML cells has yet to be verified.

Ras and the mitogen-activated protein kinase pathways

Bcr-Abl binds directly to proteins that activate Ras[48]. Autophosphorylation of tyrosine 177 generates a binding site for the adapter molecule Grb-2[33]. Grb- 2 associates with the Sos protein, which stimulates the conversion of the inactive GDP-bound form of Ras to the active GTP-bound state[48]. Ras also may be activated by two other adapter molecules, Shc and CrkL, which are substrates of Bcr-Abl[49]. Although CrkL appears to be necessary for the transformation of fibroblasts by Bcr-Abl, direct binding of Crkl to Bcr-Abl is not required for the transformation of myeloid cells. Activated Ras binds to the serinethreonine kinase Raf-1, recruiting it to the plasma membrane where it is activated by tyrosine phosphorylation and initiates a signaling cascade by way of the mitogen-activated protein kinase (MAPK) pathway. Grb-2 also recruits the scaffolding adapter Gab2, which then is phosphorylated by Bcr-Abl, resulting in activation of phosphatidylinositol 3 (PI-3) kinase/Akt and Ras/Erk[50]. Bcr-Abl activates different types of mitogen-activated protein kinases, including extracellular signal–related kinases (ERK)-1/2 and JNK or stress-activated protein kinase. Ultimately, these pathways regulate gene transcription.

Janus kinase–signal transducer and activator of transcription pathway.

Phosphorylation of members of the signal transducer and activator of transcription (STAT) family of transcription factors has been reported in BCRABL–positive cell lines[51] [104] and in primary CML cells. Physiologically, STATs are phosphorylated by Janus kinases (Jak)

that are downstream of growth factor receptors. In contrast, phosphorylation of STAT5 in Bcr-Abl–expressing myeloid cells appears to be mediated by the Src family kinase, Hck, which binds the SH2 and SH3 domains of Bcr-Abl[52]. There is evidence that activation of STAT5 by p210Bcr-Abl contributes to malignant transformation of K562 cells[53] and inhibits apoptosis by up-regulating the transcription of Bcl-xL[54]. STAT5, however, is not required for leukemia induction by Bcr-Abl in mice, casting doubt on its relevance in a more physiologic context. Interestingly, p190Bcr-Abl differs from p210Bcr-Abl in that it also is able to activate STAT6. It remains to be seen whether the predominantly lymphoblastic phenotype associated with p190Bcr-Abl is related to this property of the shorter form of the oncoprotein.

Phosphatidylinositol 3 kinase pathway.

Proliferation of BCR-ABL–positive cell lines and primary cells is dependent on PI-3 kinase. Bcr-Abl apparently activates this pathway by forming a multimeric complex with PI-3 kinase, p120Cbl, and the adaptor molecules Crk and CrkL. In BCR-ABL–expressing cells, activated PI-3 kinase stimulates the serine-threonine kinase Akt[55], which in turn phosphorylates the forkhead transcription factor, FKHRL1. The net result of activating this pathway appears to be the proteasome-mediated degradation of the key cell cycle inhibitor p27Kip1, although the precise intermediates are unknown. Activated Akt may function in an antiapoptotic capacity. A key substrate of Akt is the proapoptotic protein or ‘‘death agonist’’ Bad. Bad promotes cell death by binding to and thereby inactivating the antiapoptotic Bcl-2 and Bcl-xL. Thus, phosphorylation of Bad by Akt may prevent it from binding to these proteins, resulting in reduced apoptosis. Indeed, increased Bad phosphorylation was seen in BCR-ABL–positive cells; however, even with Bad completely dephosphorylated, a fraction of cells survived, indicating the existence of Bad-independent survival pathways.

Myc pathway.

Myc is classed as a proto-oncogene because it is overexpressed in many human malignancies. As a transcription factor and immediate early response gene, Myc converts mitogenic signals to alterations of gene expression. Not surprisingly, Myc targets include genes related to cell cycle and apoptosis. Within Bcr-Abl, the SH2 domain[56] and the C-terminus are required for full activation of Myc. It recently has been shown that Jak2 is involved in Myc induction by Bcr-Abl, apparently by way of induction of Myc mRNA and by stabilization of the protein.

1.2.3.3 Inhibition of apoptosis

Apoptosis caused by growth factor withdrawal is eliminated when factor dependent cell lines are transfected with exogenous BCR-ABL. The mechanisms by which Bcr-Abl inhibits apoptosis in cell lines are not well understood. The release of cytochrome C from mitochondria, a prerequisite for caspase-3 activation, apparently is blocked in BCR-ABL–expressing cell lines. Members of the Bcl-2 family of proteins may be involved in mediating the antiapoptotic effect of Bcr-Abl. Up-regulation of Bcl-2 by Bcr-Abl has been demonstrated in two different cellular contexts: one dependent on the Ras pathway and the other on the PI-3 kinase pathway. Bcl-2 targets Raf-1 to mitochondria where it inactivates the proapoptotic protein Bad by phosphorylating it on serine residues[57]. Down-regulation of interferon consensus sequence binding protein (ICSBP) by Bcr-Abl also has been implicated as an important antiapoptotic event; conversely, ICSBP antagonizes Bcr-Abl by decreasing Bcl-2 expression. Another regulator of apoptosis targeted by Bcr-Abl is Bcl-xL, the expression of which is dependent of STAT5 activation. Surprisingly, a recent report has demonstrated that Bcr-Abl can actively induce apoptosis when trapped in the nucleus[58]. Treatment of human and murine Bcr-Abl–positive cell lines with imatinib stimulated entry of the oncoprotein into the nucleus.

1.2.3.4 Proteasomal degradation

It recently was reported that Bcr-Abl tyrosine kinase activity induced the proteasome-mediated degradation of the Abl-interactor proteins Abi-1 and Abi-2[57]. Bcr-Abl was found to cause down-regulation of the DNA repair protein DNA-PKcs in cell lines. Loss of DNA-PKcs activity was correlated with impaired DNA repair and may facilitate the acquisition of additional genetic lesions that lead to disease progression. Another important degradation target is the cell p27, a crucial inhibitor of progression from the G1 to the S phase of the cell cycle. Furthermore, Bcr-Abl can stabilize the expression of Mdm2, a protein that targets the tumor suppressor p53 for ubiquitination, which also would promote genomic instability[59].

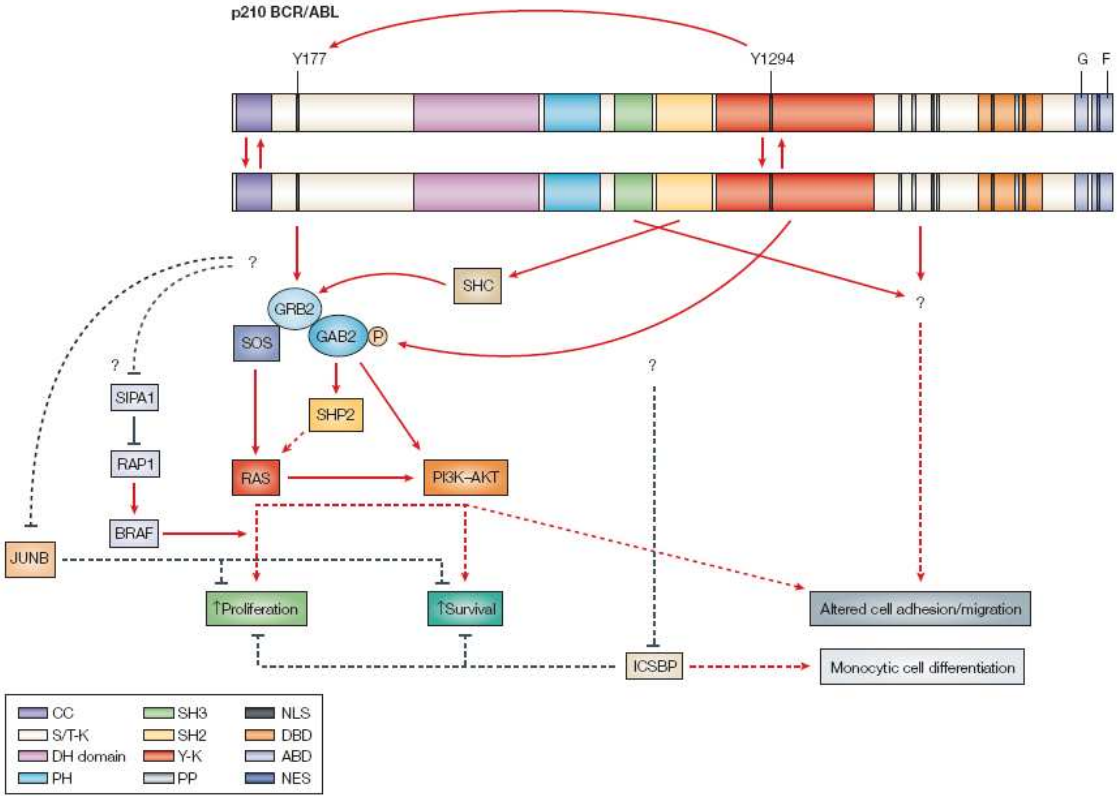

Figure 5. Leukaemogenic signalling of BCR–ABL. The BCR–ABL proteins can form dimers or tetramers through their CC domains, and trans-autophosphorylate (indicated by up and down arrows between protein structures). Phosphorylation at the Y177 residue generates a high-affinity binding site for growth factor receptor-bound protein 2 (GRB2). GRB2 binds to BCR–ABL through its SH2 domain and binds to SOS and GRB2-associated binding protein 2 (GAB2) through its SH3 domains. SOS in turn activates RAS. Following phosphorylation (P) by BCR–ABL, GAB2 recruits phosphatidylinositol 3-kinase (PI3K) and SHP2 proteins. The SH2 domain of ABL can bind SHC, which, following phosphorylation can also recruit GRB2. The ABL SH3 domain and the SH3 binding sites in the carboxy-terminal region can bind several proteins that involve regulations of cell adhesion/migration. Interferon consensus sequence binding protein (ICSBP), also known as interferon regulatory factor 8, negatively regulates proliferation and survival of myeloid cells by inducing differentiation of monocytic cells. JUNB inhibits cell proliferation and survival, partly by antagonizing the RAS downstream target JUN. SIPA1 (signal-induced proliferation-associated gene-1) is a RAP1 GAP that keeps RAP1 inactive. BCR–ABL can promote cell proliferation and survival partly by activating the RAS, SHP2 and PI3K–AKT signalling pathways. It can also downregulate transcription of ICSBP and JUNB, and might also inhibit SIPA1. Red arrows indicate direct interactions and/or activations. Black arrows indicate negative regulations. Broken arrows indicate multiple steps. ABD, actin-binding domain; CC, coiled-coil; DBD, DNA-binding domain; DH, Dbl/CDC24 guanine-nuleotide exchange factor homology; NES, nuclear exporting signal; NLS, nuclear localization signal; PP, proline-rich SH3 binding site; S/T-K, serine/threonine kinase; Y-K, tyrosine kinase.

1.3 The BCR-ABL1 Kinase Bypasses Selection for the Expression of a Pre–B Cell Receptor in Pre–B Acute Lymphoblastic Leukemia Cells

B-cell differentiation in adult bone marrow is a highly regulated process that requires a stepwise expression of particular cell surface markers and the sequential rearrangement of the genes encoding for the immunoglobulin light (IgL) chains. The transient expression on developing B-cell precursors of a functional pre-B cell receptor (pre-BCR) is the first checkpoint in B-cell development at the pro-B/pre-B transition stage. Signalling through the pre-BCR is required for allelic exclusion at the Ig heavy locus, down-regulation of the recombination machinery, cell proliferation, and differentiation to small post-mitotic pre-B cells that further undergo the rearrangement of the IgL chain genes. Structurally the pre-B-cell receptor is composed of Ig heavy (IgH) and surrogate light chains (SLC), which associate with the signaling molecules Igα and Igβ (Igα/β). In contrast to a conventional IgL chain in BCR, the SL chain is a heterodimer composed of two invariant polypeptides: an Ig V-like sequence called VpreB and an Ig C-like sequence called λ5 (Fig. 6). A critical component in the pre–B cell receptor signalling cascade is the adaptor molecule SLP65, which links SYK to downstream effector pathways, including PLCγ2 BTK, and VAV. Although somatic SLP65 deficiency is a frequent aberration in pre–B acute lymphoblastic leukaemia (ALL) in humans, SLP65-/- mutant mice exhibit a differentiation block at the pre–B cell stage, and also show autonomous proliferation, ongoing rearrangement of IgH V region genes, and development of leukaemia.

Comparing the gene expression pattern in BCR-ABL positive pre–B ALL and normal uman pre–B cells, many genes conferring B cell lineage commitment and signal transductionthrough the pre–B cell receptor were transcriptionally silenced in the leukemic cells (Fig 7). Loss of pre–B cell receptor–related molecules in the pre–B ALL cells involves nuclear transcription factors OBF1, PAX5, E2A, OCT2, EBF, and IRF4, cytoplasmic kinases and linker molecules (LYN, BLK, BTK, BRAG, SLP65, SYK, BAP37, IgαBP1,

BRDG1, PLCγ2, VAV1-3, HPK1, LCK, FYN, BAM32, AKT, SHC1, SAP, p62DOK, CIN85, NIK, and IKK), and membrane-associated receptor molecules (CD19, IGHμ, VpreB, Igα, and Igβ). Conversely, transcription factors related to primitive hematopoiesis, including AML1 and GATA1, are upregulated in the leukemia cells as compared with their normal counterpart. Also, signaling molecules related to NF-κB, JAK-STAT, GAB2, and GRB2 pathways are expressed in the leukemia cells at similar or higher levels than in pre–B cells. However, NF-κB activation and GAB2/GRB2 phosphorylation, together with expression of JAK and STAT proteins, reflect oncogenic BCR-ABL1 kinase activity or requirements for transformation by BCR-ABL1 rather than pre–B cell receptor signaling in the leukemia cells. These findings suggest that BCR-ABL1 expressing human pre-B ALL cells do not express a functional pre-B cell receptor in most of the cases. This is in striking contrast with selection processes during early B cell development, which impose the expression of a pre-B cell receptor. Presumably, the survival signals originating from the BCR-ABL1 kinase enable the pre-B ALL cells to bypass selection for the expression of a functionally rearranged Ig-μ heavy chain[60].

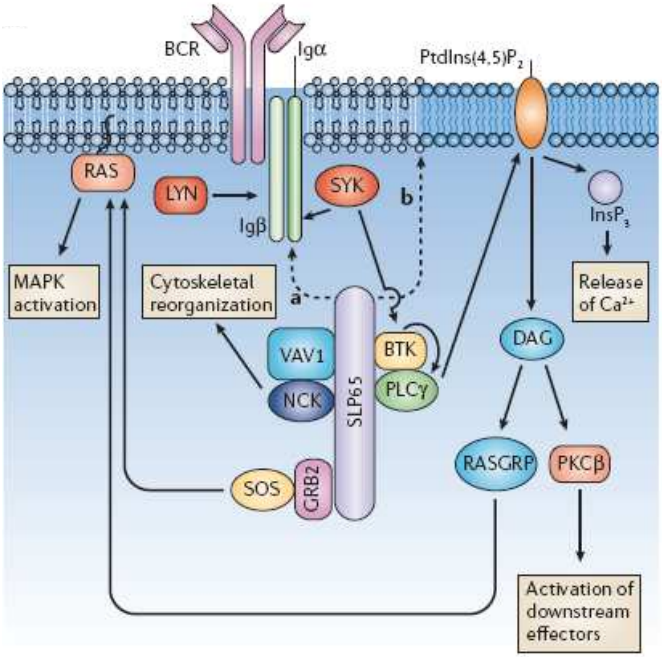

Figure 6. Role of SLP65 through the B-cell receptor. B-cell-receptor (BCR) activation results in the sequential activation of protein tyrosine kinases, which results in the formation of a signalling complex and activation of downstream pathways as shown.

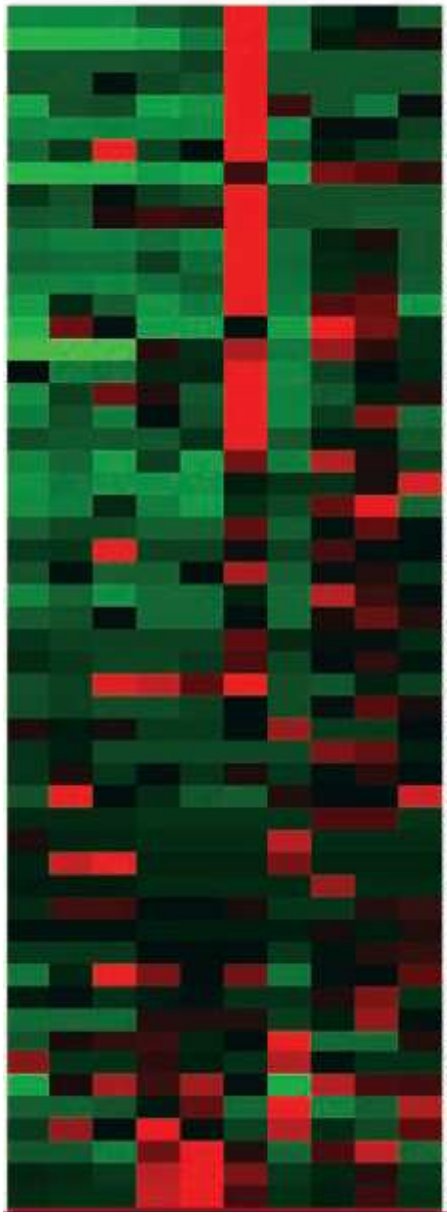

Name	Proposed function	Reference
CD19	co-ligation enhances BCR signals	Carter & Fearon, 1992
IGHCμ	IGH μ chain	Raff et al., 1976
VpreB	surrogate light chain	Kudo & Melchers, 1987
RAG2	V(D)J recombination	Schatz et al., 1989
LYN	attentuates BCR signaling	Yamanashi et al., 1991
BLK	recruits GRB2	Aoki et al., 1994
NFAT	activated by Vav2 upon BCR crosslinking	Doody et al., 2002
Igα	ITAM	Flaswinkel et al., 1995
RAG1	V(D)J recombination	Menetski & Gellert, 1990
TdT	generation of junctional diversity	Kung et al., 1975
BTK	PLCγ activation upon BCR crosslinking	Cheng et al., 1994
BRAG	enhances survival signals through BCR	Verkoczy et al., 2000
SLP65	links Syk to PLCγ2, GRB2, Vav and NCK	Fu et al., 1998
SYK	promotes BCR signaling	Kurosaki et al., 1994
CD45	antagonizes SHP1, CSK	Pani et al., 1997
Igβ	ITAM	Cassard et al., 1996
BAP37	IgM specific transmembrane signaling	Terashima et al., 1994
RHO p115	actin polymerisation upon BCR ligation	Moores et al., 2000
IgαBP1	signal transduction through Igα	Grupp et al., 1995
BRDG1	BCR-dependent activation of CREBP	Ohya et al., 1999
PLCγ2	part of downstream BCR signaling complex	Okazaki et al., 2001
VAV2	BCR signals synergistic with CD19	Doody et al., 2000
HPK1	augments BCR signaling through BLNK	Tsuji et al., 2001
PI3K p110	activates BTK	Okkenhaug et al., 2002
LCK	activated upon BCR ligation	Gold et al., 1994
FYN	reduction of BCR signaling in $FYN^{-/-}$ mice	Appleby et al., 1995
WIP	cytosceleton-associated activation signals	Anton et al., 2000
BAM32	higher Ca^{2+} upon BCR crosslinking	Niiro et al., 2002
AKT	promotes PI3K signals upon BCR ligation	Astoul et al., 1999
SHC1	Ras-activation upon BCR-crosslinking	Saxton et al., 1994
NF-κB2	reduction of BCR-signal threshold	Claudio et al., 2002
SAP	recruitment of SHIP or SHP2 to SLAM	Shlapatska et al., 2001
p62DOK	mediates ITIM-dependent BCR-inhibition	Tamir et al., 2000
CIN85	Inhibition of CBL	Beckwith et al., 1996
VAV1	B cell activation through BCR	Moores et al., 2000
IκBα	inhibits NF-κB activation upon BCR ligation	Petro et al., 2000
SHP2	links BCR to GRB2, activates RAS	Nakamura et al., 1998
CBL	recruits CBL	Wakioka et al., 1999
SIRPα1	SHP1 substrate	Cambier, 1997
SIT	inhibition of BCR by ITIM-dependent signals	Marie-Cardine et al., 1999
SLP76	Igα-downstream signaling in early B cells	Nagata et al., 1997
NIK	activates NF-κB by IκBα degradation	Claudio et al., 2002
VAV3	activation of PI3K, increased Ca^{2+} flux	Inabe et al., 2002
IKK	degradates IκBα upon activation by BTK	Petro et al., 2000
GAB1	amplifies BCR signaling via PI3 kinase	Ingham et al., 2001
REL	protects from BCR-mediated apoptosis	Chen et al., 2001
SHIP	ITIM-dependent inhibition of BCR signals	Ono et al., 1997
APS	recruits CBL	Wakioka et al., 1999
GRB2	interacts with SHC, activates Ras	Smit et al., 1994
CSK	inhibits BCR-signals together with p62DOK	Vuica et al., 1997
SHP1	antagonizes CD45	Pani et al., 1997
NF-κB	BCR-induced proliferation	Petro et al., 2000
GAB2	substrate of SHP2	Nishida et al., 1999
JAK3	required for pre-BCR signal transduction	Thomis et al., 1995

Figure 7. Expression of pre–B cell receptor–related molecules in BCR-ABL+ pre–B ALL cells (ALL, cases II and IX).

1.3.1. Defective splicing of SLP-65 transcripts

BCR-ABL1 kinase activity is linked to the expression of a truncated isoform of SH2 domain-containing leukocyte adaptor protein (SLP-65, also named BLNK or BASH), which may contribute to the compromised pre-BCR signaling. SLP-65 is the key effector for signaling downstream of the B-cell antigen receptor (BCR), it controls not only B lymphopoiesis and humoral immunity but also possesses a yet poorly defined tumor suppressor activity. Inhibition of BCR-ABL1 kinase activity by the specific inhibitor STI-571 (Imatinib mesylate, Gleevec) reconstituted selection of pre-B ALL cells expressing the pre-BCR, corrected the expression of SLP-65, and restored the capacity of the surviving cells to differentiate into IgM+ immature B cells[60]. Interestingly, defective SLP-65 expression may potentially cause the initiation of the secondary, mostly nonproductive Ig VH replacements, which would be consistent with the finding that interruption of basal IgM signaling in immature B cells, e.g., with the tyrosine kinase inhibitor herbimycin A or the PI3K inhibitor wortmannin, led to a strong induction of RAG expression. Analysis of a panel of childhood pre-B ALL samples revealed that 16 out of 34 had either complete loss or drastic reduction of SLP-65 expression. No genomic mutations in the SLP-65 locus were present, but SLP-65 transcripts contained alternative exons that introduced premature stop codons.

1.3.2 Truncated Btk splice variants

Btk signaling is not only critical for the induction of proliferation of pre-B cells, but also for cell survival, as it induces Bcl-xL expression and inhibits the pro-apoptotic effects of Fas ligation in mature B cells. Btk activation is initiated by transphosphorylation at position Y551 by Lyn or Syk kinase, which promotes the catalytic activity of Btk and subsequently results in its autophosphorylation at position Y223 in the SH3 domain[61]. BCR-ABL induces aberrant splicing of Btk, resulting in the presence of Btk-p52 (lack of exon 15, loss of

reading frame) and Btk-p62 (in frame deletions of exons 15 and 16) isoforms. Although c-Abl can phosphorylate Btk at position Y223 in the SH3 domain, BCRABL+ is unable to physically interact with full-length Btk. However, in BCR-ABL+ pre-B-ALL, the BCR-ABL1 fusion protein utilizes the expression of the truncated splice variant Btk-p52 as a linker molecule to constitutively phosphorylate full-length Btk and Btk-p52 at Y223 (Fig. 8). In this complex, full length Btk and Btk-p52 can bind to each other as a result of stable intermolecular interactions between the praline rich region within the Tec domain of one molecule and the SH3 domain of a second molecule. As a result, activated Btk provides signals that otherwise would be transmitted by the pre-BCR, such as activation of PLCγ1 and induction of Bcl-xL. Activation of Btk and PLCγ1 is independent of SLP-65 expression, which is defective in BCR-ABL+ ALL. The presence of BCR-ABL, full-length Btk, Btk-p52, and PLCγ1 is also required for autonomous Ca2+ oscillations in these ALL cells, as well as for phosphorylation and nuclear translocation of Stat5, which was previously shown to be a direct substrate of Btk.

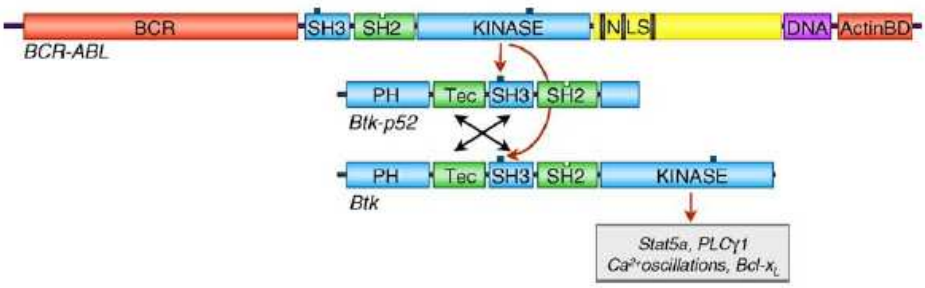

Figure 8. Model for BCR-ABL1-dependent activation of Btk in ALL. Truncated Btk-p52 acts as a linker, enabling BCR-ABL1 to phosphorylate full length Btk at position Y223 in the SH3 domain, which initiates the indicated downstream survival signals. Full length and Btk-p52 interact through association of proline-rich regions in the Tec-homology domain and the SH3 domain. PH: pleckstrin-homology domain, SH2,3: Src-homology domain-2 and -3; NLS: nuclear localization signal; DNA: DNA-binding domain; ActinBD: actin binding domain.

1.4 The role of the Ikaros gene in lymphocyte development and pre-B Ph+ ALL

Human leukaemia has been shown to be heterogeneous for the pattern of spliced isoforms of Ikaros (Ik1, Lyf-1, ZNFN1A1) proteins which are critical for the development of lymphocytes and other haematopoietic lineages[62,63].

1.4.1 Expression in the Hemo-Lymphoid Lineages

Ikaros is abundantly expressed in the day-8 yolk sac, the first site of extra-embryonic hemopoiesis. Subsequently, its mRNA is detected in the day-9.5 fetal liver primordium, a subsequent site of hemopoiesis in the embryo proper. At these sites, Ikaros is expressed in hemopoietic progenitors and in erythroid and myeloid precursors long before the appearance of fetal lymphocytes. Ikaros is expressed in the fetal thymus from the beginning of its colonization by hemopoietic progenitors that generate the fetal T lineages. High levels of Ikaros mRNA are detected in maturing thymocytes in the fetal as well as in the adult organ. It is also expressed in mature T and B lymphocytes and natural killer cells. Within hemopoietic progenitors, Ikaros is expressed in the Sca-1C/c-kitC population that is highly enriched for the pluripotent hematopoietic stem cells (HSC). It is equally expressed in multipotent progenitors with a strong erythro-myeloid (Sca-1−/c-kitC) and lymphoid (Sca-1C/ckitC/Sca-2C) potential. Although it is also expressed in erythroid and myeloid precursors, it is turned off in most of their terminally differentiated products. The highly restricted and complex pattern of Ikaros expression in embryonic, fetal, and adult hemopoietic sites qualifies this gene as a potential regulator of cell fate in the fetal and adult hemopoietic systems (Fig. 9).

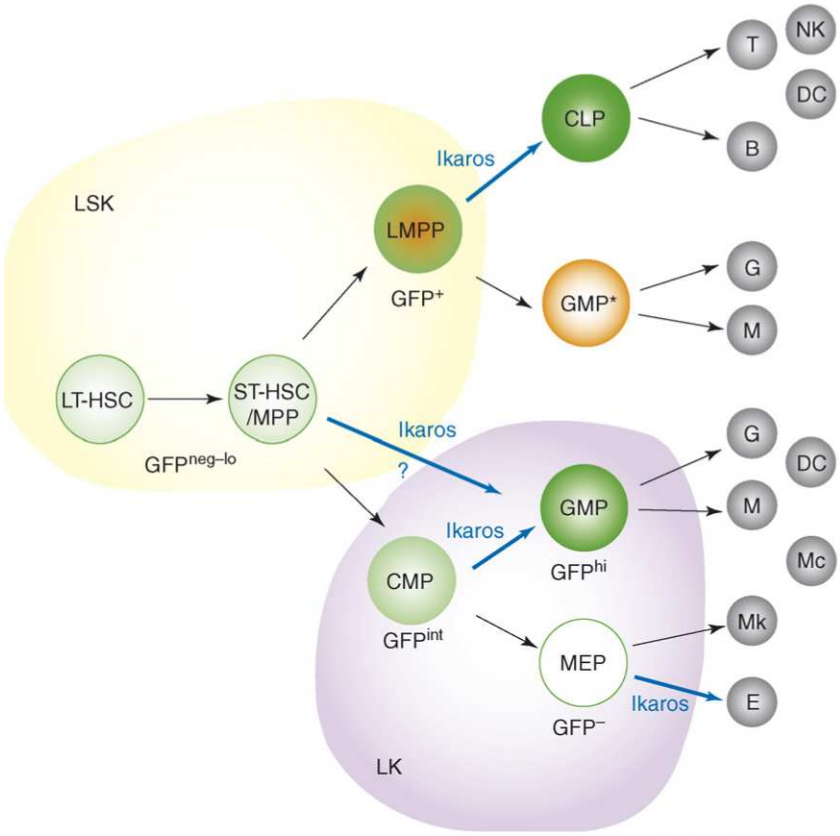

Figure 9. An Ikaros-centered view of hematopoiesis. Ikaros is important for the development of lymphoid at the expense of myeloid lineages starting in the LMPP. In the absence of Ikaros, an LMPP-mediated pathway of granulocyte macrophage progenitor development predominates. In addition, Ikaros is important for specification of the GMP at the expense of MEP in the CMP and for the development of erythrocyte progenitors at the expense of megakaryocyte progenitors from the MEP. The star indicates an alternative developmental pathway for GMPs.

1.4.2 Functionally Distinct Zinc Finger Domains Play a Pivotal Role in Ikaros Activity

Ikaros gene is comprised of eight exons, seven of which (2-8) are encoding[64]. By means of alternative splicing of exon 4-7, at least eight different isoforms were encoded (Fig. 10). All isoforms containing two C-terminal zinc fingers which mediate functionally indispensable protein-protein interactions between Ikaros family members whereas they differ in the number of N-terminal zinc finger motifs which dictate sequence specificity and DNA affinity. Only the isoforms with at least three out of four of the N-terminal zinc fingers are capable of binding to sites that contain the GGGA 8 base pair core motif. Therefore, the presence of functionally distinct combinations of zinc fingers in the Ikaros gene modulates the DNA binding potential of its protein products and, consequently, their effects in transcription. The formation of homo- and heterodimers among the DNA-binding isoforms increases their affinity for DNA, whereas the dominant-negative isoforms can dimerize with DNA-binding isoforms of Ikaros or with other members of Ikaros family such as Aiolos[65,66] and Helios [67], preventing the DNA binding of the formed dimer.

When bound to DNA through their cognate recognition sites, Ikaros protein complexes stimulate basal levels of transcription by means of a bipartite activation domain adjacent to the C-terminal zinc fingers and common to all of the Ikaros proteins. The Ikaros activation domain is comprised of two functionally distinct stretches of amino acids that are, respectively, acidic and hydrophobic in nature. The stretch of acidic amino acids activates transcription when tethered to a heterologous DNA binding domain, whereas the hydrophobic residues do not. These two subdomains, when put together, form a strong activation module. The role of the hydrophobic region may be to stabilize interactions that take place between the acidic amino acids and members of the basal transcription machinery, possibly by providing additional interaction interfaces. Such protein interactions between the two distinct components of the Ikaros activation domain may involve the same or distinct members of the holoenzyme complex. Alternatively, the hydrophobic amino

acids may control accessibility of the acidic region by influencing local protein structure. Interestingly, when the full-length Ikaros protein is tethered to a heterologous DNA binding domain, it displays a significantly weaker activation potential compared to its isolated bipartite activation module.

1.4.3 Phosphorylation Controls Ikaros's Ability To Negatively Regulate the G1-S Transition

Ikaros impedes the G1-S transition by modulating expression of genes that function as positive or negative effectors of the cell cycle (i.e., have a negative effect on cyclins and/or a positive effect on cell cycle inhibitors p27, p21, etc.). Ikaros may affect expression of some of these genes directly by binding to their transcriptional regulatory regions. In support of this model, mutations in the Ikaros DNA binding domain alleviate its ability to control the cell cycle. Under physiological conditions, Ikaros DNA binding activity is temporarily downmodulated through CKIIdependent phosphorylation of its C-terminal region that facilitates the G1-S transition. Mutations in Ikaros that abolish p1 phosphorylation eliminate this type of regulation on Ikaros DNA binding and block cells in G1. During the G1-S transition, Ikaros becomes phosphorylated in exon 8, an event that reduces its activity as a negative regulator of the G1-S transition and its DNA binding. In the M phase, Ikaros becomes phosphorylated at the zinc finger linker regions, which further reduces its DNA binding to possibly exclude it from mitotic chromosomes. The G1-S transition is a critical checkpoint in cell cycle regulation. The expression and activity of proteins involved in this transition are tightly regulated, and a failure to do so frequently results in cellular apoptosis or neoplastic transformation. Ikaros modifications may allow only lymphocytes that have received appropriate levels of signaling to enter the replicative phase of the cell cycle[68].

1.4.4 Ikaros has a dualistic role

The molecular function of Ikaros appears to be dualistic depending on whether it acts as a transcriptional activator or potentiator that enhances the activity of the promoter, or as a suppressor. For the latter, Ikaros associates with the nucleosome remodeling and deacetylation complex and has been considered as a factor to convert genes from active to inactive state. In support of this, Ikaros binds to its consensus sites in the regulatory elements of TdT and λ5 genes in vitro, and is important for the down-regulation of their activity in lymphocytes[69,70]. Ikaros recruitment to specific promoters causes the localized hypo-acetylation of core histones and repression; these effects are mediated through Ikaros association with histone deacetylases (HDACs) which have been proposed to interfere with the communication between activators, TBP and the PolII holoenzyme complex by exerting local changes in chromatin. A significant fraction of Ikaros protein is also associated with a Brg-1-based SWI/SNF complex implicated in mediating chromatin accessibility. The functional participation of Ikaros proteins in histone deacetylase complexes may provide a molecular mechanism to explain the development of lymphoid tumors in Ikaros mutant mice and possibly acute lymphoblastic leukemia. Deregulated recruitment of histone deacetylases has been observed in several leukemias. Ikaros isoforms which cannot bind DNA can still interact with mSin3 and HDAC proteins. Increased expression of these Ikaros isoforms in ALLpatients and mutant mice may result in the titration of HDAC into non-productive complexes which cannot participate in the normal molecular processes of transcription or replication. the lymphoid lineage-determining factors encoded by the Ikaros gene can repress basal transcription, through recruitment of histone deacetylases,whenbrought to promoters through heterologous DNA-binding factors. The difference in the ability of Ikaros to activate versus repress transcription appears to be determined by how it is recruited to a given promoter: when Ikaros binds DNA using its

own DNA binding-domain (DBD) it is able to activate transcription. However, when recruited via a heterologous DBD, Ikaros becomes a potent transcriptional repressor.

1.4.5 Over-expression of dominant-negative Ikaros isoforms

The fact that Ikaros functions as a critical regulator of normal lymphocyte development and the observation of rapid development of leukaemia in mice expressing non-DNA binding isoforms, prompted many studies to investigate whether normal Ikaros expression and function might be altered in human haematological malignancies. An excess of short Ikaros isoforms has been described in leukemic cells obtained from infant, children B and T acute lymphoblastic leukemias (ALLs)[71-74], in de novo adult B ALL[75], in cells from transformed chronic myeloid leukemias (CML)[76] and from de novo acute myelomonocytic and monocytic leukemias[77,78], demonstrating that aberrant regulation of splicing is a new mechanism of activation of an oncogene in ALL.

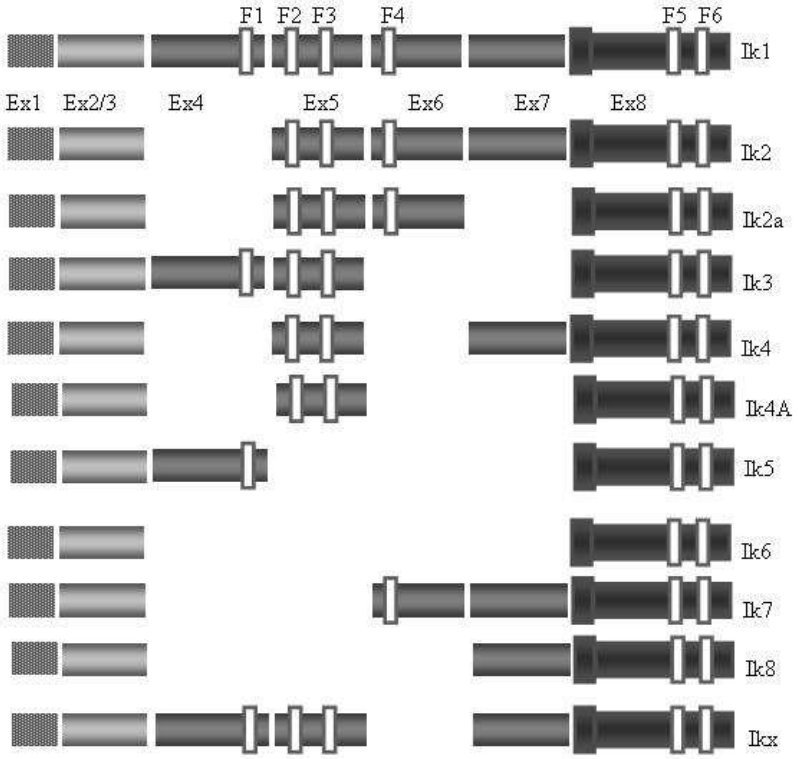

Figure 10. Schematic diagram of the full-lenght Ikaros cDNA and the different isoforms produced by alternative splicing; N-terminal zinc-fingers (F) show DNA-binding activity and C-terminal F mediate dimerization of the protein (Ex= exon).

1.5 Treatment of Ph-positive ALL

Significant advances in the treatment of Philadelephia chromosome ALL have been made since the discovery of the selective ABL tyrosine kinase inhibitors (TKIs). Optimal use of these novel agents in the treatment schema of Ph+ ALL will be paramount in ensuring continued success in the eradication of this disease.

1.5.1 Chemotherapy for Ph+ ALL in the Pre-Imatinib Era

Historically, prior to the advent of tyrosine kinase inhibitors (TKIs), outcome after chemotherapy for Ph+ ALL was dismal. Although the complete remission (CR) rates with conventional and intensive ALL regimens ranged from 60% to 90%, long-term disease-free survival (DFS) rates were less than 20% in the absence of allogeneic stem cell transplantation (SCT)[79]. Median survival ranged from 8 to 16 months owing to relapse-related mortality. Improved CR rates with the more intensive regimens did not translate into an increase in durability of response. The quality of the molecular response as measured by log reduction in the level of BCR-ABL transcripts after frontline chemotherapy correlated with outcome, even prior to the availability of TKIs. In a study using high-dose anthracycline chemotherapy, chemosensitive patients who achieved at least a 3-log reduction in BCR-ABL transcripts by quantitative real-time polymerase chain reaction (RT-PCR) after consolidation chemotherapy had 2-year DFS and overall survival rates of 27% and 48%, respectively, not dissimilar from the outcomes observed after allogeneic SCT in first CR[80]. None of the patients who had less than a 3-log reduction in BCRABL transcripts were alive at 2 years.

1.5.2 Allogeneic Stem Cell Transplantation for Ph+ ALL in the Pre-Imatinib Era

Given the dismal outcome with chemotherapy alone, allogeneic stem cell transplantation (SCT) was established as the only potential curative modality. However, allogeneic SCT

was often feasible only in younger patients without significant comorbidities and for whom a suitable donor was identified prior to disease recurrence, limiting the applicability of this approach. Although the long-term survival rates improved to 27% to 65% after allogeneic SCT in first CR, relapse remained the primary cause of failure, with persistent detection of BCRABL by RT-PCR heralding eventual recurrence[81-83]. In a retrospective review of 197 patients with Ph+ ALL who underwent allogeneic SCT, the 5-year survival rates were 34% for patients in first CR, 21% for those in second or subsequent CR, and 9% for those with active disease ($P < .0001$)[84].

1.5.3 Imatinib Mesylate in Previously Treated Ph+ ALL

The phenylaminopyrimidine compound imatinib mesylate (Gleevec/Glivec/STI571; Novartis) was among the first selective protein kinase inhibitors developed for targeted cancer therapy, and is highly effective against several tyrosine kinases such as Abl, c-kit and the platelet-derived growth factor receptor (PDGFR)[85]. Imatinib binds to the inactive moiety of Bcr-Abl while partially blocking the ATP binding site, preventing a conformational switch to the activated form of the oncoprotein (Fig 4). The activity of single-agent imatinib was initially investigated in patients with relapsed or refractory Ph+ ALL. A phase 1 clinical trial of imatinib at doses of 300 to 1000 mg daily led to a 70% hematologic response rate with a 20% CR rate. A phase 2 trial of intermediate-dose imatinib yielded a CR rate of 29%. Disease recurrence was usually observed within a median of 2 months, and responses were durable only in a minority of patients. Relapse in the central nervous system (CNS) was not uncommon, as imatinib concentrations in the cerebrospinal fluid only reach 1% to 2% of detectable serum levels, emphasizing the need for concurrent CNS prophylaxis[86].

1.5.4 Imatinib-Based Chemotherapy for de novo Ph+ ALL

Although monotherapy with imatinib demonstrated modest activity in the setting of recurrent or refractory disease, durability of responses was suboptimal. Imatinib was thus incorporated into combination chemotherapy regimens typically used for de novo Ph+ ALL, either concurrently (simultaneous imatinib and chemotherapy) or sequentially (alternating imatinib with chemotherapy). The first report of a clinical trial of this nature included 20 patients with de novo or minimally treated Ph+ ALL (no age restrictions)[87]; CR rate was 96%, with a 2-year DFS rate of 85%. Lee et al[88] also reported favorable outcomes after incorporating imatinib into a conventional L-asparaginase–based ALL regimen for newly diagnosed Ph+ ALL (up to age 67 years). In a subsequent report of outcome with imatinib-based frontline chemotherapy, two sequential cohorts of patients with de novo Ph+ ALL were treated according to German Multi-Centre Acute Lymphoblastic Leukemia (GMALL) protocols[89].

1.5.5 Allogeneic Stem Cell Transplant in the Imatinib Era

The role of allogeneic SCT for de novo Ph+ ALL in the imatinib era continues to be refined, with feasibility of this approach still limited by the availability of an appropriate donor, absence of significant comorbidities, and ability to sustain a complete remission. Several studies have reported an improvement in the rate of allogeneic SCT in first CR after imatinib-based therapy compared with the prior experience[90,91]. This success is in part related to (1) an increase in the proportion of sustained remissions, offering additional time for identification of a suitable donor, and to (2) an improvement in the quality of the remissions (e.g., lower levels of BCR-ABL transcripts after imatinib-based therapy), resulting in a lower pre transplantation tumor burden. Two of the early nonrandomized studies of imatinib-based chemotherapy for de novo Ph+ ALL applied allogeneic SCT in first CR as standard of care when feasible. Similar survival outcomes were observed with or

without allogeneic SCT, despite the selection biases favouring SCT. Post-allogeneic SCT maintenance strategies are also being explored, particularly as the detection of minimal residual disease (MRD) following SCT predicts imminent relapse in the absence of intervention.

1.6 Mechanisms of Resistance to Imatinib

Although high rates of complete remissions have been observed with imatinib in Ph+ ALL, a short duration of response with eventual emergence of resistance has also been observed. There are two possible categories of imatinib resistance: BCR-ABL independent and BCR-ABL dependent. In the first category, the leukemia cells no longer rely on BCR-ABL for their proliferative drive but grow as a consequence of the secondary oncogenic changes in these cells. Alternatively, something may change in either the patient or the leukemia clone that prevents the drug from effectively shutting down the target BCR-ABL enzyme. However, resistance to any particular drug is likely to be a multifactorial process. Imatinib is given orally and, like other oral medications, is therefore subject to variations in gastrointestinal absorption and first-pass metabolism, as well as: plasma-protein binding; cellular drug influx and drug efflux; enzymatic inactivation; changes in expression or mutations of the target molecule; defects in apoptosis, senescence, or repair mechanisms; and the development of alternative pathways of signal transduction.

1.6.1 Point Mutations

Bcr-Abl kinase domain mutations are at present the most extensively investigated and best characterized mechanism of resistance to imatinib, but nature of their origin is still not clear. They may emerge from drug-selection pressure or independently as a consequence of the genetic instability induced by BCR-ABL[92,93]. Mutation analysis has identified structural motifs that are critical for enzyme activity of Bcr-Abl, most importantly the adenosine triphosphate (ATP)–binding loop (p-loop) and the activation loop, a highly flexible structure that controls access of substrate and ATP to the catalytic site. Kinase activity is regulated by the phosphorylation of tyrosines within the activation loop. The crystal structure of the Abl KD in complex with an imatinib analogue and subsequently with imatinib itself was solved at high resolution (Fig. 11). Imatinib was found to penetrate deeply through the entire

catalytic cleft, burying a large surface area and engaging ≥ 19 amino acid residues in hydrogen bonds or van der Waals interactions. Unexpectedly, inhibitor binding was found to require a catalytically inactive kinase conformation with the activation loop in a “closed” position that precludes substrate binding. The aspartate of the DFG motif, which is highly conserved among kinases and binds the magnesium ion required to position the phosphate groups of ATP, was turned outward, preventing productive ATP binding. Therefore, rather than directly competing with ATP for binding to the active site, imatinib blocks kinase activity by stabilizing a unique inactive conformation of Abl. In contrast, imatinib cannot gain access to the activated conformation of Abl. More than 50 different point mutations encoding for distinct single amino acid substitutions in the BCR-ABL kinase domain have been identified in relapsed CML patients and Ph+ ALL. They were clustered in four regions: (1) the P-loop, a highly conserved region responsible for phosphate binding; (2) at 315, a non-conserved residue that is in part responsible for the selective inhibition of Abl by Imatinib; (3) M351 and E355, (4) mutations of the activation loop, resulting in an activated conformation of Abl insensitive to Imatinib. Kinase domain mutations could confer imatinib resistance by more about 3 mechanisms. For one, mutations affecting contact residues could abolish critical hydrogen bonds or cause a steric clash in the case of bulky substitutions in spatially confined areas. The prototype of this mutation type is T315I; it not only eliminates the hydrogen bond between the nitrogen of the pyridinyl ring of imatinib and the threonine side chain but also occurs in the “gatekeeper” position where large side chains are not tolerated. The second type of mutation leads to changes in the structure that prevent the conformational adjustments required for optimal imatinib binding. It is thought that this mechanism underlies the resistance caused by mutations in the p-loop that prevent the induced fit required to accommodate the pyridine ring of imatinib. The third type of mutation involves residues that are more remote from the imatinib binding surface. It is believed that this mutation type confers resistance by shifting the equilibrium between the

inactive and active Abl conformation toward the active state, from which imatinib is sterically excluded. Mutations in the activation loop and other domains involved in autoregulation of the kinase are thought to operate through this mechanism[94].

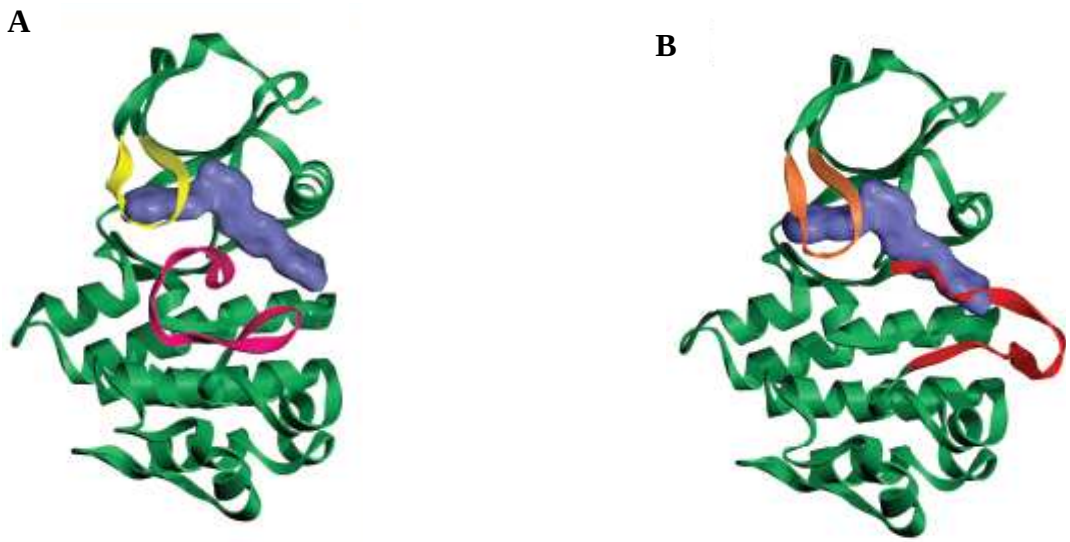

Figure 11.. (A) **Structure of Abl in its imatinib-sensitive, inactive conformation in complex with imatinib** (blue). In this conformation, the activation loop (magenta) occupies its closed position and does not interfere with imatinib binding. The distortion of the p-loop (yellow) relative to the active conformation might be induced by imatinib binding or might simply be a feature of the natural, autoinhibited state of the kinase. (B) **Placement of imatinib into the ATP-binding site of Abl kinase in its active conformation**, to which imatinib cannot bind. In this conformation, the phosphorylated activation loop (red) folds into the prospective imatinib-binding site and interferes with inhibitor binding.

1.6.2 BCR-ABL gene amplification

In a study by Mahon and co-workers[95], overexpression of BCR-ABL was shown to be the most frequent cause of resistance identified in cell lines that were engineered to develop resistance. The fact that this finding is not more frequent in clinical practice is surprising. Amplification of BCR-ABL was first reported in three of 11 patients with acquired resistance, and in one individual it coexisted with the presence of a point mutation in the ABL-kinase domain. Several case reports have since described clinical resistance to

imatinib in association with BCRABL amplification or multiple copies of the Ph chromosome, or both. However, in a large study of 66 patients with primary or acquired resistance to imatinib, only two patients showed BCR-ABL genomic amplification[96]. The chance of gene amplification is likely to be related to genetic instability and is thought to occur at a rate of 10^{-4} per cell division, whereas point mutations occur much less frequently at 10^{-9} per cell division. In practice, however, clinical resistance is much more likely to be due to a point mutation than to BCR-ABL amplification. One explanation for this could be that overexpression of BCR-ABL might itself be harmful to the cell. Cell lines that overexpressed BCR-ABL were noted to have a sudden loss of viability and decreased proliferation when imatinib was withdrawn. Additionally, cell lines that expressed varying amounts of BCR-ABL were noted to have dose dependent differences in growth-factor dependence, clonogenicity, and migration. Cells with high expression of BCR-ABL were much less sensitive to imatinib and, more importantly, took a substantially shorter time to produce a mutant subclone resistant to the inhibitor than cells with low expression levels.

1.6.3 Oral biovailability

Early studies on the pharmacokinetics of imatinib showed considerable interpatient variability in imatinib concentrations[97]. Oral bioavailability is established by gastrointestinal absorption and first-pass drug metabolism in the liver. Imatinib is largely neutralised by the cytochrome p450 isoenzyme 4A (CYP3A4). Variability in CYP3A4 concentrations between individuals, together with the potential for drug interactions, might explain, in part, the variability in imatinib concentrations. Picard and co-workers[98] assayed plasma imatinib trough concentrations in 68 patients who had been on treatment for at least 12 months and they confirmed wide variability. More importantly, mean trough concentrations were higher in patients with good responses (complete cytogenetic remission and major molecular

response) than in patients with less good outcomes, suggesting that drug concentrations should be measured in patients without optimum responses.

1.6.4 Alterations in intracellular availability of imatinib

In patients with wild-type Bcr-Abl other mechanisms of resistance have been suspected. It is now clear that blood and tissue concentrations of most drugs are influenced by inter-individual variations in genes encoding drug metabolizing enzymes (DMEs) and drug transporters. Cytochrome P450 enzymes (CYPs) are thought to have evolved as a protective adaptive response against environmental toxic effects. Imatinib is metabolized mainly by CYP3A4 and CYP3A5 isoforms, and to a lesser extent by CYP1A2, CYP2D6, CYP2C19[99]. Some imatinib metabolites have been shown to be produced by CYP1A1 and CYP1B1. Picard and co-workers[98] assayed plasma imatinib trough concentrations in 68 patients who had been on treatment for at least 12 months and they confirmed wide variability. More importantly, mean trough concentrations were higher in patients with good responses (complete cytogenetic remission and major molecular response) than in patients with less good outcomes, suggesting that drug concentrations should be measured in patients without optimum responses.

Imatinib transport into cells has been shown to be mediated by hOCT1 (human Organic Cation Transporter, isoform 1)[100], also known as SLC22A1 (Solute Carrier family 22, member 1). The OCT family mediates electrogenic and sodium-independent translocation of organic cations or weak bases, i.e., molecules with a transient or permanent positive net charge at physiological Ph, in both directions across the plasma membrane. The family comprises three members (hOCT1, hOCT2 and hOCT3 also known as EMT, Extraneural Monoamine Transporter) differing in tissue distribution and substrate specificity. Pre-imatinib hOCT1 expression levels have been demonstrated to be significantly lower in

patients who remain >65% Philadelphia-chromosome positive by cytogenetics during the first 10 months of imatinib treatment.

In contrast, imatinib efflux is thought to be mediated by ABC transporters ABCB1[100,101] (MDR1; P-glycoprotein) and ABCG2 (also known as also known as breast-cancer resistance protein, BCRP)[102,103]. Both ABCB1 and ABCG2 are expressed at the apical membrane of the small intestine and bile canalicular membranes, and gastrointestinal transport activity could affect oral drug bioavailability. Overexpression of the cell-surface transmembrane ATPase ABCB1 seemingly conferred insensitivity to many chemotherapeutic drugs by active (ie, energy-dependent) drug transport. The MDR-1 gene is commonly overexpressed in blast cells of patients in the advanced phase Ph+ leukemia. Mahon and colleagues[104] firstly reported the overexpression of ABCB1 as a possible mechanism for resistance to imatinib. They developed a resistant cell line, LAMA-84R, by gradual exposure to increasing concentrations of imatinib. Both BCR-ABL and ABCB1 were overexpressed compared with the sensitive parental cell line. The treatment with verapamil, a protein-pump inhibitor, restored imatinib sensitivity. Overexpression of ABCB1 in resistant cell lines has now been confirmed by other groups[105,106]. The role of ABCB1 in clinical resistance remain also unclear. A study of 33 patients on imatinib showed that those who did not achieve at least major cytogenetic remission showed overexpression of ABCB1, as did those who developed disease progression[106]. By contrast, Mahon and colleagues[104] were unable to identify ABCB1 overexpression in six patients in blast crisis after imatinib who did not have point mutations or BCR-ABL overexpression, although the addition of PSC833, an alternative pump inhibitor, increased the sensitivity of the primary cells, taken from these patients, to imatinib in a clonogenic assay. The relationship between imatinib and ABCG2 (BRCP), another efflux protein of the ATP binding cassette family, is, however, less clear, and the source of much controversy lately. At least 4 independent groups have investigated this issue, reaching somewhat different conclusions[99,102]. Thus,

Houghton et al[107] reported that imatinib is an inhibitor but not a substrate of ABCG2, whereas Burger et al[99] concluded otherwise when demonstrating that ABCG2-overexpressing cell lines are resistant to imatinib. Recently, Nakanishi et al[108] showed that the interaction between ABCG2 and imatinib in BCR-ABL–expressing cells is in fact rather complex, with ABCG2-mediated resistance to imatinib being counteracted by the inhibitor's capacity to down-modulate ABCG2 expression via the AKT-signaling pathway. Jordanides and colleagues suggested that imatinib is an inhibitor but not a substrate of ABCG2[102].

1.6.5 Overexpression of Src-family kinases

Another resistance mechanism could be the compensation of loss of BCR-ABL signalling by other tyrosine kinase-mediated pathways. Src-family kinases such as Lyn are involved in BCR-ABL-mediated leukemogenesis and have been found to be up regulated in cultured CML cells selected for imatinib resistance; increased Lyn expression was also found to correlate with clinical evidence of imatinib resistance in some patients, which highlights the potential clinical relevance of this resistance mechanism. Hu et al. reported that the expression of BCR-ABL in progenitors that harbour a genetic triple src-kinase knockout for fgr, lyn, and hck generate a CML phenotype, whereas wild-type progenitors develop into Ph+ lymphatic blasts[109]. This provides compelling evidence that src kinases are critical in the molecular pathogenesis of Ph+ ALL. In line with this, subsequent work demonstrated that inhibition of the src kinase Lyn is per se sufficient to kill Ph+ primary Ph+ ALL blasts. Moreover, simultaneous src kinase and BCR-ABL inhibition appears to be more effective in killing of Ph+ cells. The reason for this may be that src-kinases contribute not only as downstream targets of BCR-ABL, but also independently to the survival of the malignant clone and are thus capable to drive imatinib resistance. Indeed, when patients with Ph+ ALL or lymphatic blast crisis of CML are treated with dasatinib (an Abl/Src dual kinase inhibitor) the complete cytogenetic responses are in the range of 46–54% [110] and tended to

be higher than the frequency of responses seen with sole BCR-ABL inhibition using nilotinib in lymphatic blast crisis of CML in a phase I study (n = 1/9, 11%).The challenge for the future is to improve current clinical results with tyrosine kinase inhibitors in Ph+ leukemias, developing strategies that can eradicate residual disease and overcome or prevent resistance.

1.6.6 Loss of the tumor suppressor p14Arf is involved in imatinib resistance in Ph+ ALL

In Ph+ ALL pro B-cells have a self-renewing capacity. Recently, Williams and colleagues, have shown that loss of the tumor suppressor p14Arf is a cooperating event of BCR-ABL induced transformation in Ph+ ALL. The Arf tumor suppressor protects against the emergence of oncogene-induced cancers[111]. By antagonizing the p53-negative regulator Mdm2, the p19Arf protein induces a p53 transcriptional response that triggers either cell cycle arrest or apoptosis, thereby eliminating incipient tumor cells. Deletion or epigenetic silencing of Arf abrogates this form of tumor suppression and, not surprisingly, Arf inactivation is frequently observed in many forms of cancer[112]. Transduction of BCR-ABL into Arf-null pro-B-cells resulted in the evolution of a highly aggressive leukemia initiating cell population. Injection of very few BCR-ABL-transformed Arf−/− cells was sufficient to cause leukemia. In contrast, even large numbers of BCR-ABL transduced Arf+/+ pro-B-cells were incapable of causing leukemia, again demonstrating how decisively cooperating genetic factors control the biology of BCR-ABL. BCR-ABL-transformed Arf-null leukemias were insensitive to imatinib in vivo because interleukin-7 (IL-7)-induced Jak-Stat-5 signaling fully replaced BCR-ABL-dependence for growth and survival after inhibition with imatinib[112]. Deletion of the INK4A/ARF locus occurs in Ph+ ALL cases[72,113,114]; indeed, a recent survey of 21 pediatric and 22 adult cases has documented INK4A–ARF deletion in Ph+ ALL blasts taken from about 50% of patients at diagnosis.

This finding suggest that INK4A–ARF deletion might help leukemia-initiating cells survival and favour the emergence of drug resistant BCR-ABL variants (Fig. 12).

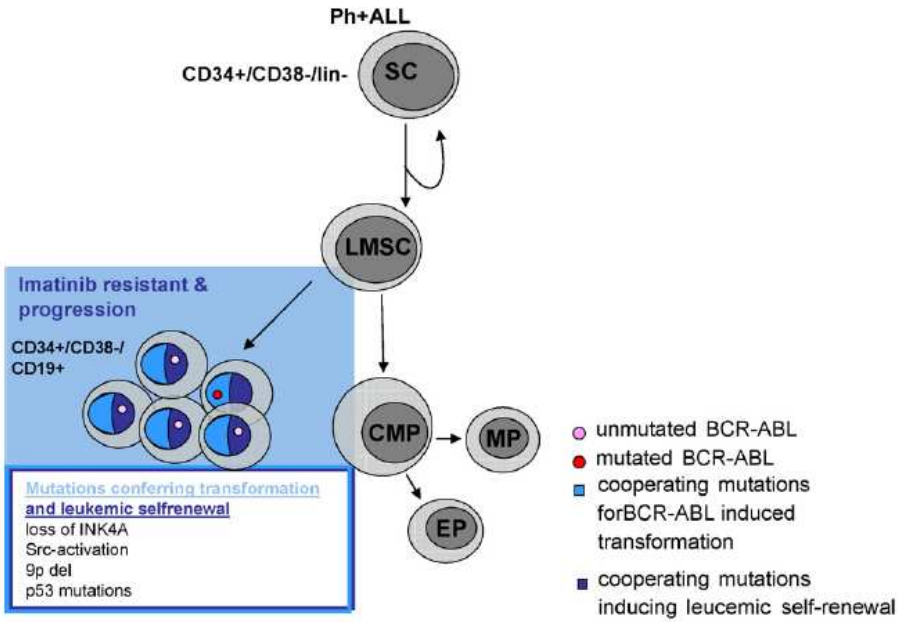

Figure 12. Proposed stem cell model of kinase inhibitor resistance in Ph+ ALL. The BCR-ABL chromosomal translocation targets a lymphatic precursor population (here: CD34+/CD38−/aberrantly CD19+) that normally has no self-renewal potential. BCR-ABL therefore requires cooperating mutations that promote transformation as well the capacity to self-renew. Imatinib cannot eradicate this population, because of the BCR-ABL-independence of leukemic self-renewal. BCR-ABL point mutations are genetic hits that are frequently detected in this population as a reflection of the substantial genetic instability, that also led to the manifestation of the disease. Abbreviations—SC: stem cell, LMSC: lymphomyeloid stem cell, CMP: common myeloid progenitor, MP: megakaryocytic progenitor, EP: erythroid progenitor, lin: lineage.

1.7 Newer Tyrosine Kinase Inhibitors for Imatinib-Resistant Ph+ ALL

The fact that imatinib resistance is usually associated with reactivation of Bcr-Abl signal transduction represents a therapeutic standpoint because there continues to be a uniform therapeutic target rather than a host of different escape mechanisms necessitating individualized therapeutic approaches. Options to restore Bcr-Abl inhibition in this situation include the design of Abl inhibitors that bind and inhibit ABL but are less affected by point mutations through their static conformation. Second-generation TKIs such as dasatinib (BMS-354825; SPRYCEL; Bristol-Myers Squibb, New York, NY) and nilotinib (AMN107, Novartis) are increasingly potent inhibitors of ABL. Several of the more recently developed multitargeted agents in ongoing clinical trials can also inhibit c-kit, PDGFR, FLT3, and other kinases with varying potency.

Dasatinib is a dual Src/Abl inhibitor with 325-fold more in vitro, and 30- to 50-fold more in vivo potency than imatinib against wild-type Bcr-Abl; it also inhibits the ckit, PDGFR, and ephrin A receptor kinases. Unlike imatinib, it binds to both the inactive and active forms of the Bcr-Abl protein. Dasatinib has demonstrated in vitro efficacy against all imatinib-resistant KD mutations tested, with the exception of T315I and F317L. In a phase I trial of dasatinib, a hematologic response rate of 80% was observed in 10 patients with imatinib-resistant Ph+ ALL. In a phase 2 program with START (Src/Abl Tyrosine Kinase Inhibition Activity: Research Trials of Dasatinib) using single-agent dasatinib 70 mg twice daily in 36 patients with imatinib-resistant Ph+ ALL, a CR rate of 33% was achieved. Responses were observed even with the presence of ABL KD mutations other than T3151. Based on the efficacy demonstrated in these and other trials, dasatinib was granted approval by the U.S. Food and Drug Administration for the treatment of all phases of CML and Ph+ ALL resistant or intolerant to imatinib. Adverse events associated with dasatinib were often amenable to dose modifications, and included myelosuppression, diarrhea and peripheral

edema. The unique toxicity of pleural effusions occurred in 5% to 20% of the patients, and has been attributed to dasatinib's potent inhibition of PDGFR. Although these effusions are amenable to dose interruptions and corticosteroids, in some patients the effusions recur with rechallenge despite dose reductions[110,115].

Nilotinib was developed by researchers at Novartis Pharmaceuticals using a rational drug design strategy based on the replacement of the metylpiperazinyl group of imatinib and optimization of drug-like properties. Like imatinib, nilotinib does not inhibit Src kinase and binds only to the inactive conformation of Bcr-Abl, with P-loop folding over the ATP-binding site, and the activation-loop blocking the substrate binding site, to disrupt the ATP-phosphate-binding site and inhibit the catalytic activity of the enzyme [116]. Nilotinib inhibits the catalytic activity of Bcr-Abl and most imatinib-resistant Bcr-Abl variants with 20- to 50-fold greater potency, compared with imatinib. The key exception is Bcr-AblT315I, which is cross resistant to nilotinib, imatinib, and dasatinib, as well as to dual combinations of these Abl kinase inhibitors. Several preclinical studies have established the bcr-abl mutations Y253H and E255V as the least nilotinib-resistant besides T315I, and the usefulness of nilotinib for treating patients with these p-loop mutations remains to be seen. Phase 1 and 2 clinical trials of nilotinib in imatinib-resistant Ph+ ALL demonstrate hematologic responses in 30% to 35% of the patients. Dose-dependent adverse events included myelosuppression, transient indirect hyperbilirubinemia, pruritis, and rash[117,118].

Development of third- or fourth-generation novel TKIs which target specific ABL KD mutations is now the focus of developmental therapeutics. Several of these agents have dual activity against the Src/ABL kinases, and are currently being investigated in clinical trials (e.g., bosutinib or SKI-60661,62 and INNO-40663). Differential selectivity for the other tyrosine kinases besides ABL, or lack thereof, as in the case of bosutinib (which does not

inhibit c-kit or PDGFR) may improve clinical outcome simply by altering the safety profile. The multi-targeted agent MK-0457 (previously VX-680), an inhibitor of the Aurora, FLT3, JAK2 and ABL kinases, is a promising agent with preliminary clinical activity against the T315I mutation, as it does not require interaction with threonine 315 for efficient binding. Several other agents are in preclinical stages of development: (1) dual specific Abl and Src kinase inhibitors such as AZD0502 and AP23464; (2) the ABL, Src, and PDGFR inhibitor ON012380 with activity in T315I mutated cell lines; and (3) pyrimidine Src/Abl inhibitors such as PD166326. Combination TKI therapy may prove of interest for further study as in vitro data suggest that nilotinib and/or dual Src/Abl inhibitors such as dasatinib or AP23464 further enhance the ability of imatinib to prevent autophosphorylation of wild-type Bcr-Abl.

2. AIMS

Pre-mRNA splicing is an important determinant of the protein repertoire in human cells but it is also a natural source of cancer-causing errors in gene expression and could contribute to the pathogenesis or resistance in leukemia. Human leukaemia has been shown to be heterogeneous for the pattern of spliced isoforms of Ikaros (Ik1, Lyf-1, ZNFN1A1) proteins which are critical for the development of lymphocytes and other haematopoietic lineages[62,63]. Mice that are heterozygous for a germline mutation which results in loss of critical DNA-binding zinc fingers of Ikaros develop a very aggressive form of lymphoblastic leukaemia, suggesting that Ikaros has an important leukaemia suppressor function[119]. Moreover, Ikaros has an important role in recruitment and centromere-associated silencing of potentially leukemogenic growth-regulatory genes[70]. The human Ikaros gene contains eight exons[64] that can, by alternative splicing, give rise to at least eight isoforms[120,121]. The isoforms differ in the number of N-terminal zinc finger motifs that bind DNA and contain the nuclear localization signals, resulting in members with and without DNA-binding properties. The fact that Ikaros functions as a critical regulator of normal lymphocyte development and the observation of rapid development of leukaemia in mice expressing non-DNA binding isoforms, prompted many studies to investigate whether normal Ikaros expression and function might be altered in human haematological malignancies. An excess of short Ikaros isoforms has been described in leukemic cells obtained from infant, children B and T acute lymphoblastic leukemias (ALLs)[71-74], in de novo adult B ALL[75], in cells from transformed chronic myeloid leukemias (CML)[76] and from de novo acute myelomonocytic and monocytic leukemias[77,78], demonstrating that aberrant regulation of splicing is a new mechanism of activation of an oncogene in ALL. In this study, we analyzed the differential expression pattern of Ikaros isoforms in Ph+ ALL patients treated with imatinib and dasatinib. Our aims were to:

- determine whether the Ikaros gene undergoes alternative splicing in Ph+ ALL;

- investigate if there were a correlation between the different Ikaros isoforms produced by alternative splicing and the BCR-ABL transcript levels;
- determine if molecular abnormalities involving the Ikaros gene could associate with the resistance to tyrosine kinase inhibitors (TKIs) in Ph+ ALL patients;
- investigate which mechanisms determine alternative splicing in Ikaros gene.

The latter point is particularly important because defects in pre-mRNA splicing can result from cis-acting mutations which can affect the use of constitutive splice sites (loss of gene expression due to aberrant splicing) or alternative splice sites (force expression of one of the alternative splicing patterns) or from trans-acting splicing mutations which can affect the function of the basal splicing machinery or factors that regulate alternative splicing. Mutations that affect the basal splicing machinery have the potential to affect splicing of all pre-mRNAs, whereas mutations that affect a regulator of alternative splicing will affect only the subset of pre-mRNAs that are targets of the regulator.

To identify cis-acting mutations in genes in which we have previously demonstrated spliced oncogenic isoforms, we will perform a genome sequence analysis of splice junctions exon regions in search of mutations. Generations of any cryptic splice site for any nucleotide variation will be assessed applied the RESCUE (relative enhancer and silencer classification by unanimous enrichment) approach.

3. PATIENTS AND METHODS

3.1 Patients and cell lines

Expression patterns of Ikaros isoforms were retrospectively studied in bone marrow and peripheral blood samples collected after informed consent from 46 adult patients with Ph-positive acute lymphoblastic leukaemia (ALL): 16 patients were treated with imatinib, 30 patients were treated with dasatinib both after imatinib failure (7 patients) and as front-line treatment (23 patients). The median age was 55 years (range, 18-76). Diagnosis of all ALL cases was made on the basis of morphologic, biochemical and immunologic features of the leukemic cells. In addition, the human lymphoblastoid SD-1, the human B cell precursor leukemia SUP-B15 and the human B-cell precursor leukaemia BV-173 cell lines were also included in the analysis. Human cell lines were obtained from DMSZ (DeutsheSammlung von Mikroorganismen und Zellkulturen GmbH, Braunschweig, Germany) and maintained in culture following the DMSZ recommendations. The cells were incubated at 37 °C in a humidified atmosphere flushed with 5% CO_2. Ph+ leukemic cells were treated with 10 μmol/l Imatinib (Novartis), 1 μmol/l Nilotinib (Novartis) and 1 μmol/l Dasatinib (Bristol Myers Squibb) for 18 hours.

3.2 RNA isolation and RT analysis

Mononuclear cells were separated by Ficoll-Hypaque density gradient centrifugation and samples stored at -190°C in RPMI 1640 with 20% FBS and 10% dimethylsulfoxid or in GTC (guanidine thiocyanate) at -80°C, as needed. Total cellular RNA was extracted from cells using the RNeasy total RNAisolation kit (Qiagen, Valencia, CA) according to the instructions of the manufacturer, and 1μg of the total RNA sample was used for cDNA synthesis with Moloney murine leukemia virus reverse transcriptase kit (Invitrogen, San Diego, CA) in the presence of 1mM dNTPs (Roche) and 5μM Random Hexamers (Perkin Elmer).

3.3 Ikaros transcript analysis

In order to set up a screening for Ikaros transcript variants, cDNA was amplified with two pairs of oligonucleotides, the forward primer of each couple conjugated with a fluorescent dye (fluorescein, excitation occurs at 494 nm and emission at 521) at its 5' end yielding amplicons A, B (Table 1). Polymerase chain reaction (PCR) was performed using 1 unit of AmpliTaq Gold DNA polymerase and a final concentration of 1.5 mM MgCl2, on a BIOMETRA Tpersonal thermal cycler set for an initial denaturation at 95°C for 5 min, 25-35 cycles with denaturation at 95°C for 30 s, annealing at 62°C for 30 s, extension at 72°C for 50 s, and a final cycle at 72°C for 10 min and at 60°C for 45 min to stabilize the fluorescence. 1µl of each amplicon was added to 9µl of Formaldehyde (Sigma-Aldrich) containing 0.2µl of GeneScan 500 (-250) LIZ size standard (Applied Biosystems) and loaded on the ABI Prism 3730 DNA Analyzer for automated capillary gel electrophoresis, and the results were plotted with the *AbiPrism GeneMapper v3.5* software (Applied Biosystems). RNA integrity was confirmed by PCR amplification of the GAPDH mRNA, which is expressed ubiquitously in human hematopoietic cells.

3.4 Cloning and Sequencing analyses

Nucleotide sequences of all the observed amplicons were validated by repeating the PCRs with 5'-unmodified primers and cloning the products into pcR2.1-TOPO vectors using the TOPO TA Cloning Kit and related protocol (Invitrogen, San Diego, CA). TOP10F' strain E. coli cells (Invitrogen, San Diego, CA) were employed as a host for transformation, and colonies containing the recombinant plasmids were screened by PCR with the primer pair for the appropriate amplicon and at the same conditions described previously. PCR product were purifed with QIAquick PCR purification kit (Qiagen, Hilden, Germany) and directly sequenced by using ABI PRISM 3730 automated DNA sequencer (Applied Biosystem,

Foster City, CA) and a Big Dye Terminator DNA sequencing kit (Applied Biosystem, Foster City, CA).

3.5 Genomic analysis

Genomic DNA was isolated using QIAamp DNA Blood Mini Kit (Qiagen). The genomic sequence surrounding the predominant splice donor and acceptor sites at the exon 2/3, exon 3/4, exon 7/8 splice junctions from leukemic patient samples and cell lines were performed in search of mutations.

To amplify the region surrounding the splice junction of Ikaros exons 2 and 3 we used for the 5' splice site a primer sense from exon 2 (F1) and an anti-sense primer (R1) on intronic region, position +608 counting from the first base of the interesting intron. For the 3' splice site we used a primer sense F2, position -703 to the end of the intron and a primer anti-sense R2 on exon 3. For the 3' splice site of the exon3/4 junction we used F3 (-601) and R3 on exon 4. To amplify the region surrounding the splice junction of Ikaros exons 7 and 8 we used for the 5' splice site a primer sense F4 on exon 7 and R4 (+ 563); The 3' splice site was tested using the intronic primer F5 (-689) and R5 on exon 8. PCR was performed using 100 ng of genomic DNA in a 50-µL reaction volume using 5 µL cDNA, 5 µL Amplitaq Buffer II (Applied Biosystems, 10x), 5 µL Amplitaq MgCl2 (Applied Biosystems, 25mM), 1 µL dNTP Mix (Amersham Pharmacia, 2.5mM), 25 pmol of each primer, 0,5 µL of the AmpliTtaq Gold^{TM} (Applied Byosystem 5U/µL) and distilled water. The long-range PCR cycling parameters were as follows: 95°C for 5 minutes (complete denaturation), which is followed by 30 cycles at 95°C for 30seconds, 61°C for 30 seconds, extension at 72°C for 70 seconds, with an additional extension at the end of 7 minutes (for F1-R1 and F4-R4); 95°C for 5 minutes (complete denaturation), which is followed by 35 cycles at 95°C for 30seconds, 57°C for 30 seconds, extension at 72°C for 80 seconds, with an additional extension at the end of 7 minutes (for F2-R2, F3-R3, F5-R5). Generations of any cryptic

splice site for any nucleotide variation was assessed applied the RESCUE[13] (relative enhancer and silencer classification by unanimous enrichment) approach. RESCUE-ESE[122,123] (exonic splicing enhancer) approach was used to predict whether exonic mutations disrupt putative exon splicing enhancers (http://genes.mit.edu/burgelab/rescue-ese/), whereas RESCUE-ISE[13] (intronic splicing enhancer) was applied to predict which intronic motifs may enhance or repress exon splicing (http://genes.mit.edu/acescan2/index.html). RESCUE-ESE identifies ESEs in human genomic sequences by searching for hexanucleotides that satisfy the following two criteria: (i) they are significantly enriched in human exons relative to introns, and (ii) they are significantly more frequent in exons with weak (non-consensus) splice sites than in exons with strong (consensus) splice sites. RESCUE-ISE predicts as ISEs hexamers that share two properties: (i) significant enrichment in introns relative to exons and (ii) significant enrichment in introns with weak (non consensus) 5'ss or 3'ss relative to intron with strong splice sites.

3.6 Western Blot analysis

Cells were lysed with sample buffer (2%SDS in 125 mM Tris HCL, pH 6.8). Cell lysates were subjected to SDS-PAGE on 12% gels and then transferred to nitrocellulose membranes (Amersham Biosciences). The blots were incubated for 60 min in Odyssey blocking buffer before incubation overnight (4°C) with polyclonal anti-Ikaros antibody (Santa Cruz). Blotted proteins were detected and quantified using the Odyssey infrared imaging system LI-COR.

3.7 Subcellular Localization Studies Using Confocal Laser Scanning Microscopy

The subcellular localization of Ikaros protein(s) was examined by immunofluorescence and confocal laser scanning microscopy. Cytospins were prepared using SD-1 and BV-173 cell

lines and leukemic cell from patients with Ph+ ALL. Cytospins were fixed with 4% paraformaldeyde and permeabilized with 0,1% Triton X-100 for 3 minutes. Cells were blocked with a solution containing: 2% Fetal Calf Serum, 2% Bovine Serum Albumin, 0.2% Fish Skin Gelatin Solution, PBS 10X for 45 minutes at room temperature. Cells were then stained with a rabbit polyclonal antibody against Ikaros (Santa Cruz Biotechnology) for 2 hrs at room temperature and washed 3 times with PBS for 3 minutes. The antibody-antigen complexes were detected by incubation for 30 minutes with a secondary goat anti rabbit Alexa Fluor 488 immunoglobulin G antibodies (1:1000, Molecular probes). Cells were washed in PBS for 5 minutes and treated with propidium iodide for 5 minutes to stain the nucleus. Cover slips were mounted with Mowiol and the cells were subsequently analyzed with Leica Gmbh fluorescence microscope using Qfluoro software (Leica Microsystem). Representative digital images were processed using the Photoshop Software (Adobe Systems).

3.8 DNA-binding assay: EMSA (Electrophoretic mobility shift assay)

The Ikaros consensus and mutant sequences (32P-labeled probe sense: 5'-GTTTCTTCAGAGCCTGGGAAACAAGTC-3, containing a known high-affinity Ikaros-binding site, underlined, and 32P-labeled probe antisense:5'-ATTCTGACTTGTTTCCCAGGCTCGAA-3') were obtained from Sigma Genosys and labeled with T4 polynucleotide kinase (LifeTechnologies, Gaithersburg, MD) and [32P]-ATP (NEN, Boston, MA) and purified over aSephadex G25 (Pharmacia Biotech) column. 40 μg of protein nuclear extracts (obtained from IK2 and IK6 patients) were incubated with 2 mg poly d(I-C) (Roche Molecular Biochemicals, Indianapolis, IN) and 10214 mol 32P-labeled probe in 10 mM HEPES, 5 mM Tris, 50 mM KCl, 1.2 mM EDTA, and 10% (vol/vol) glycerol (pH7.8) for 30 minutes at room temperature. A 200-fold molar excess of unlabeled oligonucleotide (Ikaros consensus or mutant) was added for competition assays.

Protein/DNA complexes were resolved on 6% native polyacrylamide gels in 0.25 3 TBE (25 mM Tris, 22.5 mM boric acid, and 0.25 mM EDTA). Gels were visualized by autoradiography using MS-BioMax film and intensifying screens (Kodak, Rochester, NY).

3.9 Monitoring of BCR-ABL transcript levels

BCR-ABL transcript levels were detected at diagnosis and during the follow-up by a standardized real time quantitative PCR (RQ-PCR) method that was established within the framework of the EU Concerted Action[124]. The method independently measures, in each sample by RQ-PCR, the copy number of mRNA encoding for the p210 BCR-ABL protein or the p190 BCR-ABL protein and for a control gene (ABL) to verify sample-to-sample RNA quality variations. RQ-PCR was performed on an ABI PRISM 7700 Sequence Detector (Perkin Elmer, Foster City, CA). The quantification principles and procedure using the TaqMan probe have been previously described.15 All real time RT-PCR experiments were performed in duplicate. The copy number of BCR-ABL and ABL transcripts was derived by the interpolation of threshold cycle (ct) values to the appropriate standard curve, and the result, for each sample, was expressed as a ratio of BCR-ABL mRNA copies to ABL mRNA copies per cent. The threshold was systematically set at 0.1 in order to avoid any particular problems of baseline creeping. The lowest level of detectability of the method is 0.001.

3.10 Construction of pcDNA-Ik6 expression vector

The complete Ik6 coding sequence was PCR amplified; PCR products were isolated from agarose gel, purified using a Spin Column Kit (Qiagen, Valencia, CA) and restricted with EcoRI and Xba. The restricted fragment was cloned into the pcDNA3.1 expression vector (Invitrogen Ltd, Paisley UK) treated with EcoRI and Xba. The recombinant plasmid carrying the Ik6 gene was transfected into Escherichia coli DH5-αstrain and growth in LB

(Luria Bertani) medium supplemented with ampicillin 100 μg/ml, over night at 37° C . Preparation of plasmid DNA was performed using the QiafilterTM Plasmid Maxi Kit (Qiagen) according to the manufacturer's instructions.

3.11 Transfection with pcDNA-Ik6

For transfection, $1X10^6$ SUP-B15 cells were collected on Day 2, PBS washed and resuspended in 1ml serum-free medium. Cells were transiently transfected with 16 μg pcDNA-IK6 using the geneJammer (Invitrogen) mediated DNA transfection technique, following the manufacturer's instructions. In addition, a GFP empty vector (16 μg pEGFP) was used as internal control. GFP expression was detected within 48 h after transfection using a fluorescent microscope (Qfluoro Software, Leica Microsystem).

3.12 Apoptosis assay

Apoptosis was evaluated by flow cytometry for the detection of annexin V positive cells. Transfected and treated cells were were labeled with annexin V conjugated with fluorescein isothiocyanate and propidium iodide. Briefly, cells were washed once in PBS and once in 1x binding buffer, then 5 μL each of annexin V-FITC and propidium iodide was added to the cells. Cells were incubated at room temperature for 15 minutes, after which 300 μl 1x binding buffer was added and cells were analyzed by flow cytometry. Apoptotic cells were defined as annexin V positive and propidium iodide negative.

3.13 Proliferation assay by incorporation of 3H timidine

Cells are seeded at 10 X 104 concentration in RPMI added with 10% FBS for 18 hrs and then starved. After 12 hrs 10% FBS is added. After 6 hrs 1 μCi/ml of 3H timidine is added (Amersham Bioscences, Piscataway, NJ). After 24 of incubation hrs 3H timidine is removed. Cells are then washed with PBS and 5% Tricloric Acetic Acid and re-suspended

with NaOH. The amount of incorporated 3H timidine is detected by β counter.

3.14 Clonogenic assay or colony formation assay

$5x10^5$ cells were plated in methylcellulose (Methocult 4230, Stem Cell Technologies) supplemented with 10ng/ml G-CSF, 10ng/ml GM-CSF, 10ng/ml IL3, 300U/ml EPO. Cells were plated in 35 mm Petri dishes and for each sample were prepared 4 dishes. Cells were maintained at 37°C in a fully humidified incubator with 5% CO2 for 14 days. The growth of hematopietic colonies was assessed by count at optic microscopy.

3.15 Definitions

Hematologic complete remission (HCR) was defined as: bone marrow (BM) cellularity of at least 20% and containing less than 5% blast cells; peripheral blood (PB) smears without blasts; no evidence of extramedullary involvement from leukaemia; polymorphonuclear (PMN) cells >1.5 x 109/L and platelets >100 x 109/L. Cytogenetic response (CgR) was classified in complete (CCgR, 0% Ph+ metaphases), partial (PCgR, 1-35% Ph+ metaphases), minor (MCgR, 36-94% Ph+ metaphases), and none or minimal response (NCgR, >95% abnormal metaphases). Hematologic relapse was defined as the re-appearance of >5% BM blasts or in PB in HCR patients confirmed with a second BM aspirate one week after the first one. Cytogenetic response was defined whenever a complete or a partial CgR were lost to minor or minimal/none.

3.16 Statistical analysis

To estimate whether the difference in the level of BCR-ABL transcript was statistically significant between different patient groups we performed nonparametric Mann-Whitney test and $p<0.05$ was considered statistically significant. Comparison of frequencies were made with the $\chi 2$ test or the Fisher's exact test, as appropriate. All statistical calculations

and graphs were performed using GraphPad Prism 4 (GraphPad Software, Inc.., San Diego, CA, USA).

Table 1 A. - PCR primers used for Ikaros transcript analysis

Amplicon	Primer name	Sequence (5'→ 3')	Position
A	Ikaros F_A, Fluorescein-conjugated	ATGGATGCTGATGAGGGTCAAGAC	exon 2
	Ikaros R_A	GATGGCTTGGTCCATCACGTGG	exon 8
B	Ikaros F_B, Fluorescein-conjugated	GGGGCTGATGACTTTAGGGATTTC	insertion
	Ikaros R_B	GATGGCTTGGTCCATCACGTGG	exon 8

Table 2 A. - PCR primers used for genomic analysis.

F1: 5'-ATGGATGCTGATGAGGGTCAAGAC-3'

R1: 5'-gccagtccaacaaaaccgcac-3'

F2: 5'-ctctaagcagaatacctggtg-3'

R2: 5'-CTCATCTGGAGTATCGCTTAC-3'

F3: 5'-cggaaatctgaaagggaactg-3'

R3: 5'-GATGAAGAGAATGGGCGTGC-3'

F4: 5'-CGTGCTGGACAGACTAGCAAG-3'

R4: 5'-ctaggagcattgcccagagtag-3'

F5: 5'-cgggcctgccaactacagag-3'

R5: 5'-TCCCACGTGATGGACCAAGCCATC-3'

4. RESULTS

4.1 Adult Ph+ ALL patients express different wild-type Ikaros transcript variants

The expression of Ikaros was detected in all patients and the majority of them expressed different Ikaros variants at the same time (Table 1 and Fig. 1A). In 19/46 (41%) Ph+ ALL patients valuable at diagnosis we identified by fluorescent RT-PCR a single peak of 255 bp which by cloning and subsequent sequencing we found to be corresponded to Ik6 isoform in which the exon 3 is juxtaposed to exon 8. Since this isoform lacks all zinc fingers needed to bind the DNA of target genes, it is considered to be not functional. In the remaining patients (27/46, 59%) we observed the coexistence in the same PCR sample and at the same time of many fragments ranging from more than 900 bp to less than 200 bp (Fig.1B and 1C). In addition to already identified Ik6 isoform in these patients cloning and subsequent sequencing analysis revealed that the longer PCR product was Ik-1, the full-length isoform containing all the exons (945 bp). The fragment of 684 bp was identified as Ik2 isoform which shares three of the four N-terminal zinc fingers (F2, F3 and F4), whereas the band of 558 bp corresponded to Ik4 isoform in which exon 3 and exon 5 are lost. Other spliced Ikaros isoforms were identified: Ik4A containing the exons 1, 2, 3, 5 and 8; Ik 8 in which the exons 4, 5 and 6 lack; a new isoform which we called Ik5A, containing the exons 1, 2, 3, 4, 6 and 8; furthermore we identified a new small Ikaros isoform containing just two exons: 2 and 8 (Ik 6Δ). Since patients can express different Ikaros isoforms at the same time, our aim was to determine whether some isoforms could be overexpressed and favoured by alternative splicing. We set up a fast, high-throughput method, derived from microsatellite analysis and based on capillary electrophoresis technology, to detect and quantify splice variants. Since the peak heights showed in the electrophoretograms are correlated to the quantity of amplified PCR product, we used them as an indicator of the relative expression of each Ikaros isoform in a sample. As shown in Figure 3A, in the samples which showed the co-expression of more than one Ikaros variants, the isoforms more frequently produced by alternative splicing were Ik2 (median value 19%, SD 5.14), Ik4 (median value 16%, SD

8.46), Ik6 (median value 21%, SD 10.45) and Ik8 (median value 11%, SD 3.75) (Figure 3A). Other isoforms were observed with a minor expression: Ik4A (median value 7%, SD 2.75), Ik5A (median value 9%, SD 3.22) and Ik6Δ (median value 6%, SD 5.48). In comparison, in normal bone marrow pre-B cells we observed that the major Ikaros isoforms expressed were: Ik2 (median value 23%, SD 3.15), Ik4 (median value 20%, SD 5.20) and Ik8 (median value 9%, SD 4.55). Ik6 expression was observed with a minor expression (median value 6%, SD 6.84), such as Ik5A (median value 8%, SD 2.85), Ik4A (median value 7%, SD 2.95) and Ik5 (median value 2%, SD 3.05).

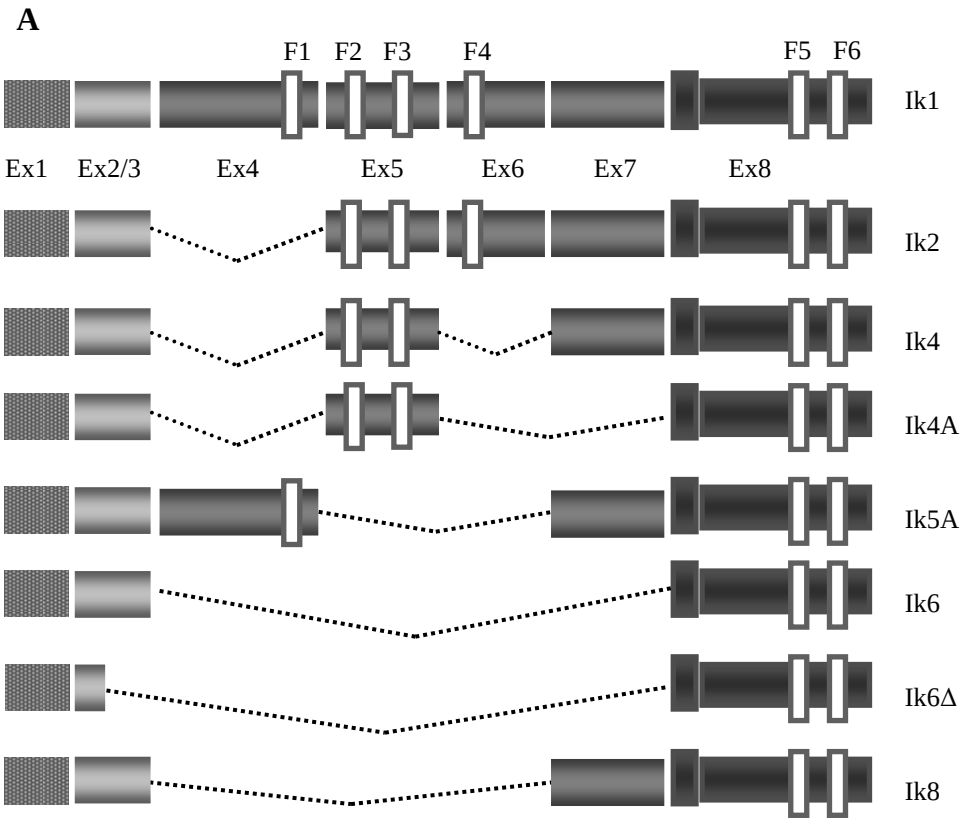

B

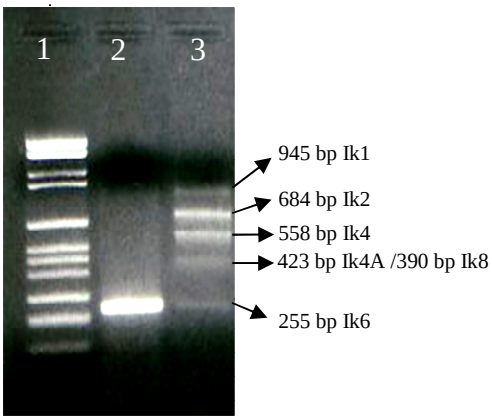

C

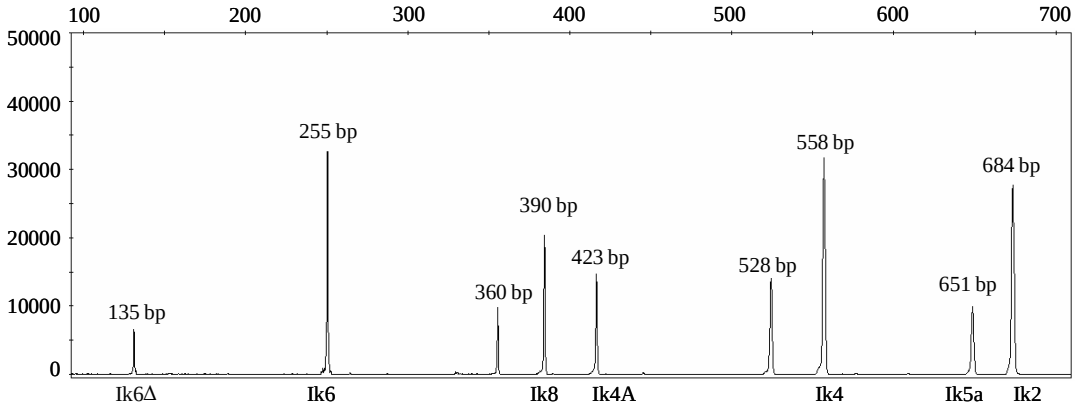

Figure 1. A. Schematic diagram of the the different Ikaros isoforms produced in our Ph+ ALL samples by alternative splicing; N-terminal zinc-fingers (F) show DNA-binding activity and C-terminal F mediate dimerization of the protein (Ex= exon). B. Bands generated by RT-PCR using primers derived on exons 2 and 8 and corresponding to the alternatively spliced products of the Ikaros pre-mRNA transcript. PCR products were detected by ethidium bromide staining of 1.5% agarose gel. The left lane is the molecular size marker,Marker VI Roche; lane2:Ik6 expression; lane 3: co-expression of Ik1, Ik2, Ik4, Ik4A/Ik8 and Ik6. C. Electrophenogram of Ikaros PCR product performed using a forward primer conjugated with the fluorescin dye at its 5'. Different Ikaros isoforms were represented in the electrophenogram by different peaks. The x-axis displays the computed lenght of PCR product in base pairs, as determined automatically by the use of an internal lane standard. The y-axis represents the peak height in fluorescence units.

Table 2. Characteristics of 59% Ph+ ALL patients who co- expressed different Ikaros isoforms. For each patient hypothetical and confirmed wild type and aberrant Ikaros isoforms are shown.

ID	Age	Blast count (%)	BCR-ABL transcript	Wild-type Ikaros isoforms	Aberrant ikaros isoforms
1	65	100	p190	Ik6Δ, Ik6, Ik8, Ik4A, Ik4, Ik2	Ik4 del, Ik8 ins, Ik4A ins, Ik4 ins+del, Ik2 ins+del, Ik2ins
2	18	71	p210/p190	Ik6, Ik8, Ik4A, Ik4, Ik5A, Ik2	Ik5A del, Ik4 del, Ik6 ins, Ik8 ins, Ik4A ins, Ik4 ins+del, Ik2 ins+del, ik2 ins
3	60	100	p210	Ik6, Ik8, Ik4A, Ik4, Ik5A, Ik2	Ik5A del, Ik4 del, Ik6 ins, Ik8 ins, Ik4A ins, Ik4 ins+del, Ik2 ins+del, Ik2 ins
4	73	91	p190	Ik6, Ik8, Ik4A, Ik4, Ik5A, Ik2	Ik5A del, Ik4 del, Ik8 ins, Ik4A ins, Ik4 ins+del, Ik4 ins, Ik5A ins, Ik2 ins
5	57	85	p190	Ik6Δ, Ik6, Ik8, Ik4A, Ik4, Ik2	Ik4 del, Ik4A ins, Ik8 ins, Ik4A ins, Ik4 ins+del, Ik4 ins, Ik2 ins+del, Ik2 ins
6	45	85	p190	Ik6Δ, Ik6, Ik8, Ik4A, Ik4, Ik2	Ik4 del, Ik8 ins, Ik4A ins, Ik4 ins+del, Ik4 ins, Ik2 ins+del, Ik2 ins
7	40	10	p210	Ik6, Ik8, Ik4A, Ik4 del, Ik4, Ik5A, Ik2	Ik4 del, Ik8 ins, Ik4A ins, Ik4 ins+del, Ik4 ins
8	50	80	p190	Ik6, Ik8, Ik4A, Ik4, Ik5A, Ik2	Ik5A del, Ik4 del, Ik6 ins, Ik8 ins, Ik4A ins, Ik4 ins+del, Ik2 ins+del, Ik2 ins
9	72	N.A.	p210	Ik6Δ, Ik6, Ik8, Ik4A, Ik4, Ik5A, Ik2	Ik4 del, Ik6 ins, Ik8 ins, Ik4A ins, Ik4 ins+del, Ik2 ins+del, Ik2 ins
10	50	85	p190	Ik6Δ, Ik6, Ik8, Ik4A, Ik4, Ik5A, Ik2	Ik5A del, Ik4 del, Ik6 ins, Ik8 ins, Ik4A ins, Ik4 ins+del, Ik2 ins+del, Ik2 ins
11	52	85	p210	Ik6Δ, Ik6, Ik4, Ik2	Ik4A ins, Ik6 ins, Ik8 ins, Ik4A ins, Ik4 ins+del, Ik2 ins+del, Ik2 ins
12	53	94	p190	Ik6Δ, Ik6, Ik8, Ik4A, Ik4, Ik5A	Ik5A del, Ik4 del, Ik6 ins, Ik8 ins, Ik4A ins, Ik4 ins+del, Ik2 ins+del, Ik2 ins
13	41	64	p210/p190	Ik6, Ik4A, Ik4, Ik5A	Ik4del, Ik6 ins, Ik4 ins+del, Ik4 ins
14	31	96	p210	Ik6, Ik8, Ik4A, Ik4, Ik5A, Ik2	Ik4del, Ik6 ins, Ik4 ins+del, Ik4 ins, Ik2 ins
15	75	73	p210	Ik6, Ik8, Ik4A, Ik4, Ik5A, Ik2	Ik4 del, Ik4A ins, Ik4 ins+del, Ik4 ins, Ik5A ins, Ik2 ins
16	48	96	p210	Ik6, Ik8, Ik4A, Ik4, Ik5A, Ik2	Ik4 del, Ik8 ins, Ik4A ins, Ik4 ins+del, Ik2 ins+del, Ik2 ins
17	54	90	p210	Ik6Δ, Ik6, Ik8, Ik4A, Ik4, Ik5A	Ik5A del, Ik4 del, Ik8 ins, Ik4A ins, Ik4 ins+del, Ik2 ins+del, Ik2 ins
18	48	70	p210	Ik6, Ik8, Ik4A, Ik4, Ik5A, Ik2	Ik5A del, Ik4 del, Ik8 ins, Ik4A ins, Ik4 ins+del, Ik4 ins, Ik2 ins
19	41	70	p210	Ik6Δ, Ik6, Ik8, Ik4A, Ik4, Ik5A, Ik2	Ik5A del, Ik4 del, Ik6 ins, Ik8 ins, Ik4A ins, Ik4 ins+del, Ik4 ins, Ik2 ins
20	34	80	p190	Ik6, Ik8, Ik4A, Ik4 del, Ik4, Ik5A	Ik4 del, Ik6 ins, Ik4 ins
21	31	80	p190	Ik6Δ, Ik6, Ik8, Ik4A, Ik4, Ik5A	Ik4A ins, Ik4 ins+del, Ik4 ins, Ik2 ins
22	75	90	p210	Ik6Δ, Ik6, Ik8, Ik4A, Ik4, Ik5A, Ik2	Ik4 del, Ik8 ins, Ik4A ins, Ik4 ins+del, Ik4 ins, Ik2 ins
23	63	55	p190	Ik6Δ, Ik6, Ik8, Ik4A, Ik4, Ik5A	Ik5A del, Ik4 del, Ik8 ins, Ik4A ins, Ik4 ins+del, Ik4 ins, Ik2 ins
24	60	72	p210	Ik6Δ, Ik6, Ik8, Ik4A, Ik5A, Ik2	Ik5A del, Ik4 del, Ik6 ins, Ik8 ins, Ik4A ins, Ik4 ins+del, Ik4 ins, Ik2 ins
25	36	70	p210	Ik6Δ, Ik6, Ik8, Ik4A, Ik4, Ik2	Ik4 del, Ik8 ins, Ik4A ins, Ik4 ins+del, Ik4 ins, Ik2 ins
26	62	94	p190	Ik6, Ik4A, k4, Ik5A, Ik2	Ik8 del, Ik4 del, Ik4A del Ik4 ins+del, Ik4 ins, Ik2 ins
27	48	90	p190	Ik6Δ, Ik6, Ik8 del, Ik4A, Ik4, Ik5A, Ik2	Ik8 del, Ik4 del, Ik4A del, Ik4A ins, Ik4 ins+del, Ik4 ins, Ik5A ins, Ik2 ins

4.2 Adult Ph+ ALL patients express different aberrant Ikaros transcript variants

In addition to wild-type isoforms generated by alternative splicing of Ikaros gene, we frequently identified transcript variants with an atypical length not corresponding to well known and characterized wild-type isoforms. By cloning and subsequent sequencing we found that Ph+ ALL patients may express aberrant spliced Ikaros isoforms. In all 27/46 (59%) patients who did not express Ik6 alone we found clones which expressed wild-type Ikaros isoforms: (Ik1, Ik2, Ik4, Ik4a, Ik5a, Ik6, Ik6Δ and Ik8) as previously described and clones which expressed aberrant Ik2 isoforms [that we called Ik2(ins)] or Ik4/4A/5A isoforms [Ik4(ins), Ik4A(ins), Ik5A(ins), respectively] with a 20–amino acid insertion (TYGADDFRDFHAIIPKSFSR) due to a 60-bp insertion immediately downstream of exon 3 (Table 2 and Fig.2A-B). This alteration was identified either alone or together with an in-frame 10–amino acid deletion, DKSSMPQKFLG, due to a 30-bp deletion at the end of exon 7. Furthermore, aberrant transcript variants containing only the deletion between the exon 7 and exon 8 were also detected [Ik2(del), Ik4(del), Ik5A(del), Ik8(del)], increasing the complex scenario of Ikaros isoforms produce by alternative splicing and suggesting that Ph+ ALL is characterized by high instability. The observed N-terminal insertions and C-terminal deletions did not cause a frame shift and, therefore, did not change the downstream amino acid sequences.

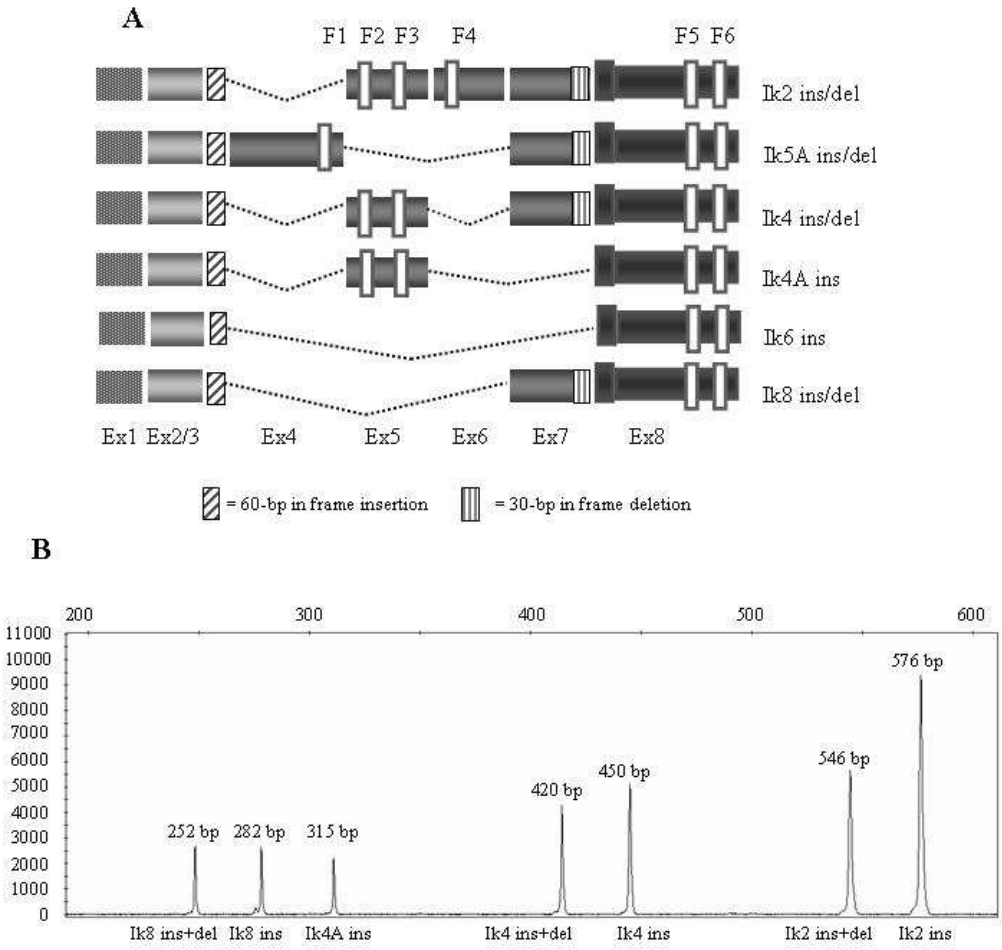

Figure 2: A. Schematic diagram of Ikaros isoforms with 60-bp insertion or 30-bp deletion identified in Ph+ ALL samples; B. Electrophenogram of Ikaros PCR product performed using the insertion primer conjugated with the fluorescin dye at its 5'. Different Ikaros isoforms were represented in the electrophenogram by different peaks. The x-axis displays the computed lenght of PCR product in base pairs, as determined automatically by the use of an internal lane standard. The y-axis represents the peak height in fluorescence units.

4.3 The aberrant Ikaros isoforms are due to the selection of an alternative splice donor and an alternative splice acceptor sites

We hypothesized that the 60-bp insertion is due to selection of an alternative splice donor and an alternative splice acceptor sites (Figure 4A). Using the Basic Local Alignment Search Tool (BLAST, http://www.ncbi.nlm.nih.gov/blast/Blast.cgi) we found that the 60-bp insertion found in [Ik2(ins)] or [Ik4(ins)] isoforms corresponded to a region in the intron 3-4. This sequence is flanked by criptic splice sites because it starts with AG and ends with GU (ie, GT in cDNA). The selection of these alternative splice sites may determine in Ik2(ins) or Ik4(ins) the skipping of the exon 4 and the introduction in the mRNA of an alternative exon (Figure 4C). In the 5A isoform the 60-bp insertion is in conjunction with the exon 3 enforcing our hypothesis on its role as alternative exon. The 60-bp insertion encodes a perfect α helix, which is followed by a flexible region (KSFSR) located upstream from the DNA binding zinc fingers (F2 and F3). The presence of this new motif may significantly alter the Ikaros-specific DNA-binding activity. Also the 30-bp deletion in exon 7 might have resulted from the selection of an alternative splice site, because it starts with a GU sequence (ie, GT in cDNA) at the 5' junction, which could very well serve as a donor site recognition sequence (Figure 4B).

4.4 Analysis of DNA-binding and non DNA-binding Ikaros isoforms containing the 60-base insertion

To obtain a more accurate characterization of aberrant isoforms, Ikaros cDNA was amplified with a forward oligonucleotide conjugated with a fluorescent dye at its 5' end and designed to specifically detect forms with the 60-base insertion following exon 3. DNA sequencing of RT-PCR products from insertion primer identified transcripts of different lengths corresponding to hypothetical aberrant isoforms. Among these the most expressed transcript variants were those of 576 bp (median value 19%, SD 7.41), 546 bp (median

value 17%, SD 4.20), 450 bp (median value 14%, SD 4.64) and 420 bp (median value 16%, SD 4.44) corresponded to Ik2(ins), Ik2(ins+del), Ik4(ins), Ik4(ins+del) isoforms, respectively (Figure 3B). In only three patients (patient 4, 15 and 27 in Table 2) we identified the Ik5A (ins) isoform expressed at high levels (median value 29%). Other isoforms were detected at lower levels: Ik4A(ins), Ik6(ins), Ik8(ins), Ik8(ins+del). All aberrant isoforms were confirmed by cloning and subsequent sequencing except for Ik6(ins), Ik8(ins) and Ik8(ins+del) (Figure 3B). Likely it is due to the fact the these isoforms are expressed very low in leukaemia cases (median value 7%, range 3-13%).

To determine whether the aberrant human Ikaros splice variants with insertion or deletion were unique to patients with Ph+ ALL diagnosis, we studied Ikaros expression in acute leukaemia cases in remission and in normal human peripheral blood. Our RT-PCR assays on capillary electrophoresis showed that Ikaros transcript variants with insert or deletion were present in normal human hemopoietic cells or in acute leukaemia cases in remission. However, these isoforms were expressed at low levels (less than 5% considering their expression respect to the other Ikaros isoforms versus a median value of 15% of leukemic cells).

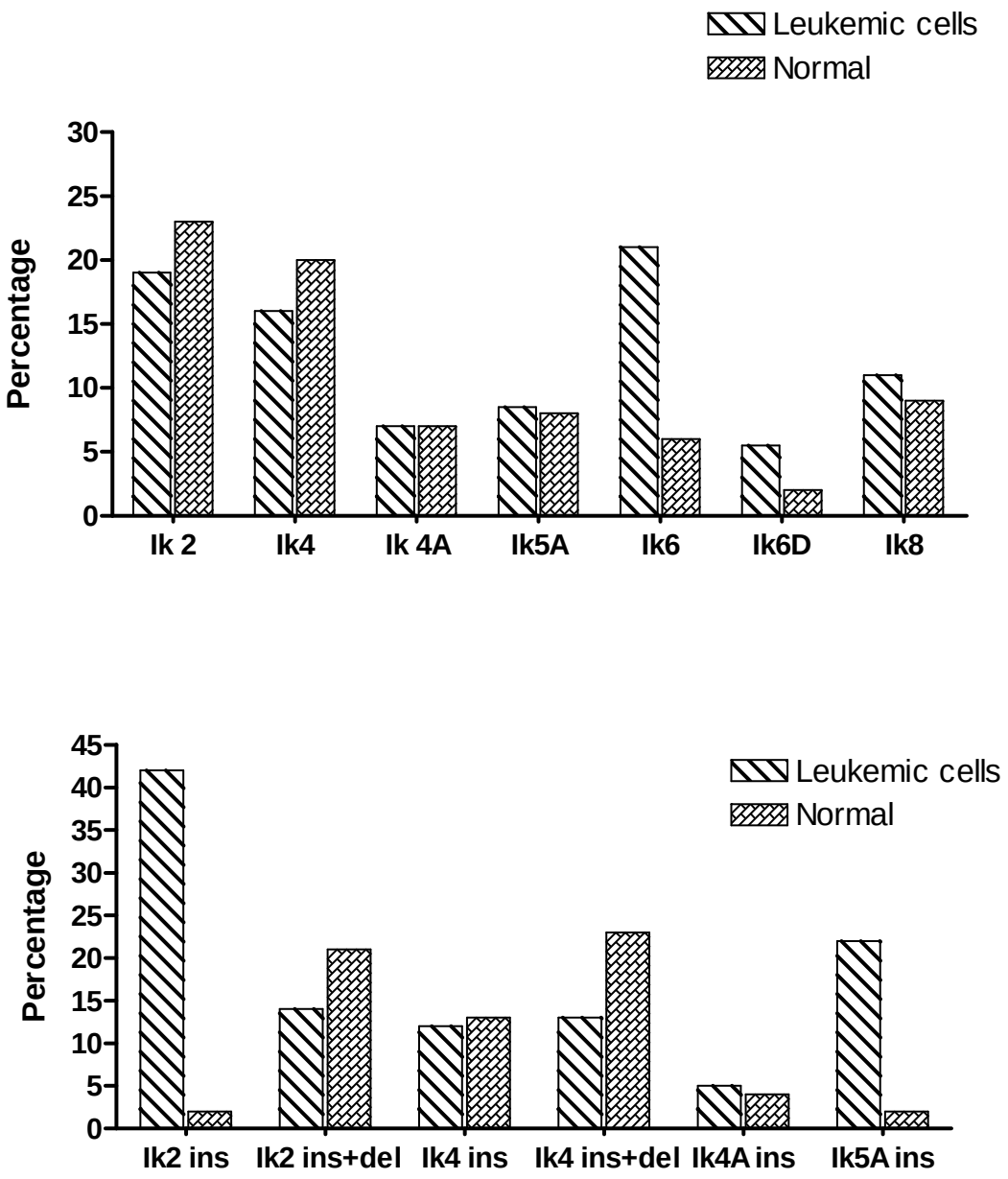

Figure 3. Relative expression of wild-type Ikaros isoforms (A) and relative expression of aberrant Ikaros isoforms (B) produced using insertion primers in Ph+ ALL samples. The relative expression of each Ikaros isoform was expressed as a percent fraction between the height of each peak and the sum of the heights of all peaks in a sample according to the following: Ik isoform A= [A/A+B]x100, where A=peak height of isoform A and B= sum of the peak heights of other Ik isoforms expressed in a sample. Ik1 isoform was omitted from the analysis.

4.5 Ik6 protein is expressed in an abnormal subcellular compartmentalization

RT-PCR and sequencing results were confirmed by Western blot analysis on primary leukemic cells from each adult Ph+ ALL patient expressing small non–DNA-binding and/or aberrant isoforms of Ikaros (Figure 5A). A 57-kDa immunoreactive protein that corresponded in size to Ik-1 and a 47- kDa immunoreactive protein that corresponded to Ik-2 were identified. In contrast, we confirmed the presence of a smaller immunoreactive protein band of approximately 37 to 40 kd, which corresponded in size to Ik6 in patients who were positive for this non-DNA binding isoform from RT-PCR. The absence of an abundant Ik1, Ik2 was not caused by a generalized proteolytic degradation because a 120-kDa Cbl protein was detected by Western blot analysis in the same whole cell lysates. The co-expression of many Ikaros isoforms in the same sample confirmed that the different splice variants identified by RT-PCR are transduced. In the patients who were positive for the expression of only Ik6, we confirmed the presence of only one band of approximately 40 kDa. The subcellular compartimentalization of Ikaros proteins in normal hematopoietic cells and in primary Ph+ leukemic cells were compared by confocal laser scanning microscopy. In normal mononuclear cells the nuclei were stained brightly by the anti-Ikaros antibody, as showed by a specific punctuate green fluorescent staining pattern. In mononuclear cells from patients who expressed the Ik6 isoform alone, we observed a cytoplasmatic localization of Ikaros, as evidenced by a bright green fluorescent ring surrounding the red nuclei. It is interesting to note that in patients who expressed different Ikaros transcript variants, we identified both nuclear proteins and cytoplasmatic proteins, suggesting that full-length Ikaros isoforms had a nuclear localization, whereas short-dominant negative isoforms and aberrant isoforms had a cytoplasmatic localization (Figure 5B).

The ability of nuclear extract proteins from normal mononuclear cells and leukemic cells to show Ikaros-specific, high affinity DNA-binding activity was tested using EMSA. In the

extracts from cell expressing Ik6 isoform alone only one very weak protein- DNA complex band was found, in contrast to normal cells expressing full-length isoforms.

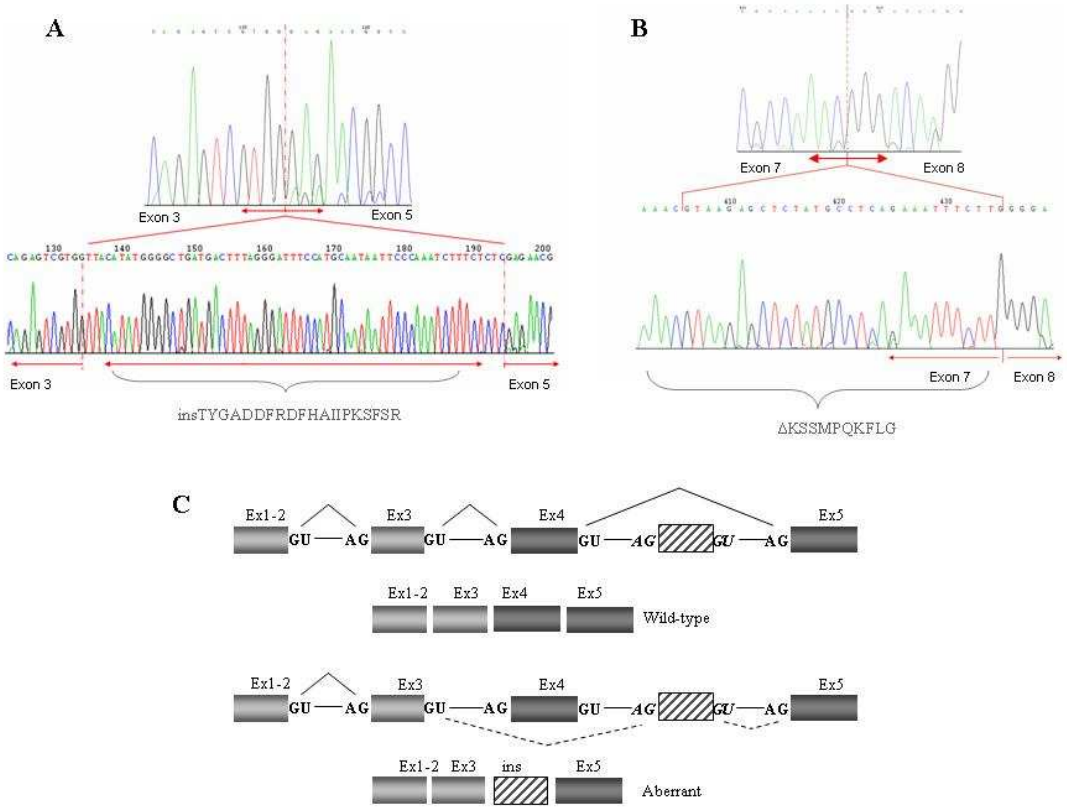

Figure 4: A. Upper the wild type junction between exon 2 and exon 4 is shown; below there is the aberrant sequence with the insertion of 60-bp (TTACATATGGGGCTGATGACTTTAGGGATTTCCATGCAATAATTCCCA) between the exon 3/exon 5 junction. B: Upper the 30-bp deletion at the exon 7/ exon 8 is shown; below there is the wild-type sequence. C: Schematic representation of the mechanism determing the insertion of a regione inside the intron 3-4 and the skipping of the exon 4.

A

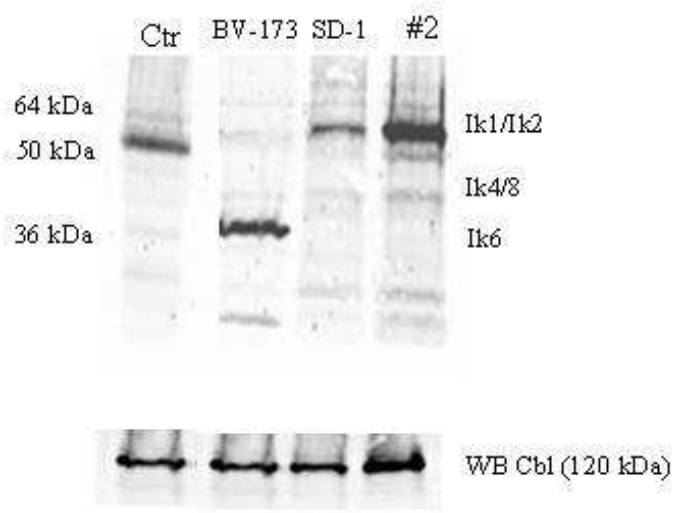
Ctr
BV-173
SD-1
#2
64 kDa
50 kDa
36 kDa
Ik1/Ik2
Ik4/8
Ik6
WB Cbl (120 kDa)

B

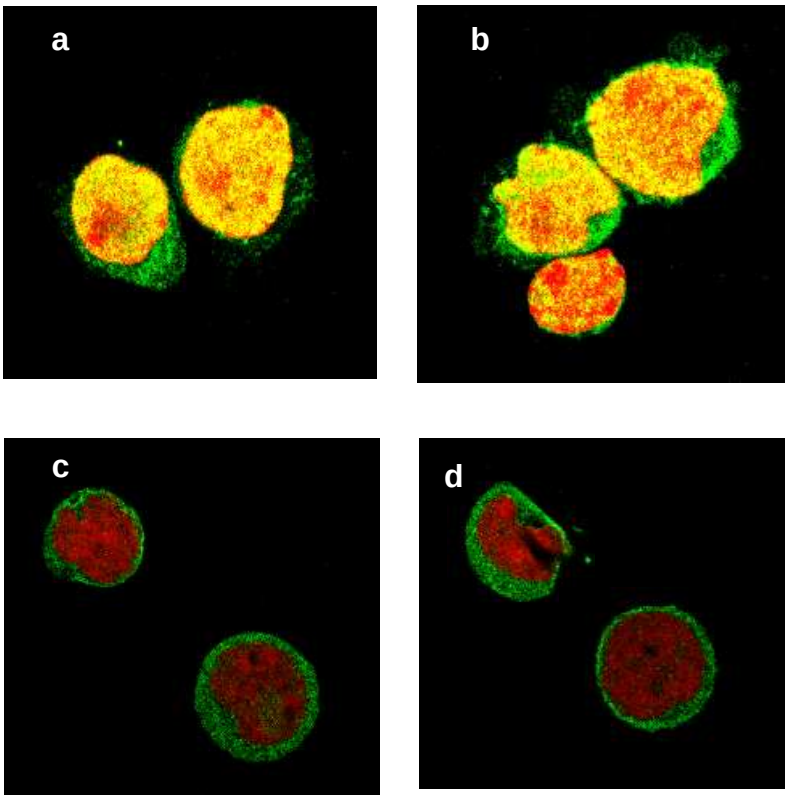
a
b
c
d

Figure 5. (A) Anti-Ikaros Western Blots of whole cell lysates from leukemic cells. Anti-Cbl Western Blots of the whole cell lysates was performed as control. (B) Expression and subcellular localization of ikaros proteins in leukemic cells from Ph+ ALL patients. In all images cells were stained with an Ikaros antibody (green) and with propidium iodide (red) to visualize DNA. In A and B confocal images of leukemic cells from patients expressing full-lenght Ikaros isoforms showed the characteristic multifocal nuclear localization pattern of Ikaros. C and D are confocal images of leukemic cells expressing Ik6 isoform and showing cytoplasmatic expression of Ikaros (e.g., bright green fluorescent rim surrounding the toto-labeled red nuclei).

4.6 Ik6 expression correlated with the percentage of blast cells

In some cases, we detected in our samples by RT-PCR and Western blot analysis the expression of the non-DNA binding isoform Ik6 both alone and in association with functional Ik1, Ik2 isoforms. Since these samples contain a mixed population of cells with a variable percentage of blast cells, it is not clear whether the larger isoforms result from normal cells present in the samples or from blast cells which have acquired a mutation in one Ikaros allele that affects isoform expression. To addressee this issue, we correlated the different expression pattern of Ikaros isoforms to the percentage of blast cells in each sample. We observed that the median percentage of blast cells in patients who expressed the Ik6 isoform alone was 90% (range, 54-100) versus 57% (range, 5-94) of patients co-expressing both the short Ik6 isoform and functional Ik1, Ik2 ($p = 0.0003$). Our hypothesis was that the co-expression of functional Ik1, Ik2 and Ik6 is due to normal cells present in the samples which express larger isoforms and to blast cells which express the short Ik6 isoform.

4.7 Ik6 expression strongly correlated with BCR-ABL transcript level in Ph positive ALL patients

After we showed a correlation between the percentage of blast cells and the expression of Ik6 isoform in the sample, the next stage was to investigate whether this alteration could depend on Bcr-Abl activity. For this purpose, BCR-ABL transcript levels were monitored in

all patients at different time points during therapy with imatinib or dasatinib. First, we demonstrated that dominant Ik6 does not depend on the type of BCR-ABL transcript rearrangement, but it can be detected both in patients carrying a p210 and in patients with p190 oncoprotein. Secondly, we found a very statistically significant difference between the BCR-ABL/ABL per cent values of the patients who expressed the DNA-binding isoforms and those of patients with only Ik6 dominant-negative isoform (Fig.*6A*). The median ratio BCR-ABL/ABL per cent of the first group was 0.01 (range, 64.49-0.0001) against 61.26 (range, 251.62-1.21) of the second group ($p < .0001$). These results showed that the expression of Ik6 strongly correlated with the BCR-ABL transcript levels, suggesting that its expression could depend on the Bcr-Abl oncoprotein activity.

4.8 Ik6 expression is associated in vivo with resistance to imatinib and dasatinib

The mechanism of aberrant over-expression of the non DNA-binding Ik6 isoform has been previously demonstrated to be restricted to certain forms of leukemia[125], such as blast crisis of CML[76] or acute lymphoblastic/myeloid leukemia[73,77,126], suggesting a role into pathogenesis of leukaemia but its role into leukaemia resistance has not yet been demonstrated. In this study, in order to provide new evidence for a possible link between the expression of Ik6 and the resistance to TKIs in Ph+ ALL patients, we examined the expression manner of Ikaros isoforms at different checkpoints during treatment with TKIs: at baseline, during remission and at the time of hematologic relapse. On the same samples and at the same time-points we performed a RQ-PCR analysis to quantify the BCR-ABL transcript levels. We divided the patients in three groups according to the Ik isoforms expressed (DNA-binding isoforms (A); co-expression of both DNA-binding and non DNA-binding isoforms (B); dominant non DNA-binding isoforms (C)) and the phase of disease (diagnosis, hematologic/cytogenetic remission and hematologic/cytogenetic relapse) (Fig. 6). Forty-one patients were evaluable for molecular analysis of BCR-ABL and Ikaros at

diagnosis. The expression of Ik6 was detected in 36 patients (88%) but in only 14 patients (34%) it was expressed alone versus 12% of patients with only Ik1, Ik2 and Ik4 isoforms (*p* = ns), suggesting that the expression of Ik6 alone was not correlated with diagnosis. Furthermore, at diagnosis we did not observe any significant difference in the BCR-ABL transcript levels among the three patient groups (p= .399). During remission following tyrosine kinase inhibitor-therapy, in all patients we detected only DNA-binding isoforms with a median BCR-ABL/ABL x100 value of 0.001 (range, 0.07-0.0001). It is important to note that in none we detected the Ik6 isoform enforcing the idea that the Ik6 expression was correlated to the amount of BCR-ABL transcript. Therefore, in patients with relapse and high levels of BCR-ABL transcript the Ik6 became the major isoform expressed both alone (67%) and in association with other isoforms (24%) versus 9% of patients expressing predominantly Ik1, Ik2 and Ik4. We did not observe any difference in the expression of Ik6 at the time of relapse between patients who were resistant to imatinib (10/16, 63%) and patients who were resistant to dasatinib (4/8, 50%). Overall, these results demonstrated that the expression of Ik6 isoform is associated with resistance to both imatinib and dasatinib.

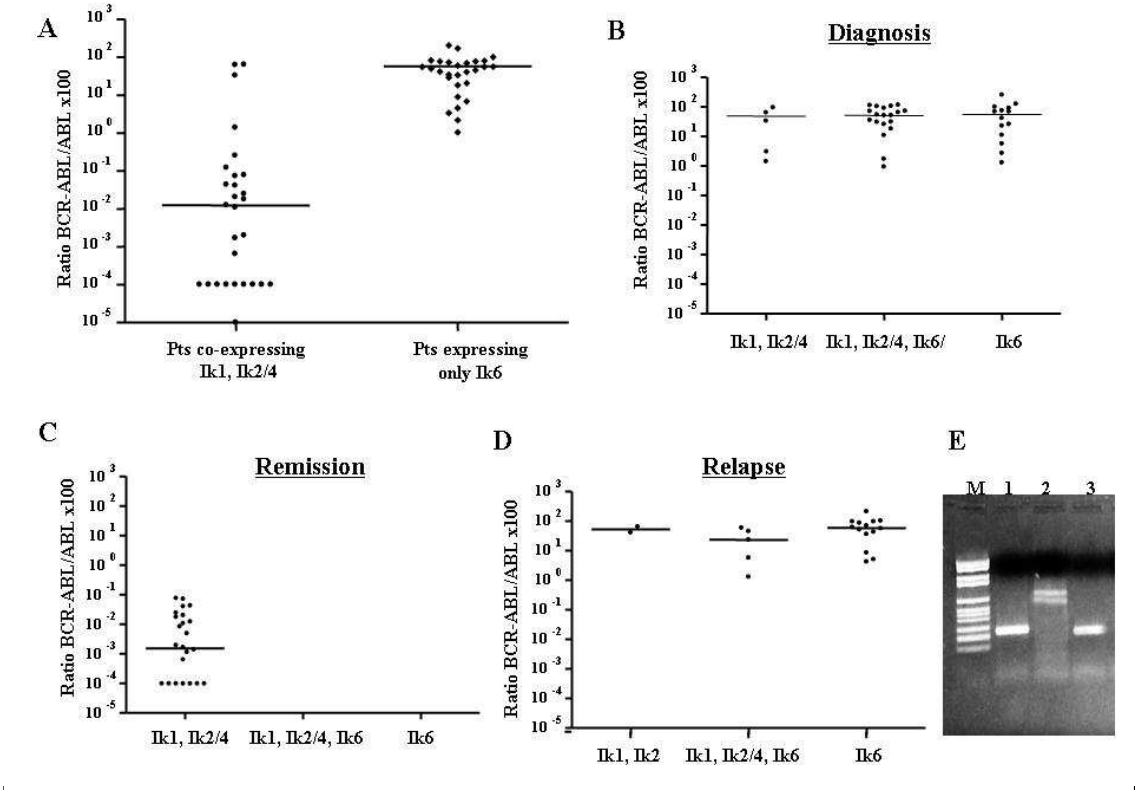

Figure 6. Comparison between the BCR-ABL/ABL per cent values of the patients who expressed the Ik1, Ik2 DNA-binding isoforms alone and those of patients with Ik6 dominant-negative isoform alone, independent on the disease clinical status. There is a strong correlation between the Ik6 expression and the BR-ABL transcript levels ($p < 0.0001$) (A).

Expression manner of Ikaros isoforms at different checkpoints during treatment with tyrosine kinase inhibitor: at baseline (B), during remission (C) and at the time of relapse (D) (both hematologic/cytogenetic and molecular). In pts with relapse and high levels of BCR-ABL transcript the Ik6 was the major isoform expressed. E. RT-PCR analysis at baseline (lane1), during remission (lane2) and at the time of relapse (lane3).

4.9 TKIs induced apoptosis in full-length Ikaros expressing-cells but not in Ik6 expressing cells

In order to assess whether also *in vitro* the selection of cells with higher expression of short Ikaros isoforms affects the sensitivity to TKIs in Ph+ALL, we treated full-length Ikaros expressing-cells (SD-1) and Ik6 expressing cells (BV-173) with different TKIs (imatinib, dasatinib and nilotinib). As shown in Figure 7 (*A*-*B*), in SD-1 cells we observed an increase of apoptotic cells of 18%, 20% and 11% after incubation with imatinib, dasatinib and nilotinib, respectively. By contrast, in Ik6 expressing cells TKIs did not increase the number of apoptotic cells when compared to the control samples. These results were confirmed by those obtained from colony growth assay (Figure *7C*). The *in vitro* incubations of SD-1 cells with imatinib, dasatinib and nilotinib resulted in a marked inhibition of colony growth when compared to the control (colony growth percentage values were 23%, 9% and 22% with imatinib, dasatinib and nilotinib, respectively). In contrast, no significant inhibition of colony growth was detected after incubation of Ik6 expressing cells with TKIs when compared to the untreated control cells (colony growth percentage values were 69%, 85% and 77% with imatinib, dasatinib and nilotinib, respectively).

4.10 Transfection of Ik6 in an Imatinib-sensitive Ik6-negative Ph+ ALL cell line decreases sensitivity to TKIs

In order to mechanistically demonstrated whether *in vitro* the overexpression of Ik6 impairs the response to TKIs and contributes to resistance we transfected an imatinib-sensitive Ik6-negative Ph+ ALL cell line (SUP-B15) with the complete Ik6 DNA coding sequence. First all, we assessed the proliferation activity of the cells transfected with Ik6 (pcDNA-Ik6) and those with the empty vector (pEGFP). Interestingly, we observed a strong increase of the proliferation rate (of about five hundred times) in cells transfected with pcDNA-Ik6 (Figure 8A). Similar results were obtained by colony growth assay as shown in Figure 8B. The

expression of Ik6 isoform in SUP-B15 cells strikingly determined an increased colony growth (of about twenty times). Moreover, in pcDNA-Ik6 SUP-B15 transfected cells number of apoptotic cells did not significantly increase after imatinib incubation when compared to the samples transfected with the empty vector (3.5 % versus 18%).

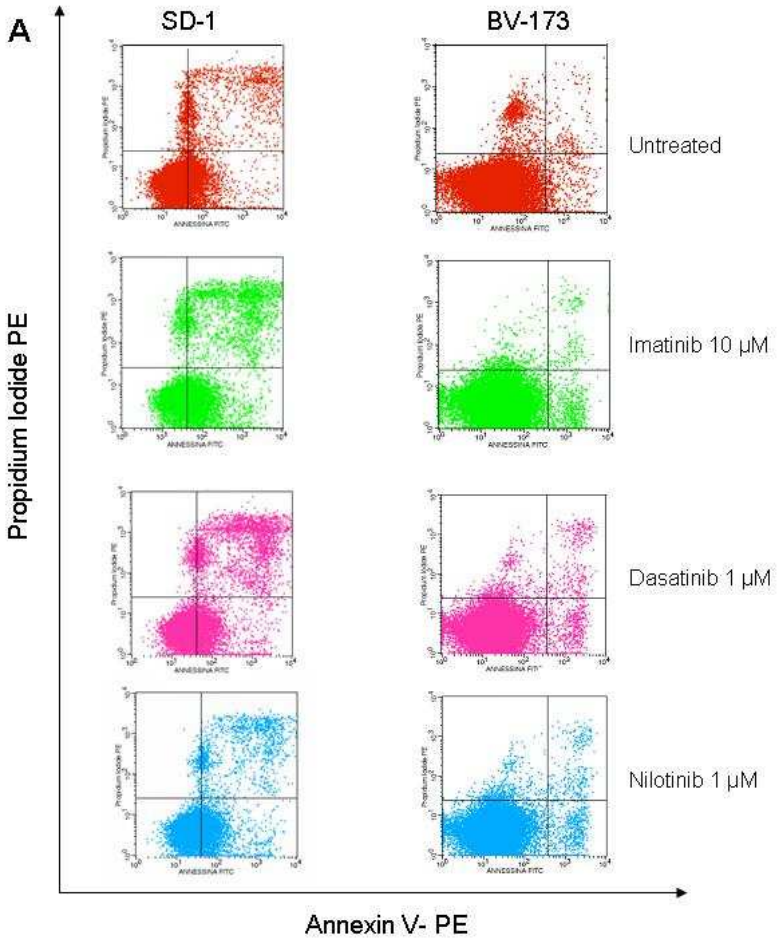

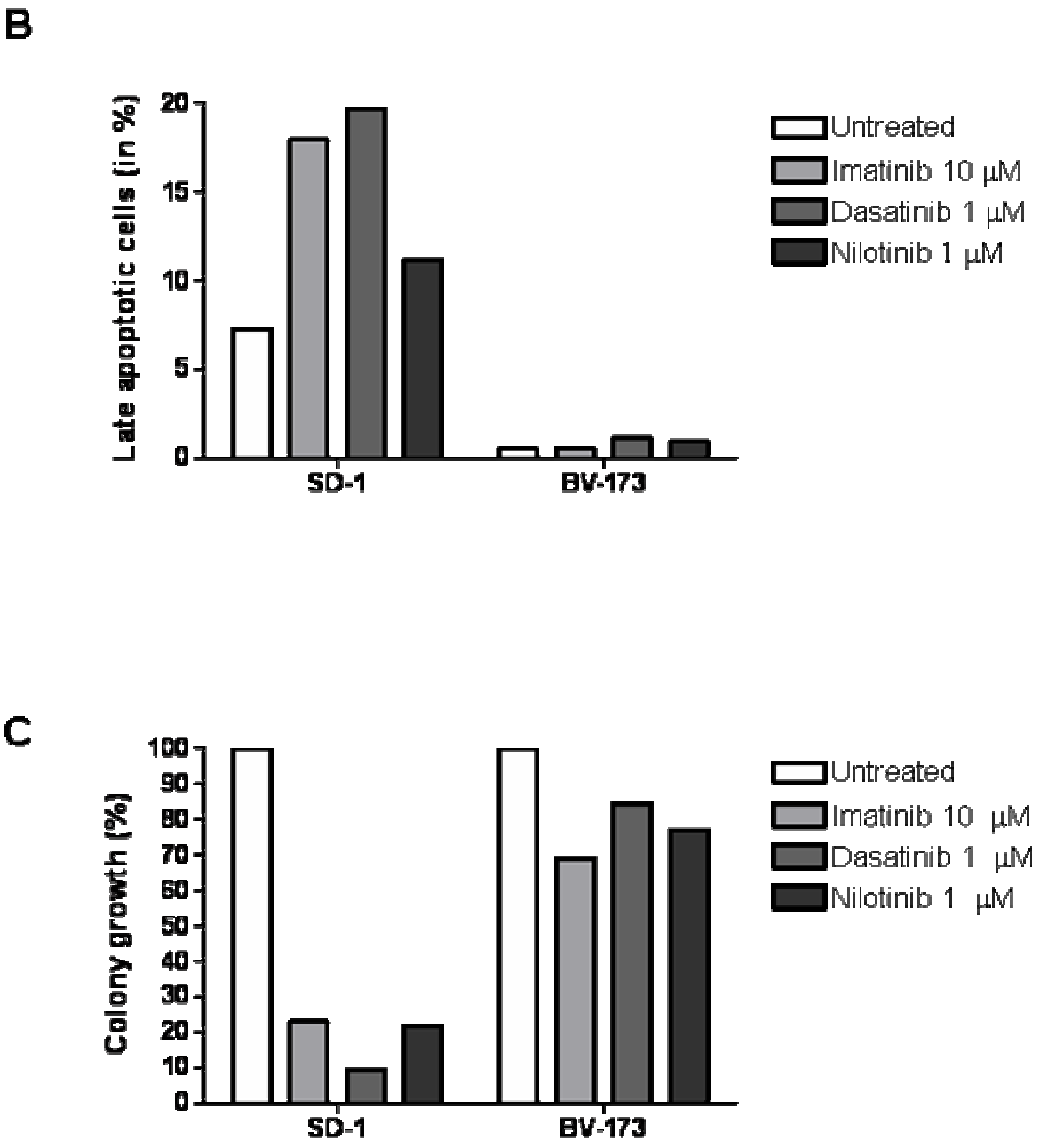

Figure 7. (A-B) Apoptotic rates of untreated and TKI (imatinib, dasatinib and nilotinib) treated-cells. Treatment with TKIs determined an incresed of apoptotic rate in Ikaros full lenght expressing cells (SD-1), whereas no differences were identified in Ik6 expressing cells (BV-173) between untreated and TKIs treated cells. C. Percentage of inhibition of colony growth compared to controls (white column). Colony growth inhibition of SD-1 and BV-173 TKIs treated cells was normalized respect to the own untreated cells.

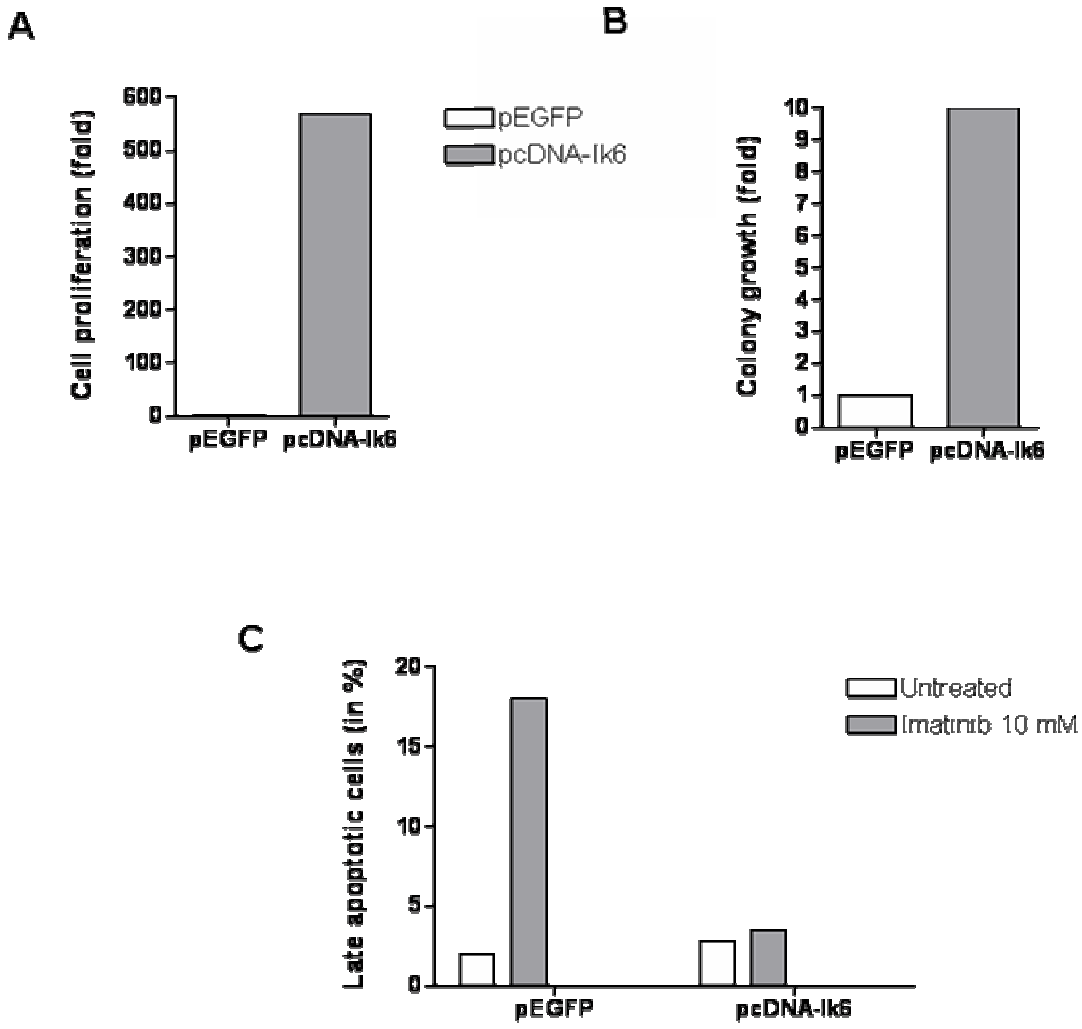

Figure 8. Induction of cell proliferation (A) and colony growth (B) in pcDNA-Ik6 SUP-B15 transfected cells. Fold induction was calculated using pEGFP SUP-B15 transfected cells as control. C. Apoptotic rates evaluated by FACS for the detection of annexin V positive cells in pcDNA-Ik6 SUP-B15 transfected cells and cells transfected with the empy vector (pEGFP) after incubation with imatinib.

4.11 Cis-acting mutations may be responsible for alternative splicing of Ikaros transcript

Amplification and genomic sequence analysis of the exon splice junction regions was performed in search of mutations in the region spanning the cryptic splice site, as well as the predominant 5' (donor) or 3' (acceptor) splice sites in Ph+ ALL patients who expressed Ik6 isoform. In these regions we observed the presence of 2 single nucleotide polymorphisms (SNPs): rs10251980 [A/G] in the exon2/3 splice junction and rs10262731 [A/G] in the exon 7/8 splice junction in 50% and 36% of analyzed patients, respectively (Fig.9). We also found a variant of the rs11329346 [-/C], in which an A was substituted by a G, in intron 3-4, in 16% of patients. Other two different single nucleotide substitutions not recognized as SNP were observed in our samples. The first one is a substitution of a G with an A in exon 2/3 splice junction at position +114 numbering from the first base of the intron 2-3, in 80% of Ik6-expressing patients. The other one is always a substitution of a G with an A in exon 3/4 splice junction at position -191 to the end of the intron 3-4, identified in 30% of patients. In Figure 9 the characterization and the position of mutations and SNPs are shown. Furthermore, we examined the expression of the single nucleotide polymorphism (SNP) affecting the third base of the triplet codon for a proline (CCC or CCA) in the highly conserved bipartite activation region of the exon 8 (A or C at position 1170 numbering from the translation start site of Ik-1, GenBank accession number U40462, NM_006060.3, http://www.ncbi.nlm.nih.gov/entrez/viewer.fcgi?val=NM_006060.3) within our Ikaros clones among different isoforms. This region is conserved in the various Ikaros splice variants, thereby allowing typing of all Ikaros isoforms. In order to assess if SNPs or point mutations in intronic or exonic sequences could affect alternative splicing creating or abolishing splicing enhancers and silencers, we applied a computational RESCUE-ESE/ISE approach, by which we analyzed the effect of sequence variation entering both the wild-type and the variant sequence into the input window. In our samples the mutation at position +114 in the intron 3-4 was identified as putative ESE creating the **A**AAAAG motif (Figure

9, A). ESE alteration events were also observed in the case of rs10251980 SNP in the same intron 3-4 where the allelic variant containing an A instead of a G was part of the GGAA**A**A or GAA**A**AG ESE motif. In the case of the mutation at position -191 at the 3' of the intron 4-5, the RESCUE approach identified a putative exon splicing silencer (ESS) site: CC**A**AGGT.

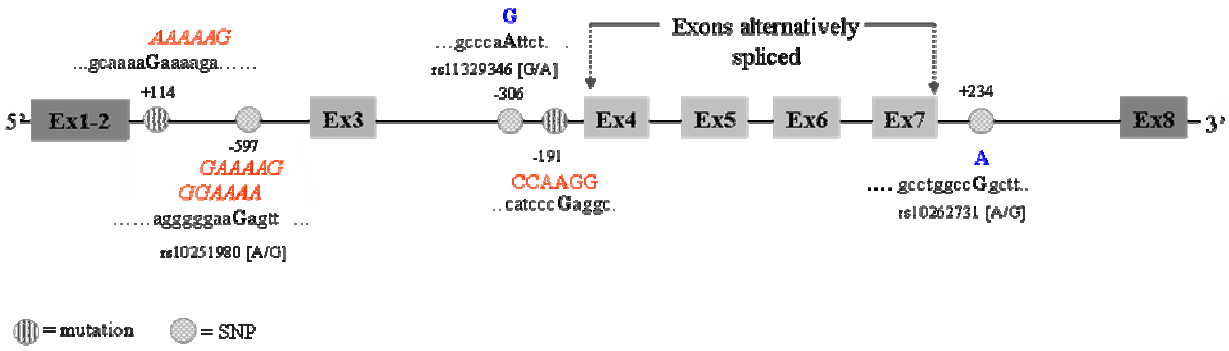

Figure 9. Results from genome sequence analysis of the splice junction regions are shown. Point mutations and single nucleotide polymorphisms (SNPs) are represented in a different way. The letters written in red represented the ESE/ESS motifs identified by using the RESCUE-ESE/ISE computational approach (http://genes.mit.edu/burgelab/rescue-ese/) and the mutated base is bold. Nucleotide substitutions which are not predicted to create ESE/ESS motifs are indicated in blue.

5. DISCUSSION

The Ph chromosome is the most frequent cytogenetic aberration associated with adult ALL and it represents the single most significant adverse prognostic marker. The constitutively active tyrosine kinase encoded by BCR-ABL blocks the differentiation of B precursor cells, prevents apoptosis and also causes genetic instability. This leads in the majority of cases to the acquisition of new mutations, resistance to tyrosine kinase inhibitors and disease progression. Despite imatinib has led to significant improvements in the treatment of patients with Ph+ ALL, in the majority of cases resistance developed quickly and disease progressed. Some mechanisms of resistance have been widely described but the full knowledge of contributing factors, driving both the disease and resistance, remains to be defined. The observation of rapid development of lymphoblastic leukemia in mice expressing altered Ikaros isoforms represented the background of this study.

Ikaros is a critical zinc finger transcription factor required primarily for the formation of more primitive lymphoid progenitors. Deletion of the Ikaros DNA-binding domain results in the absence of detectable lymphocytes or their precursors[127]. The fact that Ikaros functions as a critical regulator of normal lymphocyte development and the observation of rapid development of leukaemia in mice expressing non-DNA binding isoforms, represented the rationale for many studies to investigate whether normal Ikaros expression and function might be altered in human haematological malignancies. An excess of short Ikaros isoforms has been described in leukemic cells obtained from infant, children B and T acute lymphoblastic leukemias (ALLs)[71-74], in de novo adult B ALL[75], in cells from transformed chronic myeloid leukemias (CML)[76] and from de novo acute myelomonocytic and monocytic leukemias[77,78], demonstrating that aberrant regulation of splicing is a new mechanism of activation of an oncogene in ALL. Since expression of non-DNA binding Ikaros isoforms during early lymphopoiesis may dysregulate normal lymphocyte development, predisposing lymphocyte precursors to second hits and leukemic transformation and/or progression, we analyzed for the first time the expression pattern of

Ikaros isoforms in Ph+ ALL patients who were resistant to imatinib and dasatinib with the purpose to determine if Ik aberrant spliced isoforms could correlate with the BCR-ABL transcript levels and associate with the resistance to imatinib and dasatinib.

Given that different Ikaros isoforms can be expressed following by alternative splicing and considering the leukemic role of short and/or aberrant isoforms, it is extremely important to use a sensitive method to detect and quantify the different transcript variants. In this study, for the first time we set up a fast, high-throughput method to detect and quantify splice variants. It is derived from microsatellite analysis[128-130] and it based on capillary electrophoresis technology which is characterized by high detection sensitivity, high accurate and sizing capability and an automated format that requires minimal user intervention. Our results demonstrated that this method can be very useful to screen at high resolution different transcript variants and may become a handy tool within different research areas. It allows non only a screening of different variants but in the same experiment also the quantification of the same variants, demonstrating to be less labour intensive than other available techniques, such as real-time PCR. We were able to characterize all Ikaros isoforms expressed in adult Ph+ ALL at diagnosis and previously not identified, such as Ik5A and Ik6Δ. We demonstrated that 41% Ph+ ALL patients expressed high levels of the only DNA-binding dominant negative Ik6 isoform lacking critical N-terminal zinc-fingers which display abnormal subcellular compartmentalization pattern. Nuclear extracts from patients expressed Ik6 failed to bind DNA in mobility shift assay using a DNA probe containing an Ikaros-specific DNA binding sequence. In 59% Ph+ ALL patients we observed the coexistence in the same PCR sample and at the same time of many splice variants corresponded to Ik1, Ik2, Ik4, Ik4A, Ik5A, Ik6, Ik6Δ and Ik8 isoforms. In these patients we also identified aberrant full-length Ikaros isoforms in Ph+ ALL characterized by a 60-bp insertion immediately downstream of exon 3 and a recurring 30-bp in-frame deletion at the end of exon 7 involving most frequently the Ik2, Ik4 isoforms. Both

the insertion and deletion were due to the selection of alternative splice donor and acceptor sites. The 60-bp insertion is incorporated into the DNA-binding region and therefore may significantly alter the DNA-binding activity of Ik2 and Ik4 isoforms. The deleted sequence in these aberrant Ikaros isoforms is close to the conserved bipartite transcription activation domain within the exon 8 and it is adjacent to the C-terminal zinc finger dimerization motifs. The deletion of this peptide determines structural changes which could affect the accessibility of the Ikaros activation domain with members of the basal transcription machinery and stability of such interactions. Furthermore, the ability of these aberrant isoforms to form dimers with other Ikaros isoforms or other proteins could also be impaired and such impairments could lead to altered DNA-binding or altered subcellular localization of Ikaros. In conclusion, our findings demonstrated that alterations of the transcription factor Ikaros, involving both short spliced oncogenic isoforms and aberrant full-length isoforms are a common feature in Ph+ ALL patients. Since aberrant and short isoforms are present at low levels in normal mononuclear cells where have a potential regulatory role on the activity of the predominant Ik1 and Ik2 isoforms[131], it is probably that other factors, such as abnormalities in the splicing regulation, in this error prone system, could determine a disequilibrium which leads to the overexpression of short dominant negative isoforms or aberrant isoforms.

The presented data are consistent with the evidence from previous studies that reported an aberrant expression of spliced isoforms of Ikaros in some subtypes of human leukaemia[71,73-75,77,126,132]. Moreover, in a recent study, the comparison of the genome wide gene expression profiles of normal B-cell subsets and BCR-ABL pre-B lymphoblastic leukaemia cells by SAGE, showed loss of B-lymphoid identity and aberrant expression of myeloid lineage-specific molecules in leukemia cells[133]. In the same report BCR-ABL has been demonstrated to induce the expression of dominant-negative Ik6, which contributes to lineage infidelity observed in BCR-ABL pre-B lymphoblastic leukaemia cells. In this study

focusing on a subtype of ALL, the Ph+ ALL, we confirmed not only that BCR-ABL may induce the expression of Ik6 isoform, but we also demonstrated that the splice variant Ik6 does not depend on the type of BCR-ABL rearrangement since it was detected both in patients carrying a p210 and in patients carrying a p190 oncoprotein. Furthermore, the molecular monitoring of minimal residual disease showed for the first time *in vivo* that the dominant negative Ik6 expression correlated with the BCR-ABL transcript levels enforcing the interpretation that this alteration could depend on the Bcr-Abl activity. Patient-derived leukaemia cells expressed dominant-negative Ik6 before, but not during response to TKIs and predominantly at the time of relapse. In order to mechanistically demonstrated whether *in vitro* the overexpression of Ik6 impairs the response to TKIs and contributes to resistance we transfected an imatinib-sensitive Ik6-negative Ph+ ALL cell line (SUP-B15) with the complete Ik6 DNA coding sequence. We confirmed that expression of Ik6 strongly increases proliferation and inhibits apoptosis in TKI sensitive cells establishing a previously unknown link between specific molecular defects that involve the *IKAROS* gene and the resistance to TKIs in Ph+ ALL patients.

Expression of aberrant Ikaros isoforms in leukemic cells could result in *cis* from sequence alterations or from leukemia-associated alterations in *trans*-acting factors. While the splice sites themselves are located in the introns, additional sequences that enhance splicing from an exonic location are also known. These exonic splicing enhancers (ESEs) are short oligonucleotide sequences that are often recognized by proteins of the SR (serine-arginine) family. In order to establish which mechanism could be responsible for spliced Ikaros isoforms in our patients, amplification and genomic sequence analysis of the exon splice junction regions were performed in search of mutations. We applied for the first time on *IKAROS* gene a computational method, RESCUE-ESE/RESCUE-ISE to determine which sequences are capable of functioning as splicing enhancers, finding that some mutations in our samples can be function as splicing enhancer or silencer. Given the overwhelming

number of ESEs in human genes, it is likely that not all of them are the binding targets of the SR proteins and consequently, it is difficult to reliably determine the true incidence of ESE alteration within the set of mutations predicted to alter ESEs. The presence of some predicted ESEs may frequently occur in human genes just by chance and in this case the non-DNA binding Ikaros isoforms could be due to changes in trans-acting splicing regulators. This aspect is under investigation.

In conclusion, our data demonstrated that the post-transcriptional regulation of alternative splicing of *IKAROS* pre-mRNA is defective in the majority of Ph+ ALL patients treated with TKIs. Our hypothesis is that the overexpression of Ik6 blocking B-cell differentiation could contribute to resistance opening a time frame, during which leukaemia cells acquire secondary transforming events.

6. References

1. Hoelzer D. Therapy and prognostic factors in adult acute lymphoblastic leukaemia. Baillieres Clin Haematol. 1994;7:299-320.

2. Honma Y, Kiyosawa H, Mori T, et al. Eos: a novel member of the Ikaros gene family expressed predominantly in the developing nervous system. FEBS Lett. 1999;447:76-80.

3. Porcu P, Cripe LD, Ng EW, et al. Hyperleukocytic leukemias and leukostasis: a review of pathophysiology, clinical presentation and management. Leuk Lymphoma. 2000;39:1-18.

4. Lai R, Hirsch-Ginsberg CF, Bueso-Ramos C. Pathologic diagnosis of acute lymphocytic leukemia. Hematol Oncol Clin North Am. 2000;14:1209-1235.

5. Bennett JM, Catovsky D, Daniel MT, et al. Proposals for the classification of the acute leukaemias. French-American-British (FAB) co-operative group. Br J Haematol. 1976;33:451-458.

6. Brunning RD. Classification of acute leukemias. Semin Diagn Pathol. 2003;20:142-153.

7. Hurwitz CA, Gore SD, Stone KD, Civin CI. Flow cytometric detection of rare normal human marrow cells with immunophenotypes characteristic of acute lymphoblastic leukemia cells. Leukemia. 1992;6:233-239.

8. Huh YO, Ibrahim S. Immunophenotypes in adult acute lymphocytic leukemia. Role of flow cytometry in diagnosis and monitoring of disease. Hematol Oncol Clin North Am. 2000;14:1251-1265.

9. Bene MC, Castoldi G, Knapp W, et al. Proposals for the immunological classification of acute leukemias. European Group for the Immunological Characterization of Leukemias (EGIL). Leukemia. 1995;9:1783-1786.

10. Nakase K, Kita K, Shiku H, et al. Myeloid antigen, CD13, CD14, and/or CD33 expression is restricted to certain lymphoid neoplasms. Am J Clin Pathol. 1996;105:761-768.

11. Rowley JD. The role of chromosome translocations in leukemogenesis. Semin Hematol. 1999;36:59-72.

12. Armstrong SA, Staunton JE, Silverman LB, et al. MLL translocations specify a distinct gene expression profile that distinguishes a unique leukemia. Nat Genet. 2002;30:41-47.

13. Yap WH, Yeoh E, Tay A, Brenner S, Venkatesh B. STAT4 is a target of the hematopoietic zinc-finger transcription factor Ikaros in T cells. FEBS Lett. 2005;579:4470-4478.

14. Hunger SP. Chromosomal translocations involving the E2A gene in acute lymphoblastic leukemia: clinical features and molecular pathogenesis. Blood. 1996;87:1211-1224.

15. Secker-Walker LM. General Report on the European Union Concerted Action Workshop on 11q23, London, UK, May 1997. Leukemia. 1998;12:776-778.

16. Aguiar RC, Sohal J, van Rhee F, et al. TEL-AML1 fusion in acute lymphoblastic leukaemia of adults. M.R.C. Adult Leukaemia Working Party. Br J Haematol. 1996;95:673-677.

17. Armstrong SA, Mabon ME, Silverman LB, et al. FLT3 mutations in childhood acute lymphoblastic leukemia. Blood. 2004;103:3544-3546.

18. McKeithan TW, Shima EA, Le Beau MM, Minowada J, Rowley JD, Diaz MO. Molecular cloning of the breakpoint junction of a human chromosomal 8;14 translocation involving the T-cell receptor alpha-chain gene and sequences on the 3' side of MYC. Proc Natl Acad Sci U S A. 1986;83:6636-6640.

19. Chen Q, Yang CY, Tsan JT, et al. Coding sequences of the tal-1 gene are disrupted by chromosome translocation in human T cell leukemia. J Exp Med. 1990;172:1403-1408.

20. Mellentin JD, Smith SD, Cleary ML. lyl-1, a novel gene altered by chromosomal translocation in T cell leukemia, codes for a protein with a helix-loop-helix DNA binding motif. Cell. 1989;58:77-83.

21. Boehm TL, Werle A, Ganser A, Kornhuber B, Drahovsky D. T cell receptor gamma chain variable gene rearrangements in acute lymphoblastic leukemias of T and B lineage. Eur J Immunol. 1987;17:1593-1597.

22. Hatano M, Roberts CW, Minden M, Crist WM, Korsmeyer SJ. Deregulation of a homeobox gene, HOX11, by the t(10;14) in T cell leukemia. Science. 1991;253:79-82.

23. Mantha S, Ward M, McCafferty J, et al. Activating Notch1 mutations are an early event in T-cell malignancy of Ikaros point mutant Plastic/+ mice. Leuk Res. 2006.

24. Soulier J, Clappier E, Cayuela JM, et al. HOXA genes are included in genetic and biologic networks defining human acute T-cell leukemia (T-ALL). Blood. 2005;106:274-286.

25. Rubnitz JE, Camitta BM, Mahmoud H, et al. Childhood acute lymphoblastic leukemia with the MLL-ENL fusion and t(11;19)(q23;p13.3) translocation. J Clin Oncol. 1999;17:191-196.

26. Asnafi V, Beldjord K, Boulanger E, et al. Analysis of TCR, pT alpha, and RAG-1 in T-acute lymphoblastic leukemias improves understanding of early human T-lymphoid lineage commitment. Blood. 2003;101:2693-2703.

27. Mansour MR, Duke V, Foroni L, et al. Notch-1 mutations are secondary events in some patients with T-cell acute lymphoblastic leukemia. Clin Cancer Res. 2007;13:6964-6969.

28. Eguchi-Ishimae M, Eguchi M, Kempski H, Greaves M. NOTCH1 mutation can be an early, prenatal genetic event in T-ALL. Blood. 2008;111:376-378.

29. Matsuo Y, Drexler HG, Harashima A, Okochi A, Shimizu N, Orita K. Transcription factor expression in cell lines derived from natural killer-cell and natural killer-like T-cell leukemia-lymphoma. Hum Cell. 2004;17:85-92.

30. Ezzat S, Zhu X, Loeper S, Fischer S, Asa SL. Tumor-derived Ikaros 6 acetylates the Bcl-XL promoter to up-regulate a survival signal in pituitary cells. Mol Endocrinol. 2006;20:2976-2986.

31. Kurzrock R, Shtalrid M, Gutterman JU, et al. Molecular analysis of chromosome 22 breakpoints in adult Philadelphia-positive acute lymphoblastic leukaemia. Br J Haematol. 1987;67:55-59.

32. Bassan R, Gatta G, Tondini C, Willemze R. Adult acute lymphoblastic leukaemia. Crit Rev Oncol Hematol. 2004;50:223-261.

33. Reuther JY, Reuther GW, Cortez D, Pendergast AM, Baldwin AS, Jr. A requirement for NF-kappaB activation in Bcr-Abl-mediated transformation. Genes Dev. 1998;12:968-981.

34. He Y, Wertheim JA, Xu L, et al. The coiled-coil domain and Tyr177 of bcr are required to induce a murine chronic myelogenous leukemia-like disease by bcr/abl. Blood. 2002;99:2957-2968.

35. McWhirter JR, Wang JY. Effect of Bcr sequences on the cellular function of the Bcr-Abl oncoprotein. Oncogene. 1997;15:1625-1634.

36. Feller SM, Posern G, Voss J, et al. Physiological signals and oncogenesis mediated through Crk family adapter proteins. J Cell Physiol. 1998;177:535-552.

37. Sattler M, Salgia R, Okuda K, et al. The proto-oncogene product p120CBL and the adaptor proteins CRKL and c-CRK link c-ABL, p190BCR/ABL and p210BCR/ABL to the phosphatidylinositol-3' kinase pathway. Oncogene. 1996;12:839-846.

38. Van Etten RA. Mechanisms of transformation by the BCR-ABL oncogene: new perspectives in the post-imatinib era. Leuk Res. 2004;28 Suppl 1:S21-28.

39. Yuan Z, Mei HD. Inhibition of telomerase activity with hTERT antisense increases the effect of CDDP-induced apoptosis in myeloid leukemia. Hematol J. 2002;3:201-205.

40. Lewis ID, McDiarmid LA, Samels LM, To LB, Hughes TP. Establishment of a reproducible model of chronic-phase chronic myeloid leukemia in NOD/SCID mice using blood-derived mononuclear or CD34+ cells. Blood. 1998;91:630-640.

41. Melo JV. BCR-ABL gene variants. Baillieres Clin Haematol. 1997;10:203-222.

42. Pane F, Frigeri F, Camera A, et al. Complete phenotypic and genotypic lineage switch in a Philadelphia chromosome-positive acute lymphoblastic leukemia. Leukemia. 1996;10:741-745.

43. Konopka JB, Watanabe SM, Singer JW, Collins SJ, Witte ON. Cell lines and clinical isolates derived from Ph1-positive chronic myelogenous leukemia patients express c-abl proteins with a common structural alteration. Proc Natl Acad Sci U S A. 1985;82:1810-1814.

44. Louwagie A, Criel A, Verfaillie CM, et al. Philadelphia-positive T-acute lymphoblastic leukemia. Cancer Genet Cytogenet. 1985;16:297-300.

45. Gordon MY, Dowding CR, Riley GP, Goldman JM, Greaves MF. Altered adhesive interactions with marrow stroma of haematopoietic progenitor cells in chronic myeloid leukaemia. Nature. 1987;328:342-344.

46. Durig J, Schmucker U, Duhrsen U. Differential expression of chemokine receptors in B cell malignancies. Leukemia. 2001;15:752-756.

47. Deininger MW, Vieira S, Mendiola R, Schultheis B, Goldman JM, Melo JV. BCR-ABL tyrosine kinase activity regulates the expression of multiple genes implicated in the pathogenesis of chronic myeloid leukemia. Cancer Res. 2000;60:2049-2055.

48. Puil L, Liu J, Gish G, et al. Bcr-Abl oncoproteins bind directly to activators of the Ras signalling pathway. Embo J. 1994;13:764-773.

49. Oda T, Heaney C, Hagopian JR, Okuda K, Griffin JD, Druker BJ. Crkl is the major tyrosine-phosphorylated protein in neutrophils from patients with chronic myelogenous leukemia. J Biol Chem. 1994;269:22925-22928.

50. Sattler M, Mohi MG, Pride YB, et al. Critical role for Gab2 in transformation by BCR/ABL. Cancer Cell. 2002;1:479-492.

51. Ye D, Wolff N, Li L, Zhang S, Ilaria RL, Jr. STAT5 signaling is required for the efficient induction and maintenance of CML in mice. Blood. 2006;107:4917-4925.

52. Klejman A, Rushen L, Morrione A, Slupianek A, Skorski T. Phosphatidylinositol-3 kinase inhibitors enhance the anti-leukemia effect of STI571. Oncogene. 2002;21:5868-5876.

53. de Groot RP, Raaijmakers JA, Lammers JW, Koenderman L. STAT5-Dependent CyclinD1 and Bcl-xL expression in Bcr-Abl-transformed cells. Mol Cell Biol Res Commun. 2000;3:299-305.

54. Seki H, Seno A, Sakazume S, et al. [Clinical study of fluconazole-injectable and -granules in pediatric patients]. Jpn J Antibiot. 1994;47:289-295.

55. Gloc E, Warszawski M, Mlynarski W, et al. TEL/JAK2 tyrosine kinase inhibits DNA repair in the presence of amifostine. Acta Biochim Pol. 2002;49:121-128.

56. Afar DE, Witte ON. Characterization of breakpoint cluster region kinase and SH2-binding activities. Methods Enzymol. 1995;256:125-129.

57. Melo JV, Deininger MW. Biology of chronic myelogenous leukemia--signaling pathways of initiation and transformation. Hematol Oncol Clin North Am. 2004;18:545-568, vii-viii.

58. Vigneri P, Wang JY. Induction of apoptosis in chronic myelogenous leukemia cells through nuclear entrapment of BCR-ABL tyrosine kinase. Nat Med. 2001;7:228-234.

59. Lepelley P, Preudhomme C, Vanrumbeke M, Quesnel B, Cosson A, Fenaux P. Detection of p53 mutations in hematological malignancies: comparison between immunocytochemistry and DNA analysis. Leukemia. 1994;8:1342-1349.

60. Klein F, Feldhahn N, Harder L, et al. The BCR-ABL1 kinase bypasses selection for the expression of a pre-B cell receptor in pre-B acute lymphoblastic leukemia cells. J Exp Med. 2004;199:673-685.

61. Kersseboom R, Middendorp S, Dingjan GM, et al. Bruton's tyrosine kinase cooperates with the B cell linker protein SLP-65 as a tumor suppressor in Pre-B cells. J Exp Med. 2003;198:91-98.

62. Nichogiannopoulou A, Trevisan M, Friedrich C, Georgopoulos K. Ikaros in hemopoietic lineage determination and homeostasis. Semin Immunol. 1998;10:119-125.

63. Nera KP, Alinikula J, Terho P, et al. Ikaros has a crucial role in regulation of B cell receptor signaling. Eur J Immunol. 2006;36:516-525.

64. Kaufmann C, Yoshida T, Perotti EA, Landhuis E, Wu P, Georgopoulos K. A complex network of regulatory elements in Ikaros and their activity during hemo-lymphopoiesis. Embo J. 2003;22:2211-2223.

65. Morgan B, Sun L, Avitahl N, et al. Aiolos, a lymphoid restricted transcription factor that interacts with Ikaros to regulate lymphocyte differentiation. Embo J. 1997;16:2004-2013.

66. Wang JH, Avitahl N, Cariappa A, et al. Aiolos regulates B cell activation and maturation to effector state. Immunity. 1998;9:543-553.

67. Kelley CM, Ikeda T, Koipally J, et al. Helios, a novel dimerization partner of Ikaros expressed in the earliest hematopoietic progenitors. Curr Biol. 1998;8:508-515.

68. Gomez-del Arco P, Maki K, Georgopoulos K. Phosphorylation controls Ikaros's ability to negatively regulate the G(1)-S transition. Mol Cell Biol. 2004;24:2797-2807.

69. Gomez-del Arco P, Koipally J, Georgopoulos K. Ikaros SUMOylation: switching out of repression. Mol Cell Biol. 2005;25:2688-2697.

70. Koipally J, Georgopoulos K. A molecular dissection of the repression circuitry of Ikaros. J Biol Chem. 2002;277:27697-27705.

71. Sun L, Goodman PA, Wood CM, et al. Expression of aberrantly spliced oncogenic ikaros isoforms in childhood acute lymphoblastic leukemia. J Clin Oncol. 1999;17:3753-3766.

72. Sun L, Heerema N, Crotty L, et al. Expression of dominant-negative and mutant isoforms of the antileukemic transcription factor Ikaros in infant acute lymphoblastic leukemia. Proc Natl Acad Sci U S A. 1999;96:680-685.

73. Ruiz A, Jiang J, Kempski H, Brady HJ. Overexpression of the Ikaros 6 isoform is restricted to t(4;11) acute lymphoblastic leukaemia in children and infants and has a role in B-cell survival. Br J Haematol. 2004;125:31-37.

74. Sun L, Crotty ML, Sensel M, et al. Expression of dominant-negative Ikaros isoforms in T-cell acute lymphoblastic leukemia. Clin Cancer Res. 1999;5:2112-2120.

75. Nishii K, Katayama N, Miwa H, et al. Non-DNA-binding Ikaros isoform gene expressed in adult B-precursor acute lymphoblastic leukemia. Leukemia. 2002;16:1285-1292.

76. Nakayama H, Ishimaru F, Avitahl N, et al. Decreases in Ikaros activity correlate with blast crisis in patients with chronic myelogenous leukemia. Cancer Res. 1999;59:3931-3934.

77. Ishimaru F. Expression of Ikaros isoforms in patients with acute myeloid leukemia. Blood. 2002;100:1511-1512; 1512-1513.

78. Yagi T, Hibi S, Takanashi M, et al. High frequency of Ikaros isoform 6 expression in acute myelomonocytic and monocytic leukemias: implications for up-regulation of the antiapoptotic protein Bcl-XL in leukemogenesis. Blood. 2002;99:1350-1355.

79. Faderl S, Kantarjian HM, Thomas DA, et al. Outcome of Philadelphia chromosome-positive adult acute lymphoblastic leukemia. Leuk Lymphoma. 2000;36:263-273.

80. Pane F, Cimino G, Izzo B, et al. Significant reduction of the hybrid BCR/ABL transcripts after induction and consolidation therapy is a powerful predictor of treatment response in adult Philadelphia-positive acute lymphoblastic leukemia. Leukemia. 2005;19:628-635.

81. Radich JP. Philadelphia chromosome-positive acute lymphocytic leukemia. Hematol Oncol Clin North Am. 2001;15:21-36.

82. Barrett AJ, Kendra JR, Lucas CF, et al. Bone marrow transplantation for acute lymphoblastic leukaemia. Br J Haematol. 1982;52:181-188.

83. Avivi I, Goldstone AH. Bone marrow transplant in Ph+ ALL patients. Bone Marrow Transplant. 2003;31:623-632.

84. Yanada M, Naoe T, Iida H, et al. Myeloablative allogeneic hematopoietic stem cell transplantation for Philadelphia chromosome-positive acute lymphoblastic leukemia in adults: significant roles of total body irradiation and chronic graft-versus-host disease. Bone Marrow Transplant. 2005;36:867-872.

85. Capdeville R, Silberman S. Imatinib: a targeted clinical drug development. Semin Hematol. 2003;40:15-20.

86. Druker BJ, Sawyers CL, Kantarjian H, et al. Activity of a specific inhibitor of the BCR-ABL tyrosine kinase in the blast crisis of chronic myeloid leukemia and acute lymphoblastic leukemia with the Philadelphia chromosome. N Engl J Med. 2001;344:1038-1042.

87. Thomas DA, O'Brien S, Cortes J, et al. Outcome with the hyper-CVAD regimens in lymphoblastic lymphoma. Blood. 2004;104:1624-1630.

88. Lee KH, Lee JH, Choi SJ, et al. Clinical effect of imatinib added to intensive combination chemotherapy for newly diagnosed Philadelphia chromosome-positive acute lymphoblastic leukemia. Leukemia. 2005;19:1509-1516.

89. Wassmann B. Imatinib in relapsed or refractory Philadelphia chromosome-positive acute lymphoblastic leukaemia: a viewpoint by Barbara Wassmann. Drugs. 2007;67:2656.

90. Wassmann B, Pfeifer H, Goekbuget N, et al. Alternating versus concurrent schedules of imatinib and chemotherapy as front-line therapy for Philadelphia-positive acute lymphoblastic leukemia (Ph+ ALL). Blood. 2006;108:1469-1477.

91. Yanada M, Matsuo K, Suzuki T, Naoe T. Allogeneic hematopoietic stem cell transplantation as part of postremission therapy improves survival for adult patients with high-risk acute lymphoblastic leukemia: a metaanalysis. Cancer. 2006;106:2657-2663.

92. Soverini S, Colarossi S, Gnani A, et al. Contribution of ABL kinase domain mutations to imatinib resistance in different subsets of Philadelphia-positive patients: by the GIMEMA Working Party on Chronic Myeloid Leukemia. Clin Cancer Res. 2006;12:7374-7379.

93. Shah NP. Loss of response to imatinib: mechanisms and management. Hematology (Am Soc Hematol Educ Program). 2005:183-187.

94. Gorre ME, Mohammed M, Ellwood K, et al. Clinical resistance to STI-571 cancer therapy caused by BCR-ABL gene mutation or amplification. Science. 2001;293:876-880.

95. Mahon FX, Deininger MW, Schultheis B, et al. Selection and characterization of BCR-ABL positive cell lines with differential sensitivity to the tyrosine kinase inhibitor STI571: diverse mechanisms of resistance. Blood. 2000;96:1070-1079.

96. Hochhaus A, Kreil S, Corbin AS, et al. Molecular and chromosomal mechanisms of resistance to imatinib (STI571) therapy. Leukemia. 2002;16:2190-2196.

97. Peng B, Lloyd P, Schran H. Clinical pharmacokinetics of imatinib. Clin Pharmacokinet. 2005;44:879-894.

98. Picard S, Titier K, Etienne G, et al. Trough imatinib plasma levels are associated with both cytogenetic and molecular responses to standard-dose imatinib in chronic myeloid leukemia. Blood. 2006.

99. Hansen JD, Strassburger P, Du Pasquier L. Conservation of a master hematopoietic switch gene during vertebrate evolution: isolation and characterization of Ikaros from teleost and amphibian species. Eur J Immunol. 1997;27:3049-3058.

100. Thomas J, Wang L, Clark RE, Pirmohamed M. Active transport of imatinib into and out of cells: implications for drug resistance. Blood. 2004;104:3739-3745.

101. Ostrovsky O, Korostishevsky M, Levite I, et al. Association of heparanase gene (HPSE) single nucleotide polymorphisms with hematological malignancies. Leukemia. 2007;21:2296-2303.

102. Jordanides NE, Jorgensen HG, Holyoake TL, Mountford JC. Functional ABCG2 is overexpressed on primary CML CD34+ cells and is inhibited by imatinib mesylate. Blood. 2006;108:1370-1373.

103. Breedveld P, Beijnen JH, Schellens JH. Use of P-glycoprotein and BCRP inhibitors to improve oral bioavailability and CNS penetration of anticancer drugs. Trends Pharmacol Sci. 2006;27:17-24.

104. Mahon FX, Belloc F, Lagarde V, et al. MDR1 gene overexpression confers resistance to imatinib mesylate in leukemia cell line models. Blood. 2003;101:2368-2373.

105. Mukai M, Che XF, Furukawa T, et al. Reversal of the resistance to STI571 in human chronic myelogenous leukemia K562 cells. Cancer Sci. 2003;94:557-563.

106. Galimberti S, Cervetti G, Guerrini F, et al. Quantitative molecular monitoring of BCR-ABL and MDR1 transcripts in patients with chronic myeloid leukemia during Imatinib treatment. Cancer Genet Cytogenet. 2005;162:57-62.

107. Houghton PJ, Germain GS, Harwood FC, et al. Imatinib mesylate is a potent inhibitor of the ABCG2 (BCRP) transporter and reverses resistance to topotecan and SN-38 in vitro. Cancer Res. 2004;64:2333-2337.

108. Nakanishi T, Shiozawa K, Hassel BA, Ross DD. Complex interaction of BCRP/ABCG2 and imatinib in BCR-ABL-expressing cells: BCRP-mediated resistance to imatinib is attenuated by imatinib-induced reduction of BCRP expression. Blood. 2006;108:678-684.

109. Lam SH, Chua HL, Gong Z, Lam TJ, Sin YM. Development and maturation of the immune system in zebrafish, Danio rerio: a gene expression profiling, in situ hybridization and immunological study. Dev Comp Immunol. 2004;28:9-28.

110. Ottmann O, Dombret H, Martinelli G, et al. Dasatinib induces rapid hematologic and cytogenetic responses in adult patients with Philadelphia chromosome positive acute lymphoblastic leukemia with resistance or intolerance to imatinib: interim results of a phase 2 study. Blood. 2007;110:2309-2315.

111. Kim WY, Sharpless NE. The regulation of INK4/ARF in cancer and aging. Cell. 2006;127:265-275.

112. Baxter J, Sauer S, Peters A, et al. Histone hypomethylation is an indicator of epigenetic plasticity in quiescent lymphocytes. Embo J. 2004;23:4462-4472.

113. Primo D, Tabernero MD, Perez JJ, et al. Genetic heterogeneity of BCR/ABL+ adult B-cell precursor acute lymphoblastic leukemia: impact on the clinical, biological and immunophenotypical disease characteristics. Leukemia. 2005;19:713-720.

114. Mullighan CG, Goorha S, Radtke I, et al. Genome-wide analysis of genetic alterations in acute lymphoblastic leukaemia. Nature. 2007;446:758-764.

115. Hochhaus A. Management of Bcr-Abl-positive leukemias with dasatinib. Expert Rev Anticancer Ther. 2007;7:1529-1536.

116. Weisberg E, Manley P, Mestan J, Cowan-Jacob S, Ray A, Griffin JD. AMN107 (nilotinib): a novel and selective inhibitor of BCR-ABL. Br J Cancer. 2006;94:1765-1769.

117. Kaur P, Feldhahn N, Zhang B, et al. Nilotinib treatment in mouse models of P190 Bcr/Abl lymphoblastic leukemia. Mol Cancer. 2007;6:67.

118. Kantarjian H, Giles F, Wunderle L, et al. Nilotinib in imatinib-resistant CML and Philadelphia chromosome-positive ALL. N Engl J Med. 2006;354:2542-2551.

119. Winandy S, Wu P, Georgopoulos K. A dominant mutation in the Ikaros gene leads to rapid development of leukemia and lymphoma. Cell. 1995;83:289-299.

120. Olivero S, Maroc C, Beillard E, et al. Detection of different Ikaros isoforms in human leukaemias using real-time quantitative polymerase chain reaction. Br J Haematol. 2000;110:826-830.

121. Georgopoulos K, Moore DD, Derfler B. Ikaros, an early lymphoid-specific transcription factor and a putative mediator for T cell commitment. Science. 1992;258:808-812.

122. Wang Z, Rolish ME, Yeo G, Tung V, Mawson M, Burge CB. Systematic identification and analysis of exonic splicing silencers. Cell. 2004;119:831-845.

123. Fairbrother WG, Yeo GW, Yeh R, et al. RESCUE-ESE identifies candidate exonic splicing enhancers in vertebrate exons. Nucleic Acids Res. 2004;32:W187-190.

124. Gabert J, Beillard E, van der Velden VH, et al. Standardization and quality control studies of 'real-time' quantitative reverse transcriptase polymerase chain reaction of fusion gene transcripts for residual disease detection in leukemia - a Europe Against Cancer program. Leukemia. 2003;17:2318-2357.

125. Tonnelle C, Calmels B, Maroc C, Gabert J, Chabannon C. Ikaros gene expression and leukemia. Leuk Lymphoma. 2002;43:29-35.

126. Tonnelle C, Imbert MC, Sainty D, Granjeaud S, N'Guyen C, Chabannon C. Overexpression of dominant-negative Ikaros 6 protein is restricted to a subset of B common adult acute lymphoblastic leukemias that express high levels of the CD34 antigen. Hematol J. 2003;4:104-109.

127. Georgopoulos K, Bigby M, Wang JH, et al. The Ikaros gene is required for the development of all lymphoid lineages. Cell. 1994;79:143-156.

128. Vemireddy LR, Archak S, Nagaraju J. Capillary electrophoresis is essential for microsatellite marker based detection and quantification of adulteration of Basmati rice (Oryza sativa). J Agric Food Chem. 2007;55:8112-8117.
129. Sufliarska S, Minarik G, Horakova J, et al. Establishing the method of chimerism monitoring after allogeneic stem cell transplantation using multiplex polymerase chain reaction amplification of short tandem repeat markers and Amelogenin. Neoplasma. 2007;54:424-430.
130. Delmotte F, Leterme N, Simon JC. Microsatellite allele sizing: difference between automated capillary electrophoresis and manual technique. Biotechniques. 2001;31:810, 814-816, 818.
131. Rebollo A, Schmitt C. Ikaros, Aiolos and Helios: transcription regulators and lymphoid malignancies. Immunol Cell Biol. 2003;81:171-175.
132. Nakase K, Ishimaru F, Avitahl N, et al. Dominant negative isoform of the Ikaros gene in patients with adult B-cell acute lymphoblastic leukemia. Cancer Res. 2000;60:4062-4065.
133. Klein F, Feldhahn N, Herzog S, et al. BCR-ABL1 induces aberrant splicing of IKAROS and lineage infidelity in pre-B lymphoblastic leukemia cells. Oncogene. 2006;25:1118-1124.

Acknowlegments

Dpt of Hematology/Oncology "Seràgnoli",Bologna
Emanuela Ottaviani, Annalisa Lonetti, Federica Salmi, Simona Soverini, Nicoletta Testoni, Sabrina Colarossi, Alessandra Gnani, Marilina Amabile, Angela Poerio, Federica Salmi, Stefania Paolini, Cristina Papayannidis, Panagiota Giannoulia, Rosti Gianantonio, Fausto Castagnetti, Francesca Palandri, Francesco De Rosa, Pier Paolo Piccaluga, Barbara Lama

Giovanni Martinelli and Michele Baccarani

Dpt di Scienze Cliniche e Biologiche, Orbassano (TO)
Francesca Messa, Francesca Arruga, Enrico Bracco, Daniela Cilloni, Giuseppe Saglio

Università "La Sapienza", Roma
Robert Foà, Antonella Vitale, Sabina Chiaretti